

University of Connecticut
School of Engineering
Environmental Engineering Program
Undergraduate Honors Thesis



Hydrogeological Conceptual Model of La Villa River Watershed, Republic of Panama



Maria Gabriela Castellon Romero
April 29th, 2016

For my grandfather, the first to show me the
beauty of the natural environment surrounding us

Acknowledgements

Firstly I would like to thank Dr. Allison Mackay, who introduced me to the wonderful world of groundwater during my second semester of college and was a role model for me at the very beginning of my career. I would like to thank Dr. Gonzalo Pulido, Project Supervisor from IDAAN Panama, who helped me put the proposal for this project together. A very special thanks to Dr. Amvrossios C. Bagtzoglou, my thesis advisor, who guided and helped me build the story presented in this Thesis. Thanks to Melissa Berkey for helping me write a proposal for the IDEA Grant, and thanks to the Office of Undergraduate Research at the University of Connecticut for granting me the IDEA Award with which I was able to fund the field work for this project. Thanks to Julia Guardia, Director of IDAAN for supporting my project. Thanks to Dr. Octavio Smith, GIS Analyst and Dr. Valentina Opolenko, Hydrogeologist from CATHALAC; Dr. Christine Kirchhoff, Honors Advisor, Dr. Gary Robbins, Professor of Hydrogeology and Dr. Amy Burnicki, GIS Professor at the University of Connecticut, for answering all my questions and providing me with the necessary background knowledge that I needed to complete this project. Thanks to the members of the Department of Groundwater Sources at IDAAN Panama: Iván Cedeño, Director; Edgardo Vergara, Geologist; Gilberto Sánchez, Manuel Medina, and all Field Assistants that helped me gather data; Mathilde Le Goff and Noemie Le Heurte, Interns.

Table of Contents

Acknowledgements.....	ii
Table of Contents.....	iii
1. Introduction.....	1
1.1 The Dry Arc Region of Panama.....	1
1.2 Use and Management of Groundwater in Panama.....	2
1.3 El Niño Phenomenon and its effects in Panama.....	3
1.4 Statement of the Problem.....	5
1.5 Project Proposed.....	6
2. La Villa River Watershed.....	7
2.1 Location and Topography.....	7
2.2 Geology and Geomorphology.....	8
2.2.1 Geological History of Panama.....	8
2.2.2 Geology of Azuero and La Villa Watershed.....	9
2.3 Weather and Hydrology.....	11
2.4 Land Use and Forest Cover.....	13
3. Materials and Methods.....	15
3.1 Acquisition of Well Data.....	15
3.2 Selection of Monitoring Wells.....	16
3.3 Groundwater Elevation Measurement.....	17
3.4 Hydraulic Testing and Hydraulic Conductivity Calculations.....	18
3.4.1 Slug Tests: Data Collection and Analysis.....	18
3.4.2 Pumping Tests: Data Analysis.....	20
3.5 Geological Model.....	25
4. Results and Discussion.....	30
4.1 Groundwater Elevation and Flow Patterns.....	30
4.2 Change in Groundwater Elevation.....	34
4.3 Hydraulic Conductivity and Transmissivity.....	37
4.4 Precipitation.....	40
4.5 Recharge Areas.....	43
4.6 Hydrological Analysis.....	44

5. Conclusions..... 48

 5.1 Summary 48

 5.2 Recommendations 49

 5.3 Further Research 49

6. References..... 51

7. Appendices..... 54

 7.1 Appendix A: Figures and Maps 54

 7.2 Appendix B: Tables..... 66

 7.3 Appendix C: Calculations 68

1. Introduction

1.1 The Dry Arc Region of Panama

The Dry Arc Region of Panama includes part of the provinces of Herrera, Los Santos and Coclé, and is located in the central south part of Panama. According to ANAM (2013) this region has an area of approximately 18,000 square kilometers. However, according to Castillo and Patiño (2014) the Dry Arc Region comprises 18 out of 20 districts of the provinces of Coclé, Herrera and Los Santos as well as two districts of the province of Panama. Also, according to the Atlas of Panama, the Dry Arc Region is the region that extends from “Punta” Chame in the province of Panama to “Punta” Mala in the province of Los Santos (Castillo and Patiño, 2014). In the context of the present thesis this discrepancy in definitions is not relevant since the area of interest (the border between the provinces of Herrera and Los Santos) is included in all three definitions.

The driest part of the Dry Arc Region, located near the coastal areas surrounding the Gulf of Parita, receives an average precipitation that varies from 900 mm/year to 1300 mm/year (ETESA, 2007). The highlands of the Azuero Peninsula, as well as the highlands of the provinces of Panamá and Coclé receive an average precipitation that varies from 3000 mm/year to 3500 mm/year (ETESA, 2007). The average temperature in the region varies from 22.5 to 27.0 degrees Celsius (ANAM, 2013). Following Köppen’s climate classification, the majority of the Dry Arc Region has tropical savanna climate and some smaller areas with tropical humid climate (ETESA, 2007). The Dry Arc Region is covered in its majority by montane dry forest and tropical dry forest (Castillo and Patiño, 2014).

The main economic activities of the Dry Arc Region historically had been agronomy and livestock breeding. As a result of years of intensive agriculture, cattle farming and non-sustainable use of natural resources, the region suffers from environmental degradation characterized by the loss of mature forest, desertification and the loss of soil’s productive capacity (ANAM, 2013). The region’s natural vegetation cover has almost entirely disappeared and has been converted to pasture and farm land. The only ecosystems that remain unaltered are the mangroves (Castillo and Patiño, 2014). As a consequence of the intense desertification the Dry Arc has been experiencing, the dry season is extending and the surface water sources are becoming scarce. Therefore, people are becoming very dependent upon groundwater resources.

1.2 Use and Management of Groundwater in Panama

In certain areas of Panama, groundwater is used as the main source of water, especially in locations where surface water is not available or its quality is compromised. Groundwater in Panama is used for domestic purposes, irrigation of agricultural fields, industries, and recreational purposes as well. In the last decades, Panama has experienced a growth in the consumption of groundwater. According to the National Institution of Drinking Water Supply and Sanitation (IDAAN), domestic groundwater supply represents 6.5% of the total national production of water (ANAM, 2013).

Groundwater in Panama is a public resource, and thus it is the responsibility of government institutions to exploit and manage these resources. According to Panama's Constitution, groundwater is owned by the Panamanian State and is available for public usage (Tejeira et al., 2010). Law No. 35 from September 22nd, 1966 establishes the National Water Commission as the entity in charge of the management of water resources in the country. Executive Order No. 70 from 1973 further regulates the use of groundwater resources by implementing the use of permits for the drilling of wells and the exploitation of groundwater resources by private owners (Justia Panama, ND).

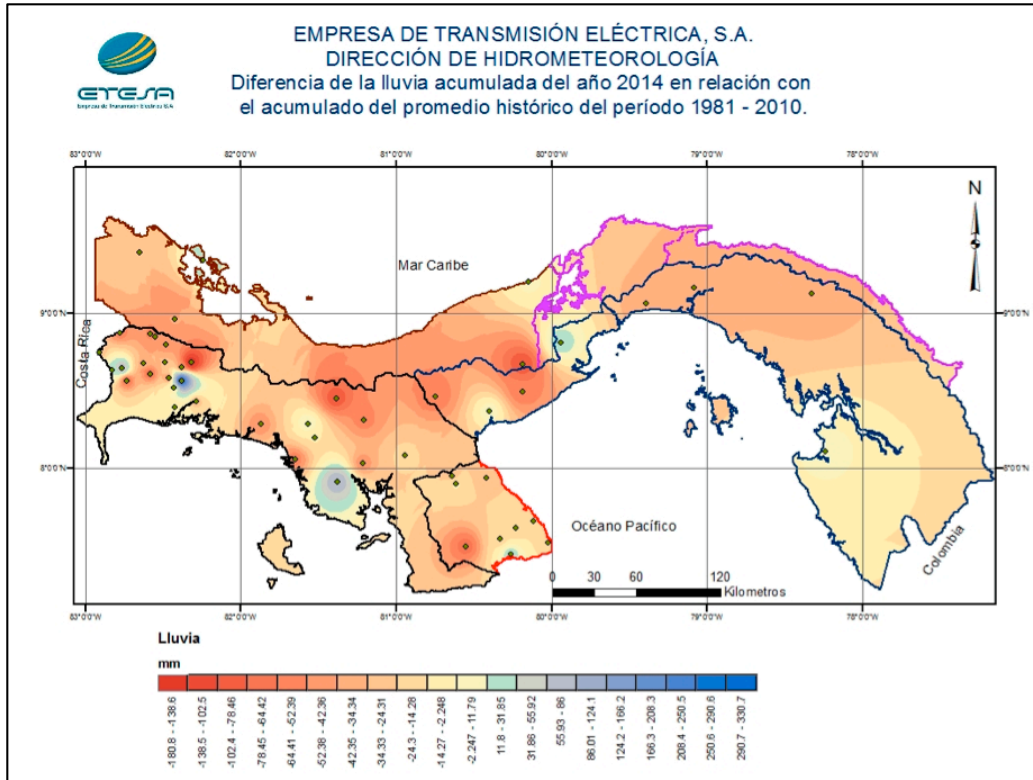
Nowadays, there are four institutions in Panama involved in the exploitation and management of groundwater resources. The National Institution of Drinking Water Supply and Sanitation (IDAAN) drills wells to provide water for domestic use to rural communities and towns with a population higher than 1500 inhabitants. The Ministry of Health (MINSa) drills wells to supply drinking water to small towns and villages with populations lower than 1500 inhabitants. The Ministry of Agriculture (MIDA) drills wells in private farms for agricultural purposes. The Ministry of Environment, previously known as the National Authority of Environmental Protection (ANAM), is the government institution responsible for managing the hydrologic resources of the country, including groundwater. The Ministry of Environment regulates the use of groundwater in Panama and it coordinates the actions of the different public institutions and private companies that exploit the country's aquifers. In Panama it is illegal for individuals to drill wells and extract groundwater without having a special permit granted by the Ministry of Environment (ANAM, 2013).

1.3 El Niño Phenomenon and its effects in Panama

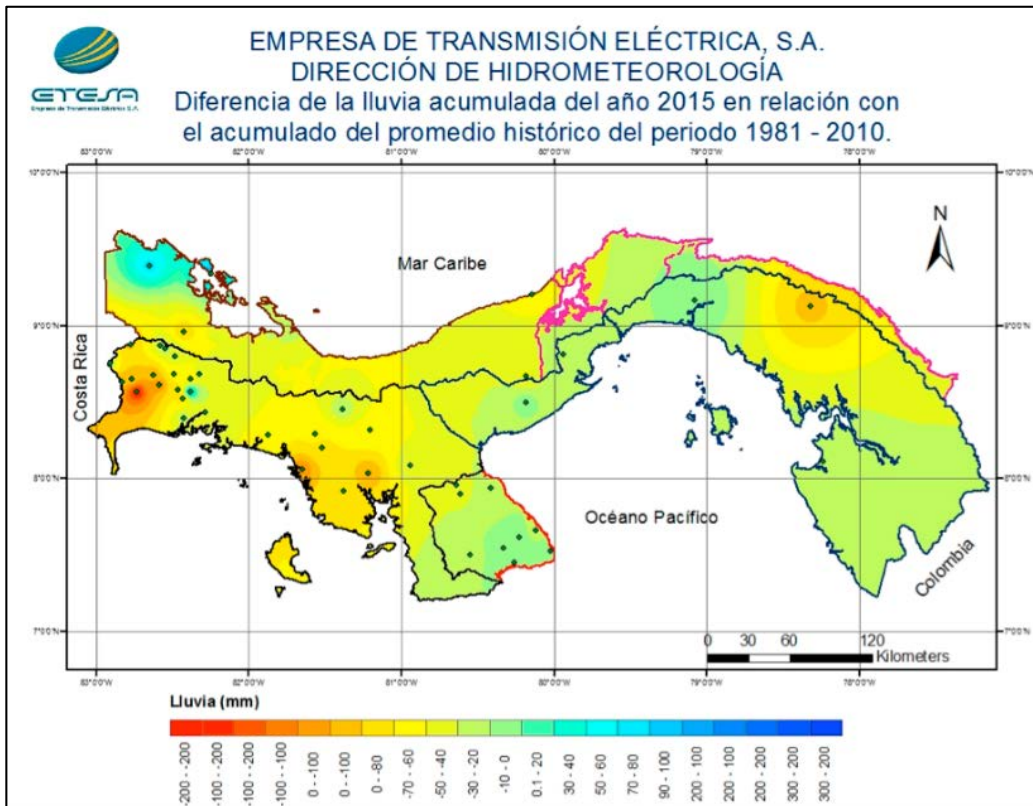
The oceanic and atmospheric disturbance known as El Niño is one stage of the climate phenomenon known as El Niño Southern Oscillation (ENSO). ENSO has the ability to shift circulation patterns of the atmosphere and in consequence, precipitation and temperatures are altered throughout the globe (L'Heureux, 2014). ENSO has three stages: El Niño, La Niña and Neutral. El Niño refers to an increase in sea surface temperatures (SST) of the tropical Pacific Ocean; La Niña refers to a decrease in SST of the tropical Pacific Ocean; and Neutral refers to average SST of the tropical Pacific Ocean (L'Heureux, 2014). It is important to note that ENSO is a “coupled” phenomenon, which means that in order for El Niño or La Niña to occur, both the ocean and the atmosphere have to be altered. Sometimes the central tropical Pacific Ocean will exhibit SST that resembles El Niño or La Niña; however, if the atmosphere is not altered then neutral conditions will occur (L'Heureux, 2014).

The El Niño phenomenon has variable duration and frequency and it affects different regions of the world in different ways. According to the department of hydrometeorology of ETESA, El Niño has a duration of 12 to 18 months and has a frequency of two to seven years (Olmedo, 2015). In California and the southern United States, El Niño brings stronger winter storms and the possibility of flood and landslides. In Indonesia, Australia and parts of the western Pacific, El Niño reduces average precipitation with the potential for severe droughts (Herring, 1999). In Panama, El Niño produces a decrease in precipitation on the Pacific coast and a slight increase in precipitation on the Caribbean coast. Although the effects will vary spatially and temporally, during El Niño years, precipitation and baseflow in rivers reduce significantly in most of the country (Olmedo, 2015).

Panama has been experiencing the effects of El Niño since 2014. The Pacific Ocean has been warmer than normal since the mid of 2014 and the Caribbean Sea has been colder than normal, a combination of circumstances that causes rainfall to be scarce across the Isthmus of Panama. Although Panama has areas that are prone to receive less rainfall than others, El Niño affects the whole country almost evenly. According to maps from ETESA, some areas of Panama received 100 mm of rain less than average in 2014, and 70 mm of rain less than average in 2015 (Figure 1.1). Models indicate that there is an 80% probability that El Niño will extend until April or May 2016 (Olmedo, 2015).



(a)



(b)

Figure 1.1: Change in rainfall accumulation due to El Niño phenomenon in 2014 (a) and 2015 (b) in Panama relative to historic averages (Department of Hydrometeorology, ETESA).

1.4 Statement of the Problem

It is common knowledge that groundwater will be of paramount importance in the future since it is the most abundant source of fresh water in the planet. Fresh groundwater makes up 0.76% of the total water of the planet, while fresh surface water (rivers and lakes) correspond to only 0.0072% (Chow et al., 1988). The natural arid conditions of the Dry Arc region and the threats of climatic uncertainty have put an immense pressure on the groundwater resources of Panama. The unorganized and intensive use of groundwater in Panama has generated a lot of problems that could threaten the quantity and quality of the resource. One important problem occurs in the coastal areas in which wells are sometimes over pumped, causing salt intrusion and therefore contaminating the aquifers with brackish water (ANAM, 2013). Other regions of the country may be at risk of depleting the aquifers because of the unregulated extraction of water and the lack of knowledge of volume of water available and safe pumping rates. The exploitation of groundwater in the Dry Arc Region increased 75% from 2002 to 2010 reaching a total value of 700,000 m³/day (185 MGD). However, it is impossible to evaluate the effect that this increase in extraction rates had on the aquifer water levels since monitoring of piezometric levels had not been implemented yet (Souifer, 2010).

It is very difficult to estimate the number of wells in the Dry Arc Region since the drilling, construction and installation of wells in the area and in the whole country is disorganized (Souifer, 2010). The different institutions in charge of drilling wells in the country keep separate databases, and they seldom share their information. Most of the times their databases are incomplete since crucial information such as well coordinates, elevation and borehole information is lacking (ANAM, 2013). The Ministry of Environment (previously known as ANAM) has put together a database of the wells in the Dry Arc Region; however, even this database is very basic and lacks important information about the hydrogeological units and aquifer conditions in the region.

Panama is in need of a better understanding of how the groundwater behaves in order to protect the quantity and quality of this vital resource and ensure the availability of potable water to the population (ANAM, 2013). According to a study done by the group *Nómadas de Centroamérica*, it is urgent that authorities in Panama install a network of piezometers in the Dry Arc Region in order to monitor the behavior of groundwater and how the water levels in the aquifers change over time (Souifer, 2010). Also it is important

to have a complete and unified database of all the wells drilled in the country with inputs from IDAAN, MIDA, MINSA and ANAM. Moreover, an inventory of all the consumers of groundwater, especially in the Dry Arc Region, is needed in order to better monitor and manage this important resource (ANAM, 2013).

1.5 Project Proposed

This thesis proposes to study the groundwater of the Dry Arc Region by analyzing the hydrogeological characteristics of individual watersheds. This project is the first attempt to develop a conceptual hydrogeological model of one of the most important watersheds in the Dry Arc Region: La Villa River Watershed.

A conceptual model improves the understanding of the characteristics of a system or a particular site before introducing quantitative metrics (Hesch, 2009). A conceptual hydrogeological model qualitatively describes the hydrogeology of a site and improves our understanding on how groundwater is behaving. The Conceptual Hydrogeological Model of La Villa River Watershed has the following goals:

- Identify the location of the potential recharge areas of the watershed
- Describe the general groundwater flow pattern
- Detect the seasonal high and low of groundwater elevation

The scope of the thesis is to integrate available hydrogeological information of the watershed with new data gathered from selected monitoring wells located in the watershed. The manipulation, presentation and analysis of the data is done using ArcGIS. The final result will be a series of maps, a database containing the information from the monitoring wells, and a set of layers that could be imported to other more sophisticated groundwater modeling software for future analysis.

Although La Villa watershed is just a small part of the Dry Arc Region, a conceptual model including characteristics of the wells and aquifer conditions will be the first step for the understanding of the dynamics of the resource in the region, and thus will be the first step for a sustainable management plan for groundwater in the region. Furthermore, it will serve as a pilot study that can be followed and applied to other parts of Panama, hence helping the country as a whole.

2. La Villa River Watershed

2.1 Location and Topography

Panama has 52 watersheds, of which 18 drain to the Caribbean Sea and 34 drain to the Pacific Ocean. La Villa Watershed is located in the Azuero Peninsula, between the provinces of Herrera and Los Santos (Appendix A, Figures A1 and A2). The main river of this watershed is the La Villa River, which drains to the Pacific Ocean and serves as the border between the two provinces for most of its length. The watershed has an area of 1,284 km² and the La Villa River has a total length of 125 km (Souifer, 2010).

The topography of this watershed is characterized by plains and lowlands (less than 200 m in elevation) that extend all the way from the coast to the middle part of the watershed with a gradually increasing elevation. Further upstream it is possible to find steeper hills (above 200 m) and mountains in the upper watershed (above 350 m). Only a few areas of the watershed surpass the 500 m of elevation. The highest elevations (above 750 m) occur mainly in the southwestern corner of the watershed, and according to the Digital Elevation Model (DEM), the highest elevation in the watershed is 941 m.

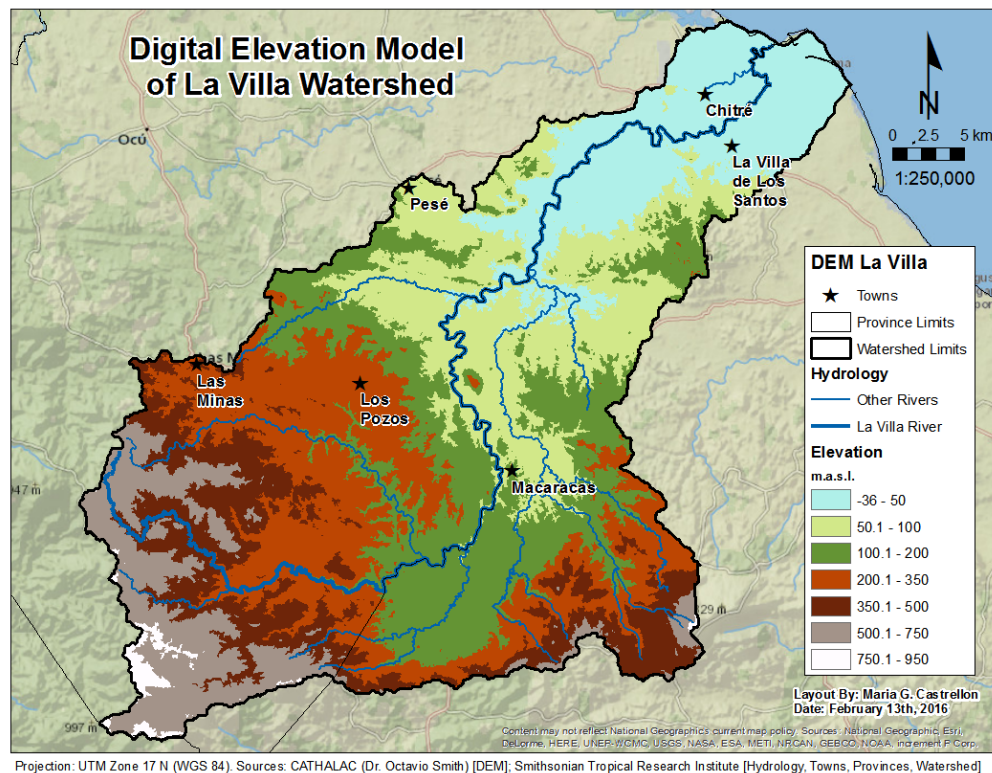


Figure 2.1: Topography of La Villa Watershed. The light blue and pale green represent the lowlands (less than 100 m). The brown, grey and white represent the highlands (higher than 350 m).

2.2 Geology and Geomorphology

2.2.1 Geological History of Panama

Panama formed as a result of very complex tectonic movement that has been taking place since 150 million years ago. Most of the Isthmus of Panama is formed by igneous rocks that resulted from volcanic activity during Tertiary time (Harmon, 2005). Around 20 million years ago, the Farallón oceanic plate, predecessor of today's Cocos plate (Figures A3 and A4), collided with the Caribbean oceanic plate creating a subduction zone with the Cocos plate sliding underneath the Caribbean plate (Kumar, 2014). The collision of these plates caused the ocean floor to rise and underwater volcanoes formed. According to Coates (1997) around 11 million years ago volcanic islands appeared in the location of today's eastern Panama and southern Central America. An archipelago formed over the next few million years, and by 6 million years ago, the deep water circulation between the Pacific and the Caribbean had stopped (Coates, 1997). The shallow ocean in between the newly formed volcanic islands filled with marine sediments and volcanoclastic materials, causing the seaway to close completely around 3.5 million years ago (Harmon, 2005).

However, not all of Panama formed in its current location. The Azuero, Soná and Burica peninsulas in Panama and the Nicoya and Osa peninsulas in Costa Rica (Figure A4), are exotic terranes that formed in the late Jurassic or early Cretaceous time as a result of hot spots in the western and southern Pacific Ocean. The movement of the Pacific plate caused this older oceanic arc to dock with the newly formed volcanic arc in eastern Panama and southern Costa Rica. These peninsulas contain the oldest exposed rocks in southern Central America (Coates, 1997; Harmon 2005).

However, other interpretations or hypotheses have been made known recently. As a result of the digging for the expansion of the Panama Canal, new geological information is now available for paleontologists and geologist to study. As a study from the University of Florida proposes, Panama was not formed as a set of volcanic islands connected by marine sediments. Instead, the age of rocks and fossils found in the Gaillard Cut of the Panama Canal suggests that Panama existed as a peninsula attached to the North American continent about 19 million years ago. Then due to tectonic forces, probably the sliding of the Cocos Plate beneath the Caribbean Plate, the Panamanian peninsula attached itself to South America about 4 million years ago. It is still unclear however, how this peninsula formed and for how long it existed (Donovan, 2008).

2.2.2 Geology of Azuero and La Villa Watershed

As is evident by the geological history of Panama, the core of the Isthmus is formed by igneous rocks above which rests a layer of tertiary sediments (Rubio, 1949). Geologists in Panama have not developed a formal classification of formations by stratigraphy, instead the formations are named after the place where they were found (Caballero, 2009).

In Azuero it is common to find evidence of volcanic activity with explosion of pyroclastic material and lavas, followed by episodes of sediment deposition. This feature has made it possible to identify two different volcanic events, one in the Cretaceous and another one in the Eocene (Caballero, 2009). The first volcanic event created the oldest rocks in the Azuero peninsula, the basalts and lavas that conform to the Playa Venado Formation, denoted as K-VE in the official geologic map of Panama (Souifer, 2010). In La Villa Watershed, this formation appears mainly in the highlands of the upper watershed, as well as in a section of the lower watershed north of the river (Figure 2.2). The oldest sedimentary rocks in Azuero are limestones and tuffs from the Ocú Formation (K-CHAO) which deposited after the volcanic event of the Cretaceous (Souifer, 2010). In the study area, this formation occurs as a layer that runs from west to east in the middle part of the watershed (Figure 2.2). The second volcanic episode occurred in the early Eocene and created the plutonic rocks of the Valle Riquito Formation (Table 2.1).

Tertiary deposits in the Isthmus occur as long and narrow “embayments” (Rubio, 1949). The oldest sedimentary deposits from the Eocene belong to the Tonosí formation (TEO-TO), and consist of sandstone, shale and tuff (Souifer, 2010). Sediments from the Oligocene are formed by very thick layers of conglomerates or sandstones, usually accompanied by limestone and shale of marine origin (Rubio, 1949). The Macaracas (TO-MAC) and Pesé (TO-MACpe) formations originated during this period and they cover the lowlands in between the mountains of volcanic origin (Figure 2.2). According to Caballero (2009) within these formations it is also usual to find layers of silty clay with a very low content of sand. Sediments from the Miocene are composed by conglomerates or sandstones created in beaches or shallow waters. Traces of these sediments can be found in the Santiago Formation (TM-SA), located in the lowlands of the provinces of Coclé, Veraguas, and in lesser quantities in Herrera and Los Santos (Rubio, 1949). The youngest sediments conform the Río Hato Formation (QR-Aha) located near the coast (Table 2.1).

Table 2.1: Description of the types of rocks found in the different geological formations of La Villa Watershed, and their approximate age (Adapted from ANAM, 2013).

Type	Age	Formation	Symbol	Description
Volcanic	Cretaceous	Playa Venado	K-VE	Basalt and lava
Plutonic	Cretaceous	Loma Montuoso	K-LM	Quartz-diorite, gabbro, granodiorite
Plutonic	Cretaceous	Dacitas Loma Montuoso	K-LMda	Dacite
Sedimentary	Cretaceous	Ocú	K-CHAO	Limestone and tuff
Plutonic	Eocene	Valle Riquito	TEO-RÍQ	Quartz-diorite and gabbro
Sedimentary	Eocene	Tonosí	TEO-TO	Sandstone, shale and tuff
Sedimentary	Oligocene	Macaracas	TO-MAC	Sandstones and tuff
Sedimentary	Oligocene	Pesé	TO-MACpe	Sandstone, tuff and limestone
Sedimentary	Miocene	Santiago	TM-SA	Sandstone and conglomerate
Sedimentary	Holocene	Río Hato	QR-Aha	Conglomerate, sandstone, shale, tuff

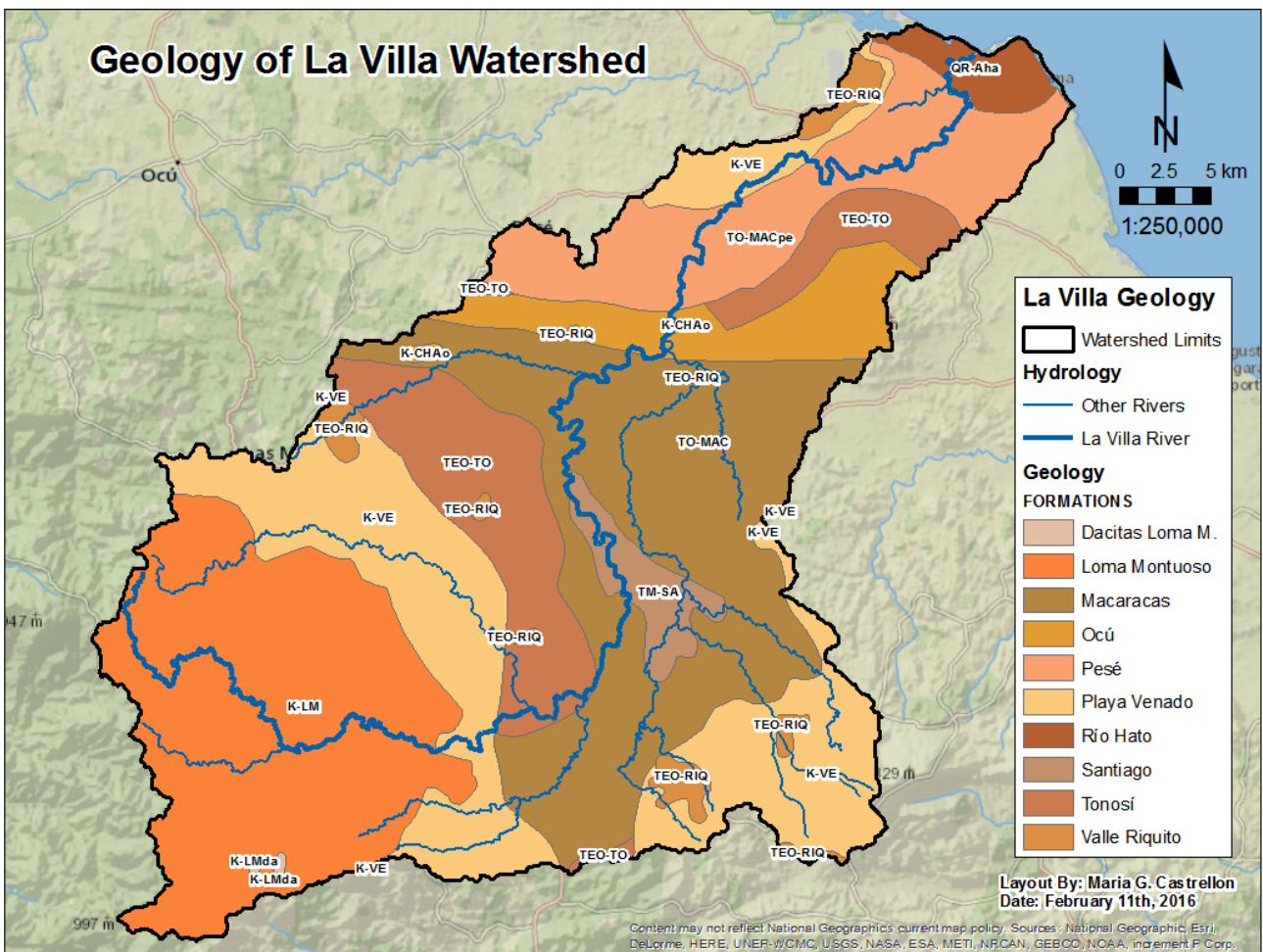


Figure 2.2: Geology of La Villa Watershed classified by characteristic formations.

2.3 Weather and Hydrology

La Villa Watershed is located in the Pacific coast of Panama, therefore it experiences two seasons: A rainy season from late April or early May to December and a dry season from December to April. During the rainy season it is common to have rain showers, and even thunderstorms almost every day. The strongest rainstorms occur in September and October. During the dry season the days are sunny and bright, with some rain showers but not as frequent or strong as in the rainy season. In extremely dry years (El Niño years), the dry season could last from December to late June.

Precipitation in La Villa Watershed is currently measured at four meteorological stations (Appendix A, Figure A6). According to the Hydrometeorology Department of ETESA, the average precipitation in La Villa watershed is 1868 mm/year, average evapotranspiration is 1264.48 mm/year and average runoff is 722.03 mm/year. During the rainy season 91% of the total yearly precipitation occurs, and only the 9% occurs during the dry season (Souifer, 2010). According to data from ETESA, published by Souifer (2010), the lowest average precipitation is less than 1 mm, and occurs in February and March in the Los Santos station, located in the lower part of the watershed; the highest average precipitation is about 320 mm, and occurs in October in the Pan de Azúcar station located in the upper part of the watershed in the province of Herrera (Figure 2.3).

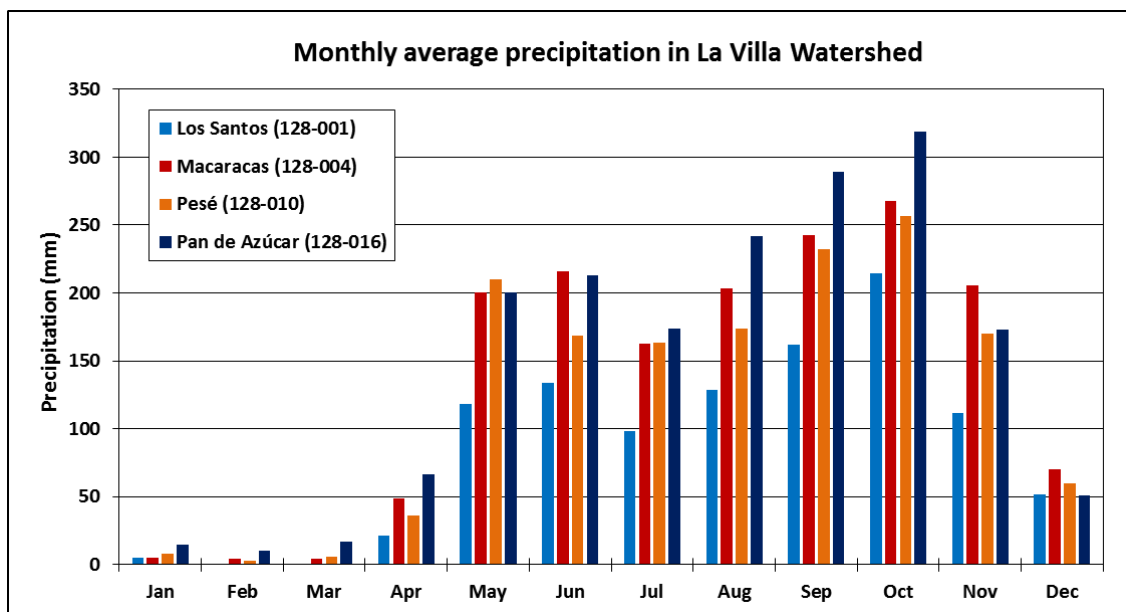


Figure 2.3: Monthly average precipitation calculated from nearly 50 years of data measured in four met stations in La Villa Watershed (Created from table published by Souifer, 2010).

The rain distribution in the watershed creates a distinctive fluvial regime in La Villa River and its main tributaries, rivers Estivaná, Tebárito and Gato. As the average annual hydrograph of La Villa River reflects (Figure 2.4), minimum flows occur in the months of January to April when precipitation is scarce, and flow starts increasing from June to December, when precipitation becomes more abundant.

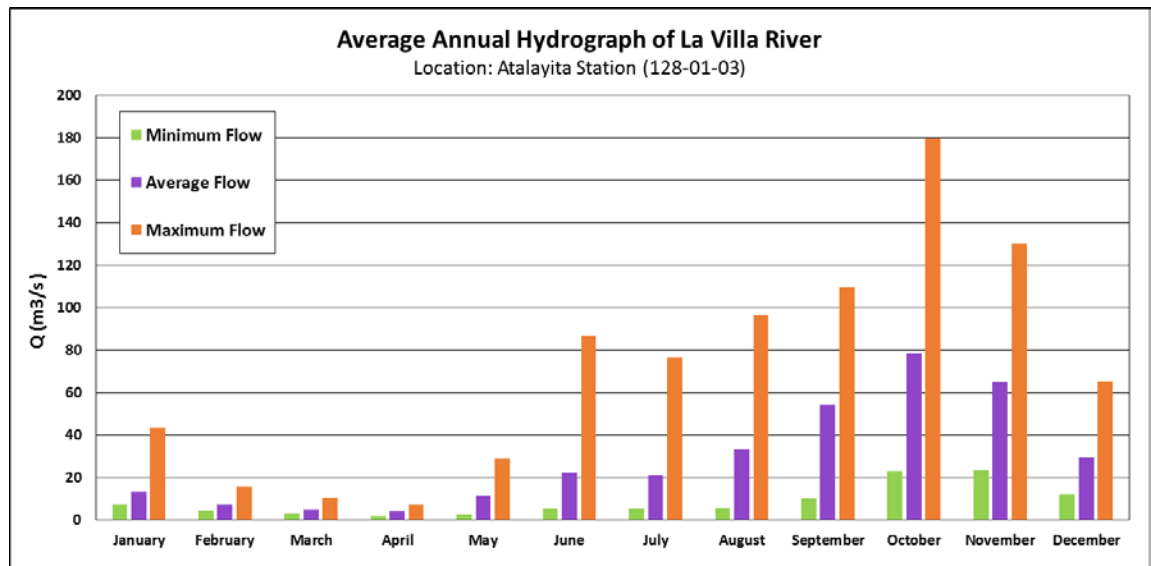


Figure 2.4: Average annual hydrograph of La Villa River measured at the Atalayita station, located in the lower part of the basin. Orange is maximum, green is the minimum, and purple is average recorded flow (Department of Hydrometeorology, ETESA).

According to the Hydrometeorology Department of ETESA, the highest average flow occurs in October and corresponds to $78.7 \text{ m}^3/\text{s}$, and the lowest average flow occurs in April and corresponds to $4.2 \text{ m}^3/\text{s}$. The average annual flow in the river is $28.8 \text{ m}^3/\text{s}$. It is important to point out that these values are averaged over more than 50 years of record. However, in the last decade the rainfall pattern has changed, causing a change in the annual hydrograph. As a result of El Niño and climate change, each year precipitation is scarcer and the dry season gets longer, causing many rivers to solely depend on groundwater generated base-flow to maintain water in their channels. However, groundwater is not enough to maintain healthy flows in some rivers of the region. The Estivaná River, one of the main tributaries of La Villa River, was almost dry in August 2015 (Cortez, 2015), and by the beginning of February 2016, about 99% of the low order streams in the province of Los Santos had completely dried (Aizprúa, 2016).

2.4 Land Use and Forest Cover

The forest cover in Panama has reduced from 70% to 45% in the last 50 years (ANAM, 2011). In no other part of the country this change has been as dramatic as in the La Villa Watershed. The main economic activities in La Villa Watershed are cattle farming and agriculture. Poor agricultural practices and unsustainable land management have led to a degradation of the quality of the soil and transformation of forest to pasture land and agricultural fields. According to the land use and forest cover map developed by ANAM in 2000, the provinces of Herrera and Los Santos have the least percentage of forest cover in the country with only 0.28% and 0.83%, respectively (ANAM, 2011).

The land cover/land use map of the watershed from the year 2000 (Figure 2.5) shows a small portion in dark green, representing the few pristine mature forests left in the watershed. The lighter shades of green represent younger forests. A large portion of the watershed is shown in yellow, which represents land for agriculture and cattle farming. The orange path surrounding the city of Chitré represents the most developed or urbanized land in the watershed.

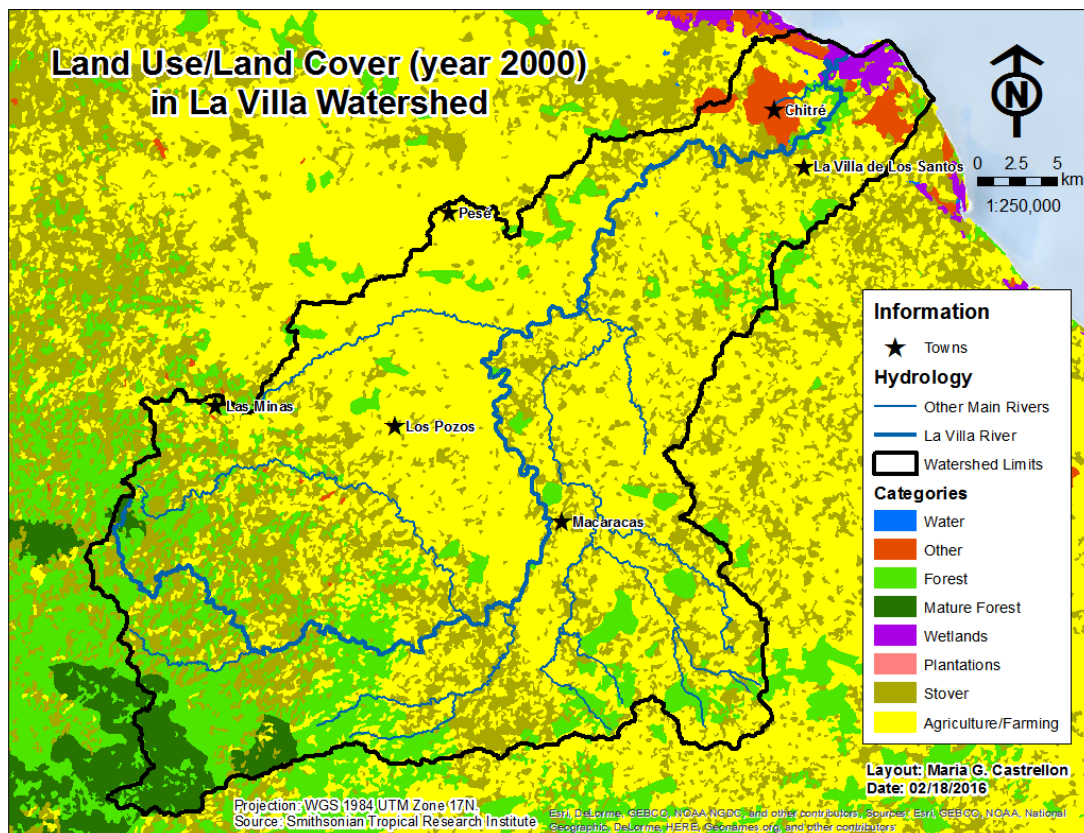


Figure 2.5: Forest cover and land use distribution in La Villa River Watershed in the year 2000.

Thanks to the creation, in 2009, of the National Committee Against Drought and Desertification (CONALSED) by ANAM, the deforestation rates have reduced and there has actually been an increase in forest cover in some areas of the country (Souifer, 2010). Unfortunately, as the forest cover map from the year 2012 (Figure 2.6) reveals, this trend has not impacted the Azuero region due to the large amount of land still dedicated to agriculture in the area (ANAM, N.D.; Souifer, 2010). Therefore, the land use/land cover map of La Villa Watershed in 2012 looks very similar as the map from 2000.

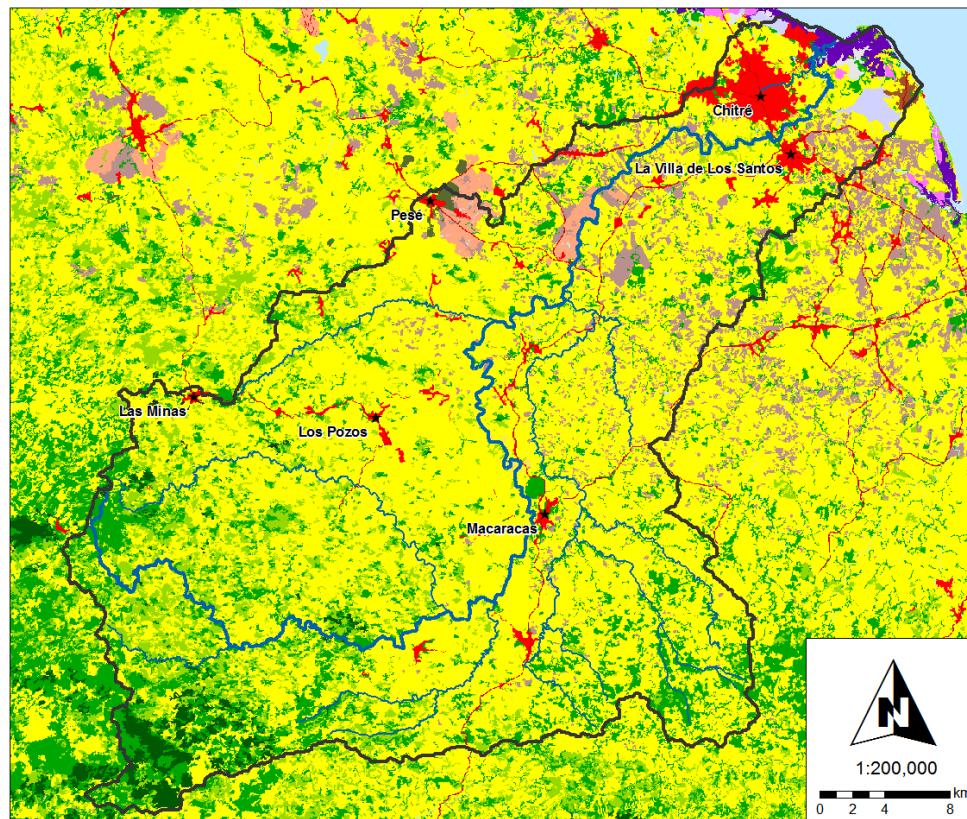


Figure 2.6: Forest cover and land use map published by ANAM in 2012
 (<http://miambiente.gob.pa/mapa2012/>)

This map includes a more detailed description of the urbanized or developed land, shown in red, as well as more specific characterization of the crops planted with pink being sugar cane and the greyish purple being corn. Same as before, the marine wetlands are shown in purple, the yellow represents pasture/farming land, and the green is forest. Notice that the extent of mature forest (dark green) reduced from 2000 to 2012, but this characterization has to do more with an improvement in remote sensing technologies than actual changes.

3. Materials and Methods

3.1 Acquisition of Well Data

The first step in the development of this project was to gather all the data available regarding the number and location of wells in the La Villa Watershed. Dr. Gonzalo Pulido, the project supervisor from IDAAN Panama, provided a database of wells in the provinces of Herrera and Los Santos compiled by ANAM. The file contained information of wells drilled by government institutions (IDAAN, MIDA and MINSA) as well as privately owned wells. However, after mapping the location of these wells (Figure 3.1), it became obvious that this database is probably incomplete because the density of wells is much higher in the province of Herrera than in Los Santos. Also personnel from IDAAN, MIDA and MINSA agree that around 30% of wells drilled for water production are not reported (ANAM, 2013). Logically, the next step would have been to go to each institution in charge of drilling wells and ask for their individual databases, however due to internal bureaucracy, this process is very complicated. Since IDAAN is one of the institutions supporting this Thesis, I had access to their archives and was able to collect additional information of the wells drilled in the watershed. After putting the two files together, the final database contained 205 wells (Appendix A, Figure A7).

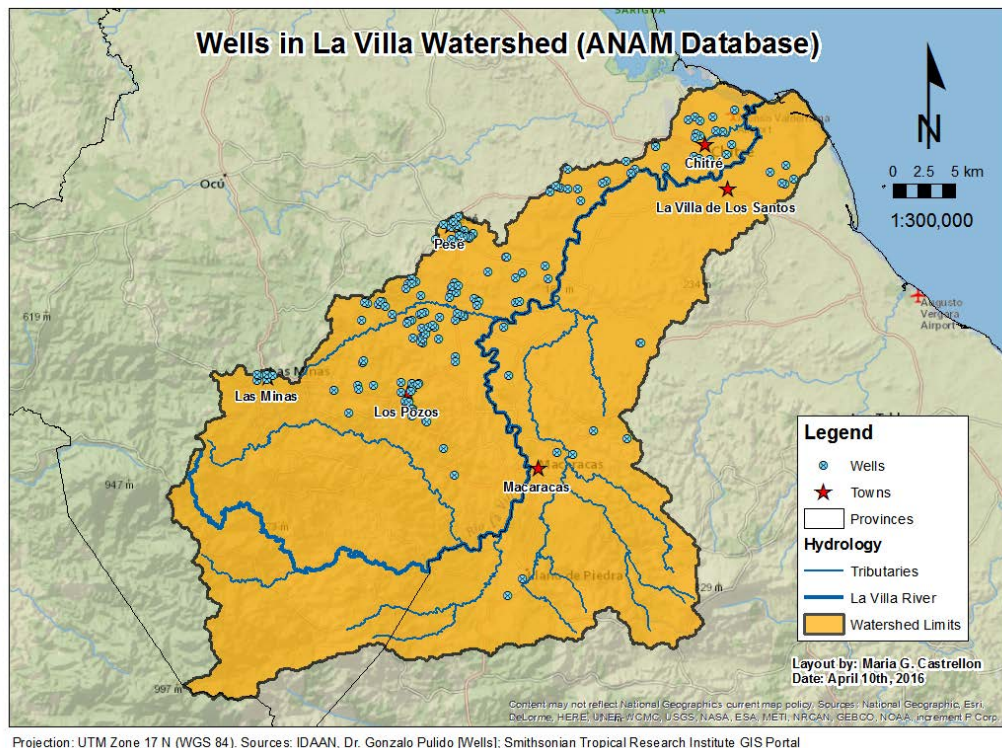


Figure 3.1: Location of the 169 wells in La Villa Watershed according to the ANAM database.

3.2 Selection of Monitoring Wells

The latest groundwater report published by ANAM (2013) suggested the need to build piezometers in the Dry Arc Region to monitor the levels of groundwater on a monthly basis. They proposed the placement of 2-inch diameter piezometers and 10 to 20 m in depth distributed spatially so there is one piezometer per 100 km². Given the size of the watershed in this study (1,284 km²) using 12 to 13 piezometers would be ideal.

An alternative to the installation of new piezometers is to use inactive or abandoned wells as monitoring points. In Panama, wells are drilled in a disorganized manner with little to no previous geophysical exploration. In the case of IDAAN, many of the wells they drill are in low permeability units, thus they are not productive enough. As a result there are many wells in the watershed that have never been equipped and connected to the distribution network. These inactive wells of IDAAN were considered as the perfect candidates to become monitoring wells.

Within the combined database of 205 wells, the inactive IDAAN wells were identified and a pre-selection of monitoring wells was made taking into account parameters such as depth (deeper wells were preferred), geology (attempted to have wells in each geological formation), and location in the watershed. Since IDAAN only drills wells in towns with more than 1500 inhabitants, some wells drilled by other entities had to be selected in order to achieve a homogeneous distribution of monitoring wells in the watershed. This preliminary selection contained about 25 wells.

The final selection of monitoring wells was made after traveling around the watershed visiting the locations of the pre-selected wells. Trying to locate the pre-selected wells in the watershed would have been an impossible task without the help of the local geologist Mr. Edgardo Vergara. Some of the wells that appeared on the list could not be located, in most cases due to the fact that the information recorded was wrong. However, with the help of Mr. Vergara, the wells were located and their geographic coordinates taken, and more inactive wells were added to the original list to reach a total of 39 monitoring wells (Figure 3.2). This final selection of monitoring wells included 2 inactive private wells, 2 abandoned wells drilled by MINSA, 2 intermittent wells from rural communities and 33 inactive wells from IDAAN located inside and near the boundaries of the watershed.

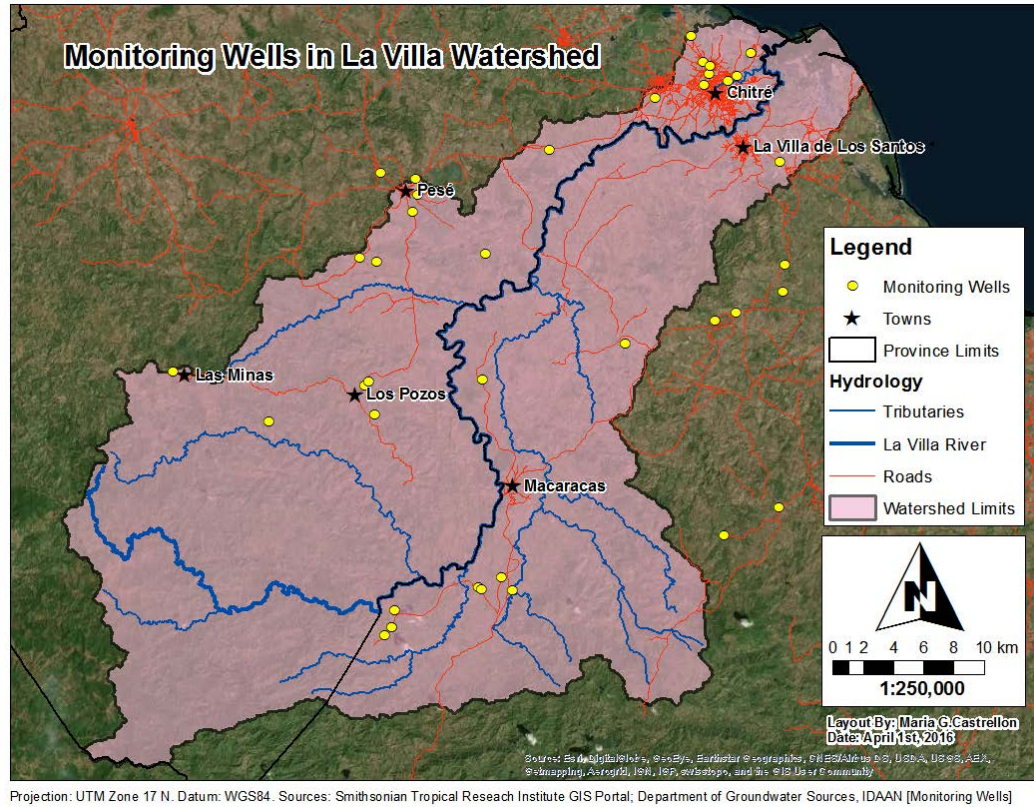


Figure 3.2: Location of the 39 monitoring wells in La Villa Watershed.

3.3 Groundwater Elevation Measurement

ANAM (2013) suggested in their report about the groundwater of the Dry Arc Region that the depth to water in the monitoring wells should be measured twice a month. For this study the depth to water in the selected wells was measured once a month starting in May 2015. In order to do this, two crews of personnel from IDAAN traveled around the watershed for one or two days and manually measured the depth to water in the monitoring wells assigned to their route using a water level sounder. I participated in the first three rounds of groundwater elevation measurements (May, June and July 2015). Starting from August 2015, the number of monitoring wells was reduced to 32 because some wells were connected to the distribution system, and the depth to water could not be measured in the intermittent wells and one of the private wells. Also, by administrative decision, the wells located outside of the southeast corner of the watershed were no longer used as monitoring points. The recorded depth to water values were subtracted from the ground elevation of the well read from Google Earth in order to obtain monthly values of groundwater elevation

in each well. These values were interpolated using the Topo to Raster tool in ArcGIS to create monthly continuous surfaces of water elevation in the watershed.

3.4 Hydraulic Testing and Hydraulic Conductivity Calculations

Hydraulic conductivity (K) is one of the most important parameters in the study of groundwater behavior. Also known as permeability, the hydraulic conductivity is defined as the capacity of fluids to move through a geological material (Sterret, 2007). A parameter related to permeability is the transmissivity (T), which was introduced by Theis (1935) and is defined as the product of the hydraulic conductivity and the thickness of the aquifer, $T = Kb$ (Sterret, 2007). Either of these parameters can be used in the Darcy equation to determine the flow rate of groundwater.

There are several types of hydraulic tests that can be implemented to determine the hydraulic properties of an aquifer, including hydraulic conductivity. The most common types or tests are pumping tests such as constant-head (variable-rate), constant-rate, and step-drawdown tests, which are applied to evaluate the parameters of highly permeable aquifers and large scale production wells (Sterret, 2007). Another type of tests, the slug tests, are used to determine the hydraulic conductivity of sites with relatively low permeability using small diameter piezometers (Fetter, 2001). The main difference between these two types of tests is that pumping tests most accurately represent the characteristics of an aquifer, because the cone of depression extends through larger areas and depths, while a slug tests only can assess the characteristics of the materials immediately surrounding the well.

3.4.1 Slug Tests: Data Collection and Analysis

Slug tests are relatively easier to perform, less expensive and require less logistics than pumping tests. For those reasons, in this study slugs tests were selected as the method to evaluate hydraulic conductivity in the watershed. Slug tests are based on the principle of altering the level of water in a well without using a pump. This is achieved by removing or adding a small volume of water to the well or by completely submerging a solid cylinder into the water to displace the water level (Kruseman and De Ridder, 1994). After the water level has been disturbed, the rate at which it recovers is measured, and then the data is analyzed to obtain the corresponding hydraulic conductivity value (Fetter, 2001).

In La Villa Watershed, 29 out of the 39 monitoring wells were suited for performing of slug tests. Due to the large diameter of these wells (6 to 8 inches), it was determined that the use of a solid rod to displace the water was the best approach. The rod consisted of a PVC pipe 1 m long and 4 inches diameter filled with gravel (Figure 3.3a). The rate of recovery was measured using a Mini-Diver or small size water data logger (Figure 3.3b). In each well at least two slug tests were performed: The first one when the rod was dropped, and after the water had decreased to its static level, the second one was performed by quickly extracting the rod from the well (see Figure 3.4 for example of data recorded).

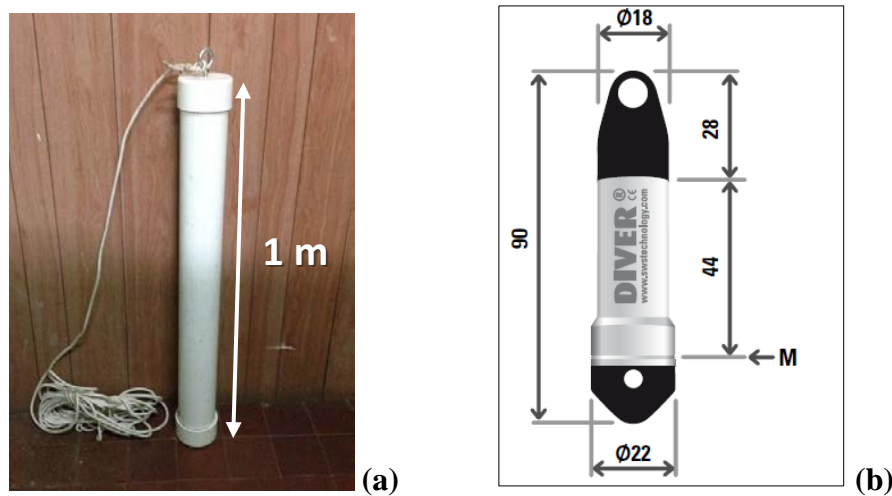


Figure 3.3: (a) Solid cylinder 1 m long and 4 inch diameter used in the slug tests, build with PVC and filled with gravel (photo by Maria G. Castellon). (b) Mini-Diver used to record the displacement every second during the slug test; M refers to the membrane and all the dimensions are in mm (<http://www.novamatrixgm.com/index.php/groundwater-monitoring/groundwater-dataloggers/mini-diver>).

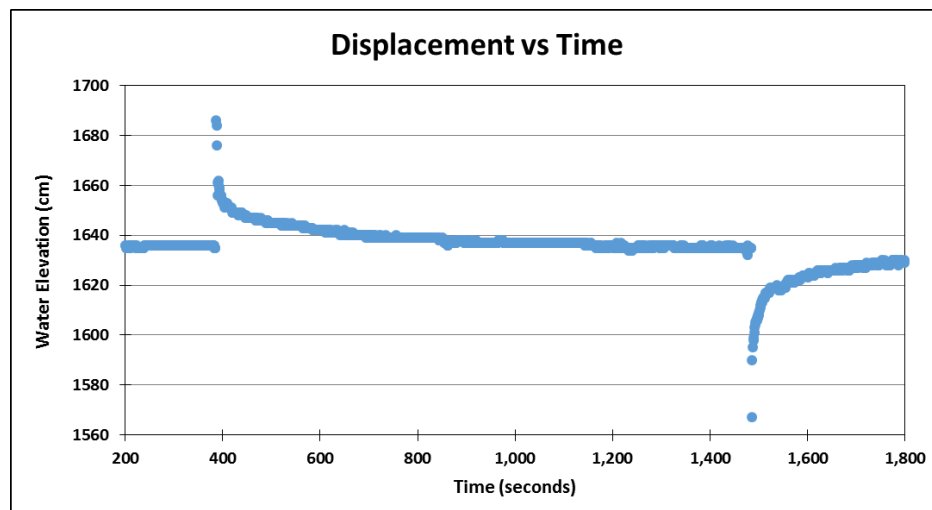


Figure 3.4: Slug Test data from MW-01 recorded with the mini data logger.

The time-drawdown data generated from the slug tests (Figure 3.4) were analyzed using the Hvorslev (1951) method. According to Fetter (2001) this method is implemented by plotting the ratio of displacement to initial displacement (h/h_0) versus time. From this graph, the time at which the well reaches 37% of recovery is used in Equation 4.1 to calculate the hydraulic conductivity:

$$K = \frac{r^2 \ln(L_e/R)}{2L_e t_{37}} \quad (\text{Eq. 4.1})$$

Where,

K is hydraulic conductivity (m/s)

r is the radius of the well casing (m)

R is the radius of the well screen (m)

L_e is the length of the well screen or saturated thickness of the aquifer (m)

t_{37} is the time the water takes to reach 37% of its original level (s)

Overall, more than 29 slug tests were performed because in several wells the test had to be performed two or three times to obtain good quality data. There were two wells in which the data could not be analyzed because the well did not recover to its static level (Appendix A, Figure A9). In some cases the data was difficult to analyze because the well recovered very quickly, and time for 37% recovery could not be accurately detected because displacement was only being recorded each second. For such cases the recovery point was approximated by using the 36% recovery.

3.4.2 Pumping Tests: Data Analysis

For this study no pumping tests were performed due to their difficulty and logistics. Instead, pumping test data was collected from the archives of the Department of Groundwater Sources of IDAAN. Every well drilled by IDAAN requires a performance test to determine its specific capacity. According to Sterret (2007), the specific capacity is the discharge divided by the drawdown at equilibrium and it is useful to determine how productive a well is and which equipment can be used.

The pumping tests performed by IDAAN are single-well tests in which the drawdown and flowrate are monitored from a period of time that goes from 48 to 72 hours. Earlier pumping tests (the ones performed in the early 1990s) only lasted for 24 hours; however, newer pumping tests last for 72 hours. For this study, data from 12 pumping tests

in wells strategically located in the watershed was collected from IDAAN's archives and analyzed using the Theis (1935) method for non-equilibrium flow. This method assumes that water is being pumped at a constant rate; the aquifer is confined, has an infinite extend and is homogeneous and isotropic; the well fully penetrates the aquifer and has infinitesimal radius (Driscoll, 1986; Kruseman and De Ridder, 1994). Theis developed the first formula able to describe the behavior of groundwater flow under unsteady pumping conditions (Eq. 4.2) by implementing an analogy between conduction of heat and groundwater flow:

$$s = \frac{Q}{4\pi T} * W(u) \quad (\text{Eq. 4.2})$$

Where,

s is the drawdown measures at a distance r away from the pumping well (m)

Q is the constant pumping rate (m^3/s)

T is the transmissivity or $K*b$ (m^2/s)

$W(u)$ is the well function represented by (Eq. 4.3) and (Eq. 4.4)

$$W(u) = \int_u^\infty \frac{e^{-y}}{y} dy = \left[-0.5772 - \ln u + u - \frac{u^2}{2 * 2!} + \frac{u^3}{3 * 3!} - \frac{u^4}{4 * 4!} + \dots \right] \quad (\text{Eq. 4.3})$$

$$u = \frac{r^2 S}{4Tt} \quad (\text{Eq. 4.4})$$

Where,

r is the distance away from the pumping well where drawdown is measured (m)

S is the storage coefficient (unitless)

T is the transmissivity or $K*b$ (m^2/s)

t is the time since the start of the pumping test (s)

The traditional approach for the use of Theis non-equilibrium formula is to plot the Theis type curve and the time-drawdown in separate pieces of logarithmic paper. The data points are then fitted to the curve and the values of transmissivity and storage coefficient are calculated using (Eq. 4.2) and (Eq. 4.4) (Driscoll, 1986). In this project the time-drawdown data was fitted to the Theis type curves using Excel spreadsheets designed by Dr. Gonzalo Pulido (Figure 3.5); and also using the Theis solution for confined aquifers in AQTESOLV Demo, an aquifer data analysis software designed by HydroSOLVE, Inc. (Figure 3.6).

Since IDAAN performs single-well tests in order to calculate their specific capacity, the data recorded does not always comply with the assumptions of the Theis (1935) method. For instance, the wells tested have significant radius (3 to 4 inches), the fractured rock aquifer is rarely homogeneous or isotropic, and the tests were not performed at a constant pumping rate. This poses a problem when trying to fit the data to the type curve and consequently it makes the calculation of the average hydraulic conductivity more difficult. For the cases in which pumping rate varied, an average rate was used for the analysis using the Excel spreadsheets. AQTESOLV Demo has the ability to calculate the combined effect of different pumping rates in the type curve, therefore no average calculation was required. In the Excel spreadsheet the fit to the curve was done semi-manually while in AQTESOLV Demo an automatic estimation was implemented for fitting later data points and a manual fit was estimated for fitting early data points. A table with the results from this analysis is included in the next section.

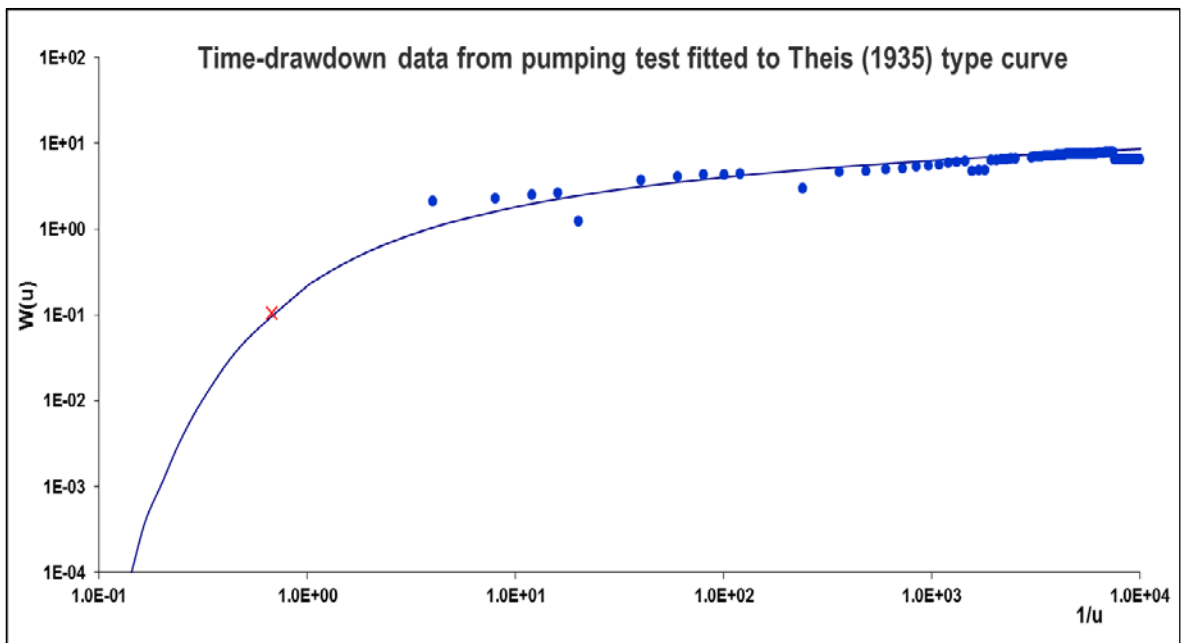


Figure 3.5: Pumping test data from MW-29 semi-manually fitted to a Theis type curve using Excel. The result of this analysis yielded a transmissivity of $178.61 \text{ m}^2/\text{day}$.

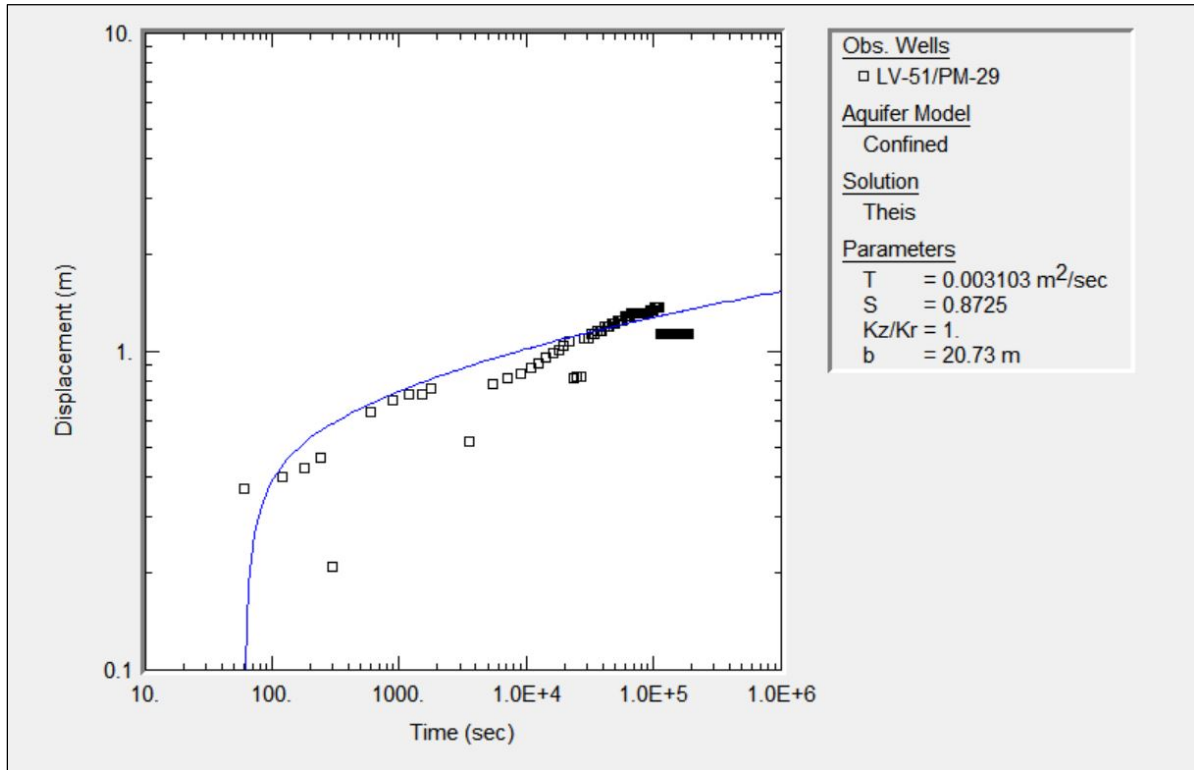


Figure 3.6: Pumping test data from MW-29 fitted to a Theis type curve using AQTESOLV Demo. The transmissivity calculated using this method is $268.10 \text{ m}^2/\text{day}$. This image is a screenshot from the displacement data interface of the aforementioned software. Only 11 out of the 12 pumping tests data sets collected could be analyzed.

The result from the well labeled as LV-31 (Los Pozos – Vía Macaracas) could not be analyzed because a match between the data points and the type curve could not be achieved. The pumping rate was reported as being reduced over time, however the data points showed the complete opposite behavior (Figure 3.7) thus the data were discarded. In other instances, the pumping rate was reported as constant, however the time-drawdown data behavior is more consistent with an increase in pumping rates, or unconfined aquifer characteristics (Figure 3.8). Therefore, for these cases only early time data were fitted during which it is believed that the rate remained constant. In general the data from the pumping tests was difficult to analyze, not only because of unsteady pumping activity, but also because the time-drawdown data were sometimes inconsistent with the reported pumping rate values.

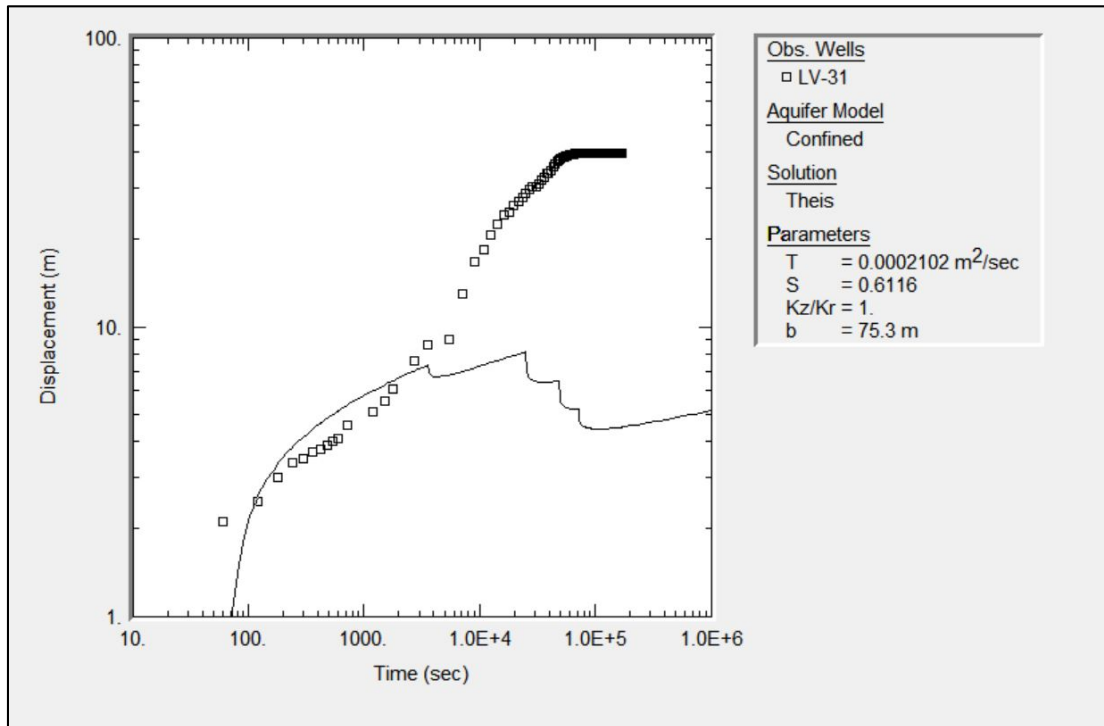


Figure 3.7: Pumping test data from well LV-31 plotted with AQTESOLV Demo. This data set was discarded because a proper fit could not be achieved and the data are in contradiction to the well operation reported by field personnel. This image is a screenshot from the displacement data interface of the aforementioned software.

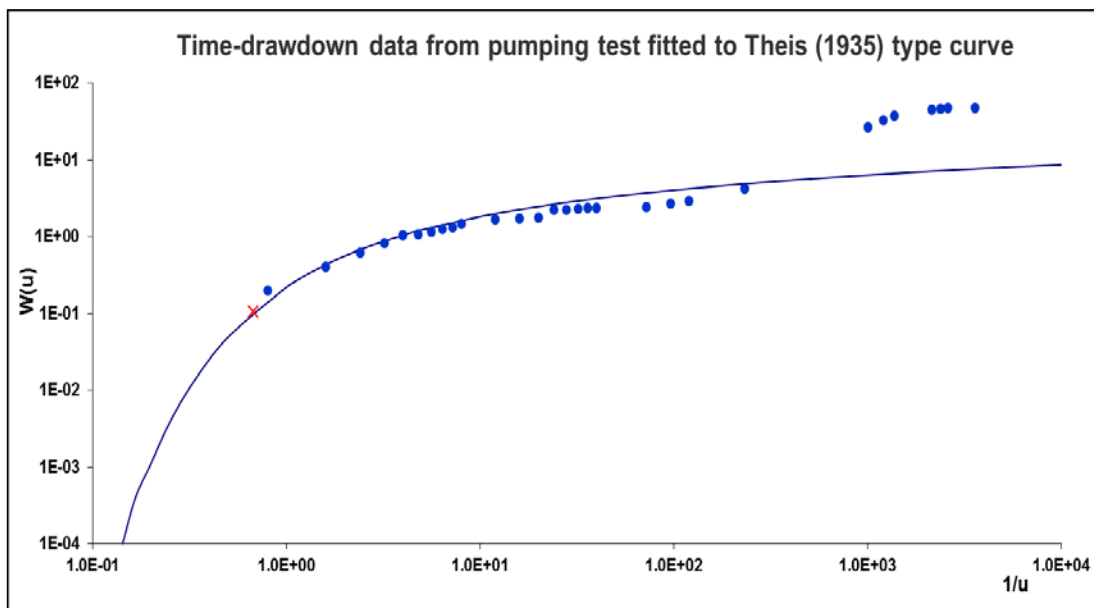


Figure 3.8: Pumping test data from MW-12 plotted using Excel. In this case only early data was fitted to the type curve. It is believed that an increase in discharge occurred afterwards and was not noticed or reported by field personnel.

3.5 Geological Model

A very important aspect in the study of groundwater is understanding the geology and stratigraphy of the study area. In order to expand on the knowledge about the geology of La Villa Watershed, 98 drilling registries (boring logs) from wells located in the watershed were gathered from the archives of the Department of Groundwater Sources of IDAAN. The boring logs consisted of paper copies of the design of well and the type of lithology found when the well was drilled. The well information and the lithology information were manually inputted into a spreadsheet. The older boring logs (from the 1980s and early 1990s) do not have coordinates associated with the well, thus the well had to be located using the provided hand-drawn map and Google Earth. The coordinates were used to map the location of the boring logs around the watershed (Figure 3.9).

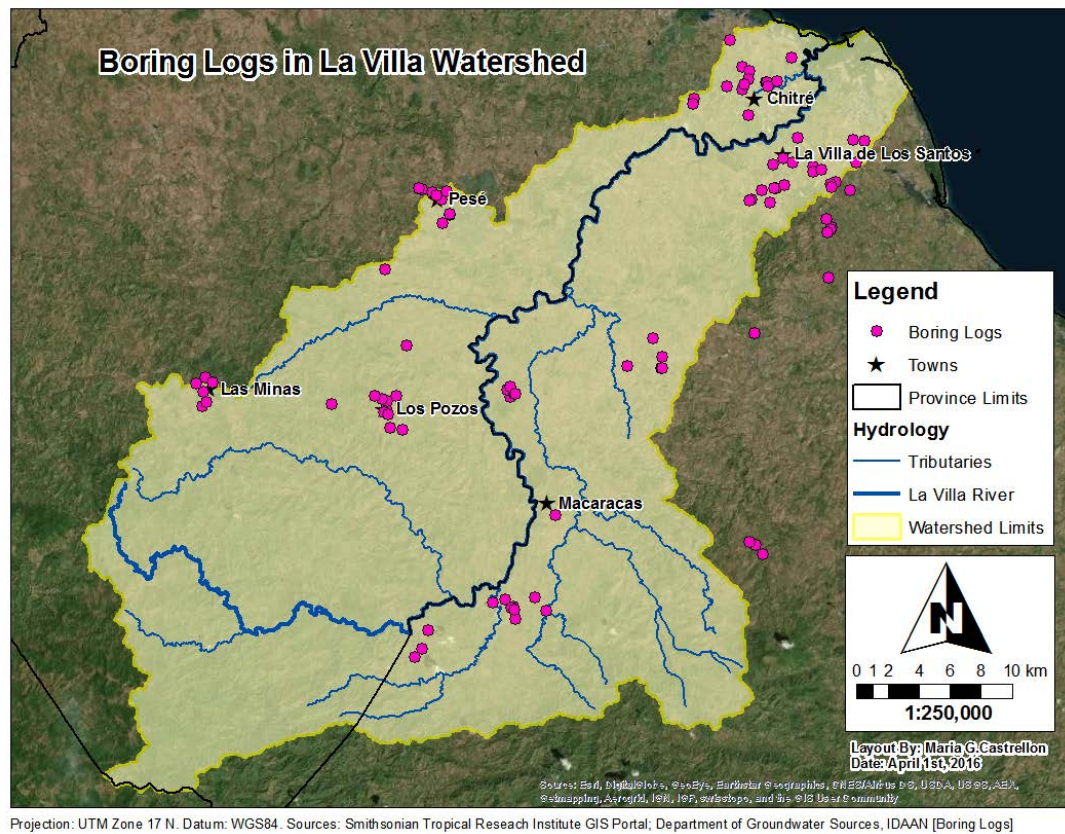


Figure 3.9: Location of boring logs in La Villa Watershed.

Also, with the aid of local geologist Mr. Edgardo Vergara, the information from the boring logs was simplified by classifying the lithological descriptions into 8 main categories: (1) tuff and breccia; (2) andesite and basalt; (3) shale; (4) clay; (5) sand, gravel and conglomerate; (6) sandstone and limestone; (8) metamorphic rocks (hornfels).

Based on the distribution of boring logs in the watershed, 8 different cross-sections (4 from north to south and 4 from west to east) were proposed to analyze the stratigraphy and lithology distribution of the watershed (Figure 3.10). For cross-section A-A' located in the northeastern side of the watershed, a stratigraphic profile was drawn using AutoCAD (Figure 3.11).

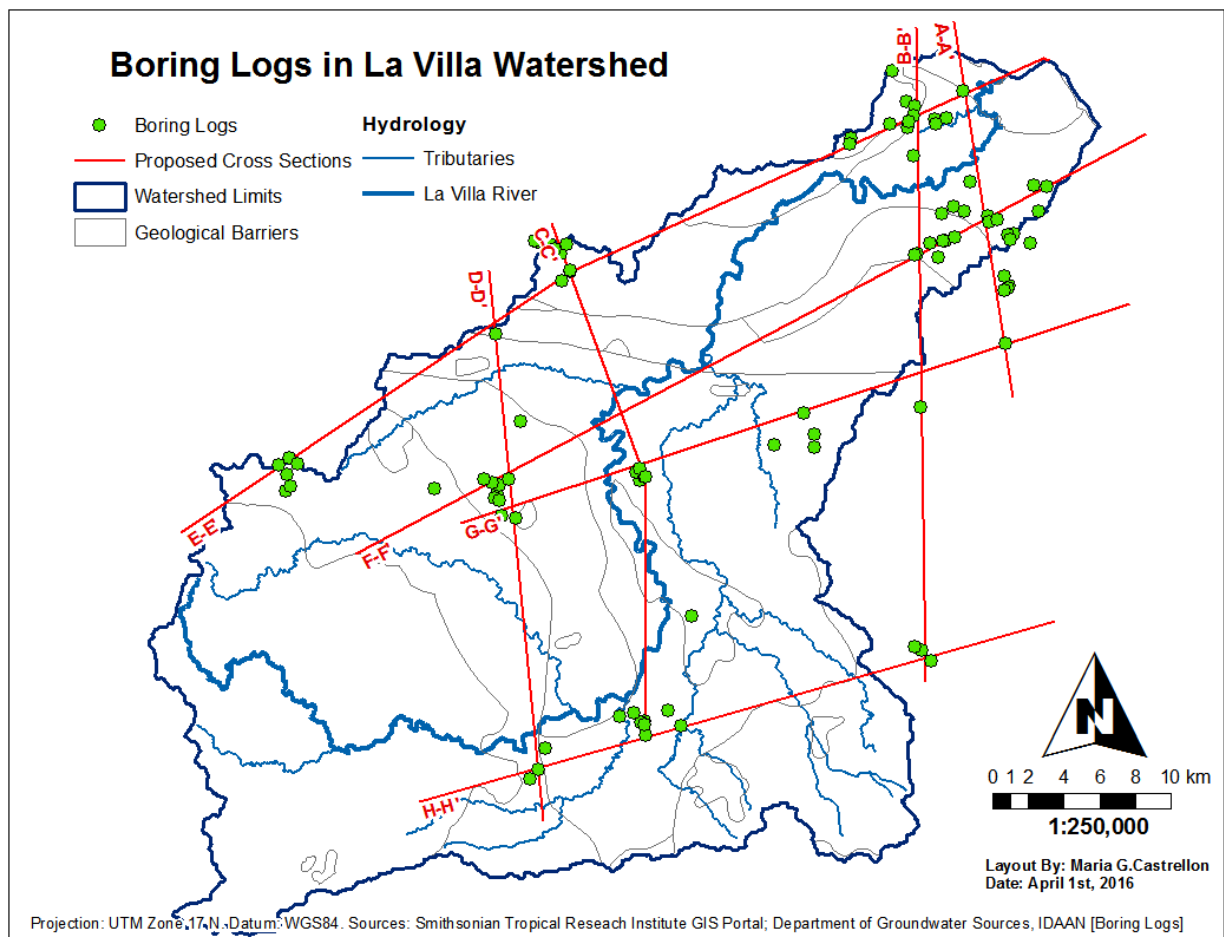


Figure 3.10: Proposed geological cross-sections in La Villa Watershed.

Cross-section A-A' shows a continuous top layer of clay with uniform thickness, an important layer of agglomerate and a significant lens of conglomerate, located in the north of the line located near Chitré. The difficulty in drawing this cross-section arose from the existence of many different stratigraphic layers in the wells that do not seem to connect with one another. Due to the great distance in between the wells, it is very difficult to predict if the layers are continuous or not. Based solely on the information provided by the boring logs, this is the best cross-section that could be drawn semi-manually. Due to the high uncertainty of this drawing, no other manual interpolation was attempted.

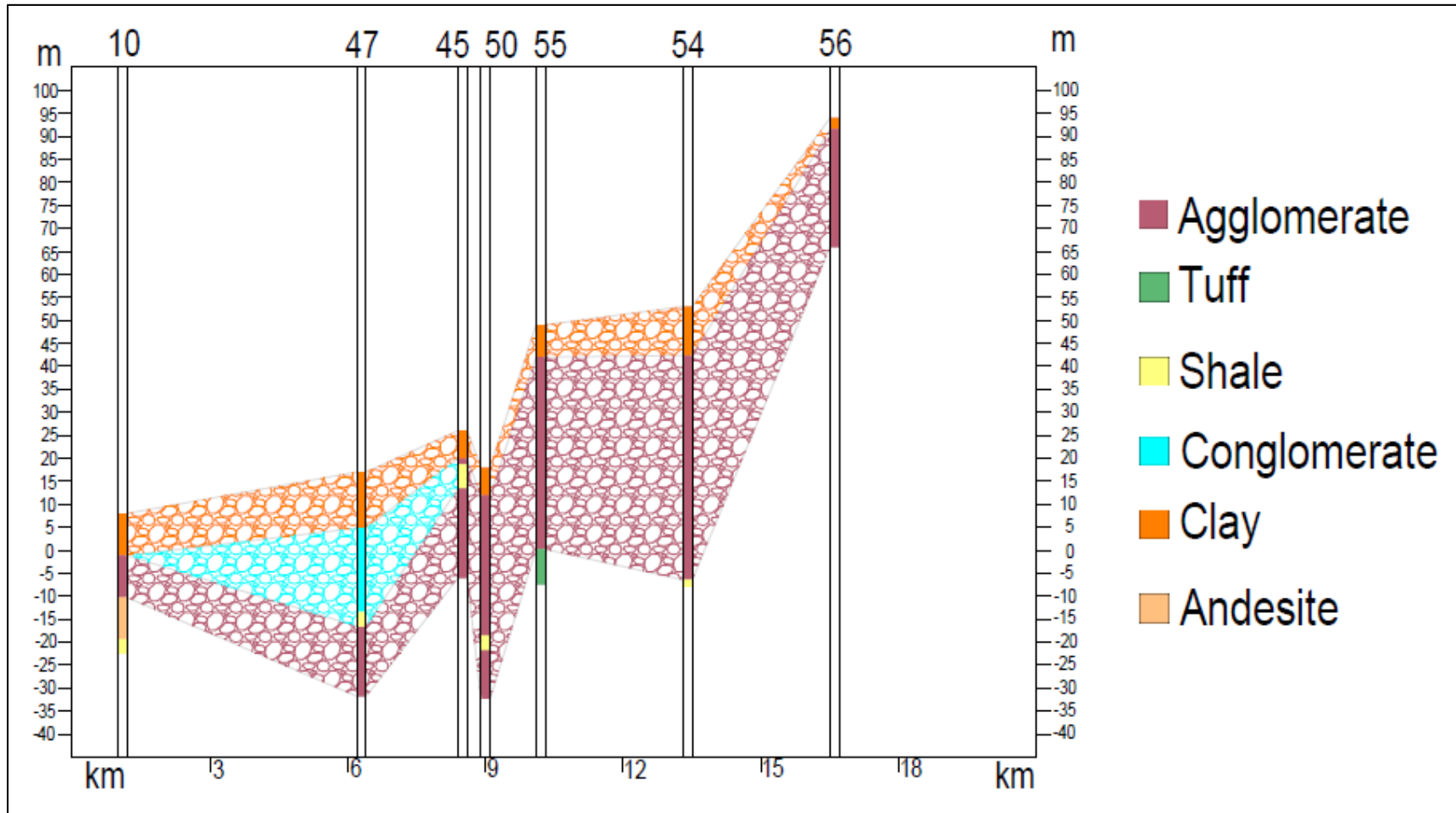


Figure 3.11: Cross-Section A-A' drawn using AutoCAD. The left and right axes are meters above or below main see level; the bottom scale is the distance in km between the wells; the top indicates the identifier of wells used to generate the cross-section (Drawing by Diego Castellon).

Also, with the aid of Dr. Valentina Opolenko from CATHALAC, a more sophisticated geological model of the city of Chitré was attempted. The model was developed using Rockworks 16, a subsurface modeling software developed by RockWare, Inc., and included the information of the 15 boring logs located in the city of Chitré.

A cross-section was drawn passing through Chitré from southwest to northeast (Figure 3.12) and a profile was generated using information from the 3D model. The resulting 2D profile revealed that even in a smaller area, the location and relationship between the different stratigraphic layers is very complex (Figure 3.13). There are clay layers that vary in extent and thickness; there are layers of lava intercalated with shale and tuff; there are some lenses of andesite and sandstone, and the more persistent strata are the agglomerates. This result also shows the immense capabilities of robust modeling software such as Rockworks 16. Ideally, several of these small scale cross-sections should have been drawn in other parts of the watershed.



Figure 3.12: Cross-Section in the city of Chitré, which is 7 km long and is oriented southwest to northeast (Image generated using Rockworks 16 and Google Earth).

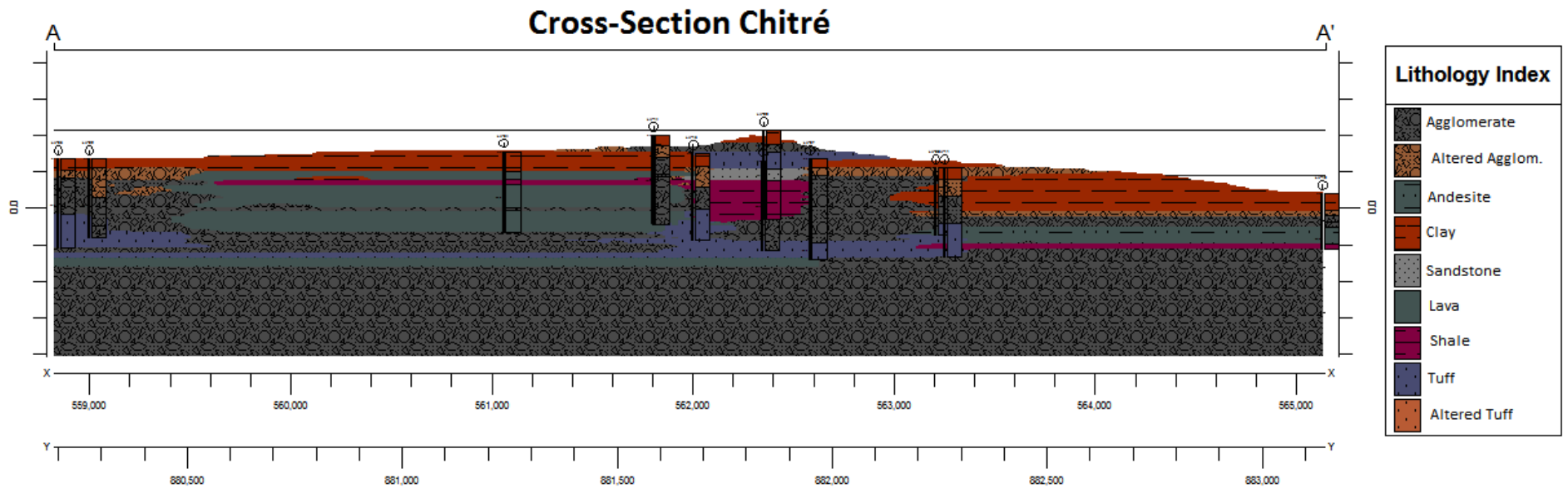


Figure 3.13: Chitré Cross-Section, generated with the aid of Dr. Valentina Opolenko from CATHALAC using Rockworks 16. This geologic profile is roughly 7 km long and includes information from 9 out the 15 boring logs located in the city of Chitré.

4. Results and Discussion

4.1 Groundwater Elevation and Flow Patterns

The groundwater (GW) elevation data measured each month were interpolated to generate continuous surfaces of groundwater elevation across the watershed (Figure 4.1). The map shown, which corresponds to May 2015, indicates that the elevation of groundwater is consistent with the topographic relief of the watershed (Figure 2.1).

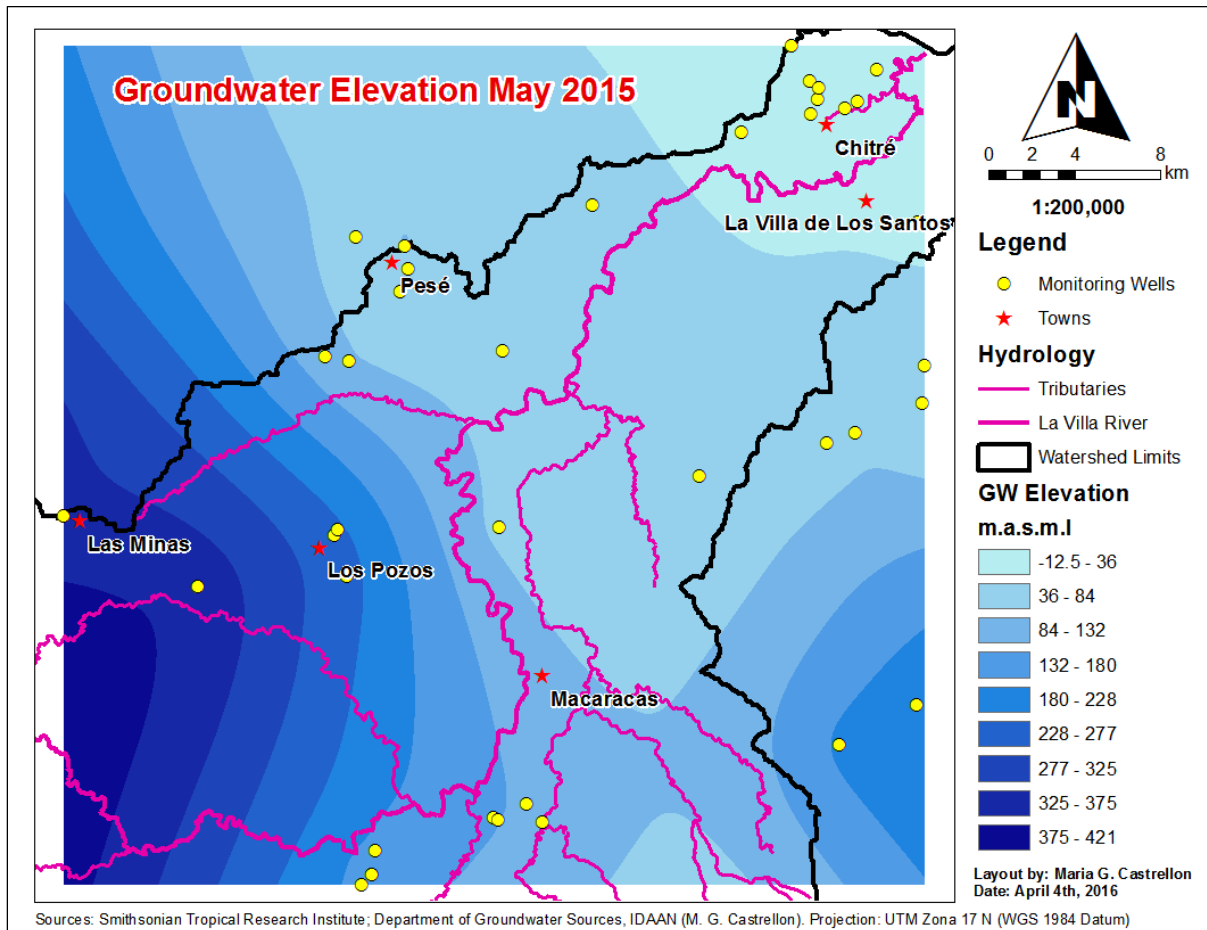


Figure 4.1: Map of groundwater elevation for May 2015.

The June through October groundwater elevation continuous surfaces look very similar to the one shown in Figure 4.1, thus these maps are not shown. Instead, maps with groundwater elevation contours of 10 meters were created based on the aforementioned surfaces (Appendix A, Figures A11 to A16). Flow lines perpendicular to the contours were hand-drawn on two of these maps (May and October) in order to portray the behavior of groundwater flow in the watershed (Figures 4.2a and 4.2b).

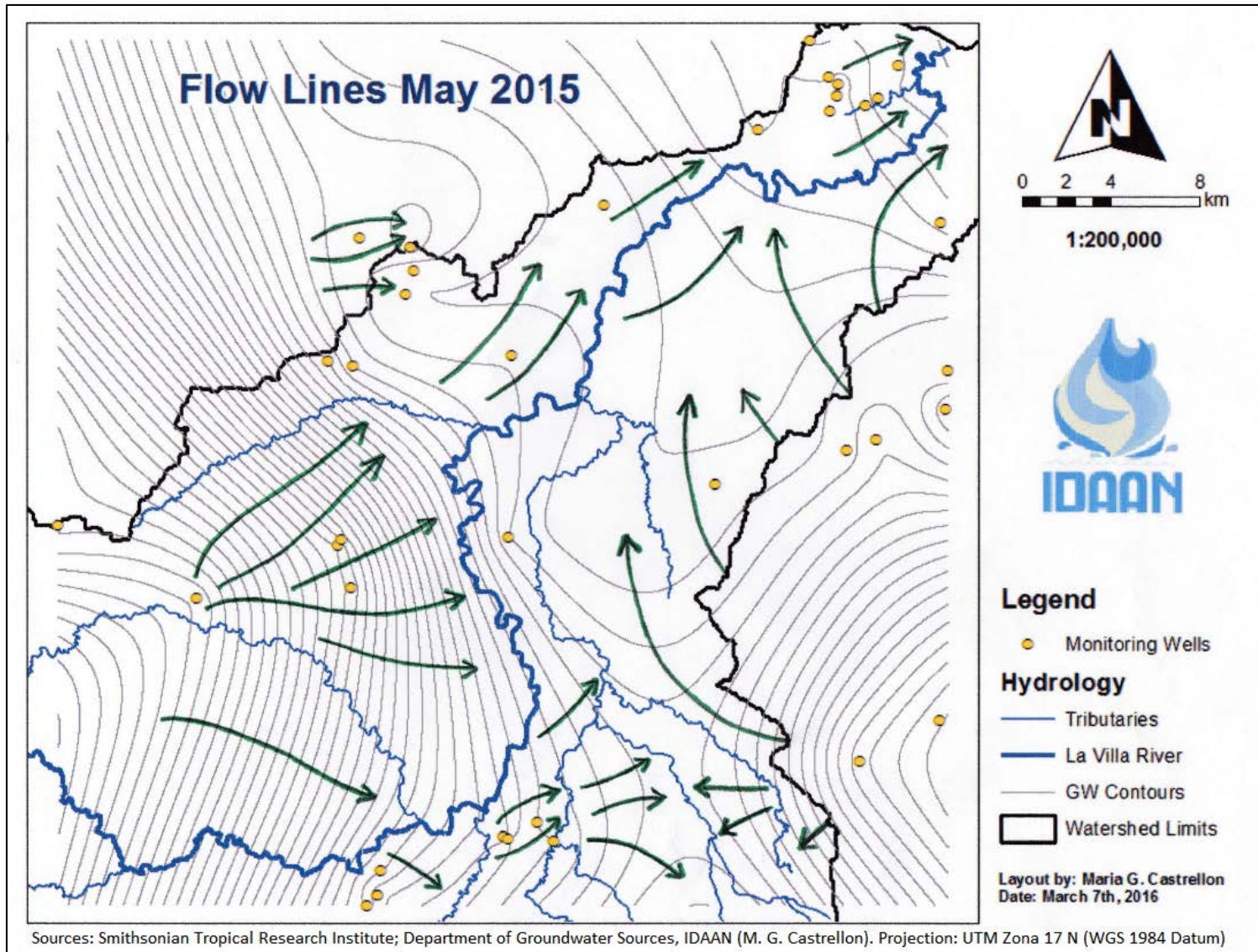


Figure 4.2a: The green arrows show the approximate direction of groundwater flow for May 2015. GW elevation contours are 10 m.

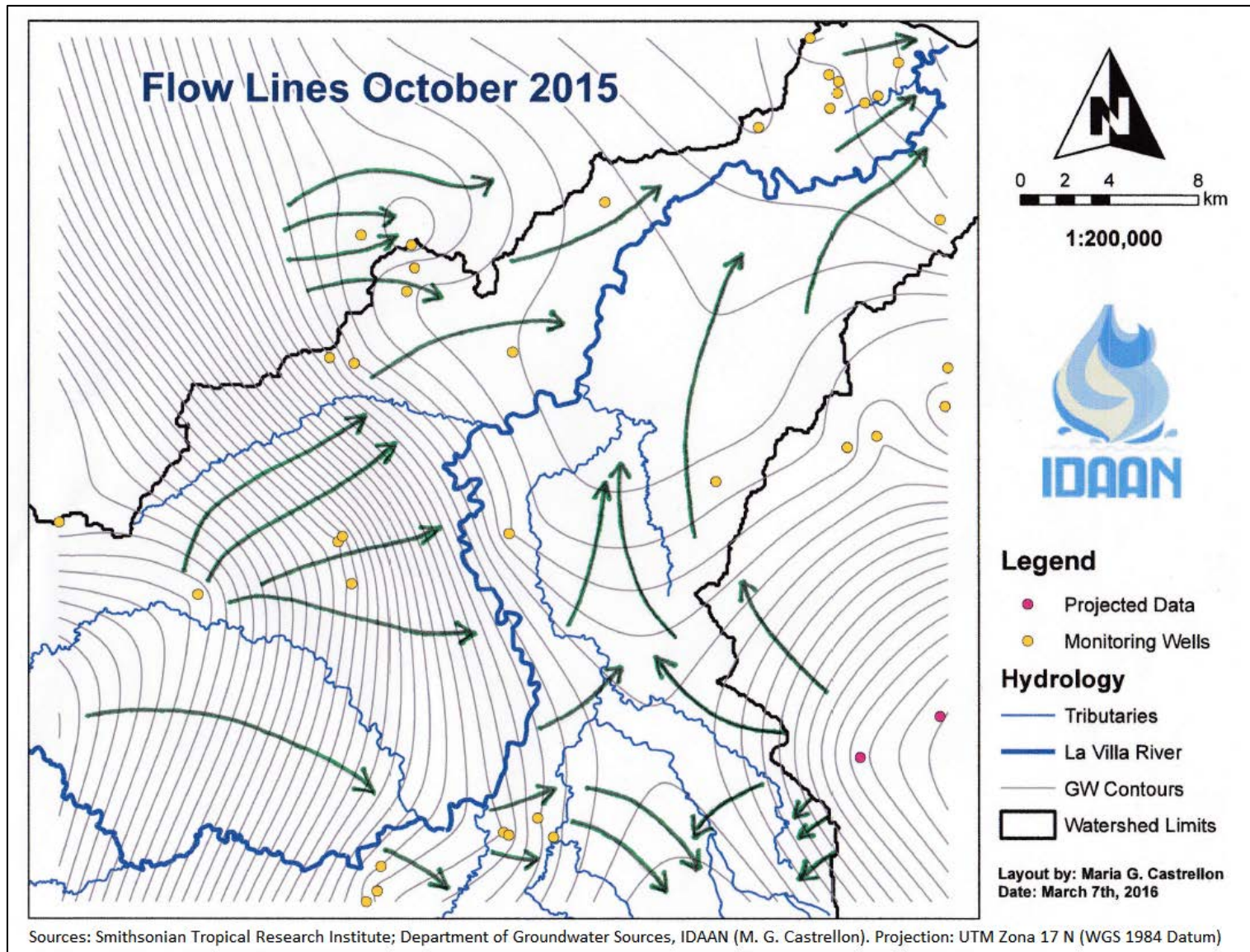


Figure 4.2b: The green arrows show the approximate direction of groundwater flow for October 2015. GW elevation contours are 10 m.

The green arrows shown in the previous figures portray the approximate direction of the groundwater flow. Several flow lines originate in the northwestern part of the watershed, which corresponds to the highlands of the Herrera Province. These lines travel almost perpendicular to the La Villa River and one of its tributaries, which is an indication that the river's baseflow is nurtured by groundwater coming from the highlands. The closeness of the contour lines in this area suggests that water is flowing very fast towards the river.

Once the groundwater reaches the mid portion of the watershed it slows down and starts traveling parallel to the river in direction to the Pacific Ocean. Near the town of Pesé, located close to the north boundary in the mid part of the watershed, there exists a cone of depression, reflected by the fact that several flow lines converge at that point. A closer look to the water elevation contour maps (Appendix A, Figures A11 to A16) suggests that this cone of depression is almost constant throughout the six months of observation. This behavior, in conjunction with the fact that 2015 is an unusually dry year, suggests that the intense pumping activity going on in the area to supply both domestic and industrial demands, could be sustained throughout the year without adverse effects to the GW resources of the area.

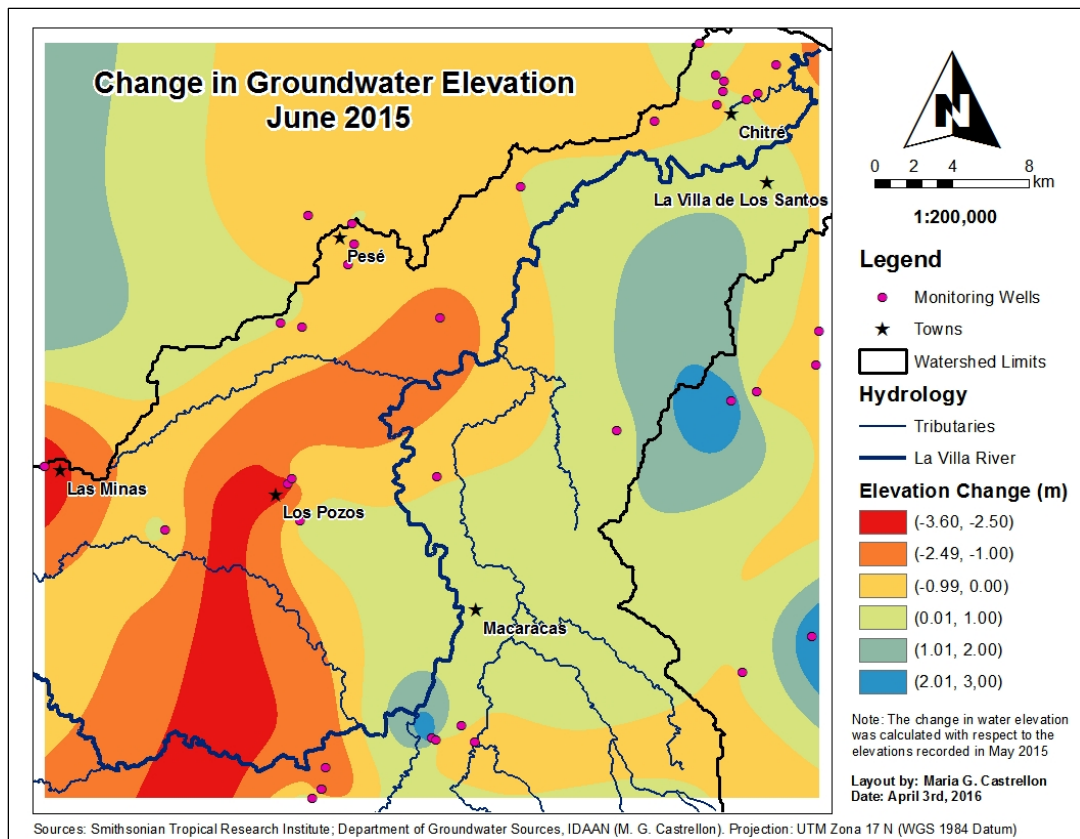
In the southeastern portion of the watershed, which corresponds to the Macaracas Valley, groundwater is generally flowing towards the tributaries of the La Villa River. There is also water coming from the highlands located to the east. This water is entering the higher portion of the watershed in the direction of the tributaries, and is entering the mid-section of the watershed and traveling parallel to the La Villa River towards the ocean. The northeast portion of the watershed near the town of Chitre may have a problem with saline intrusion, especially near the coastline, since groundwater elevations there are below main sea level (Figure 4.1 and maps in Appendix A).

The groundwater behavior described above remains constant throughout the period of observation since the May 2015 flow lines (Figure 4.2a) look very similar to the October 2015 flow lines (Figure 4.2b). Also, the GW elevation contour maps (Appendix A) support this hypothesis, since the general shape of the contours varies only slightly from May to October 2015. This variation in groundwater elevation is discussed in the following section.

4.2 Change in Groundwater Elevation

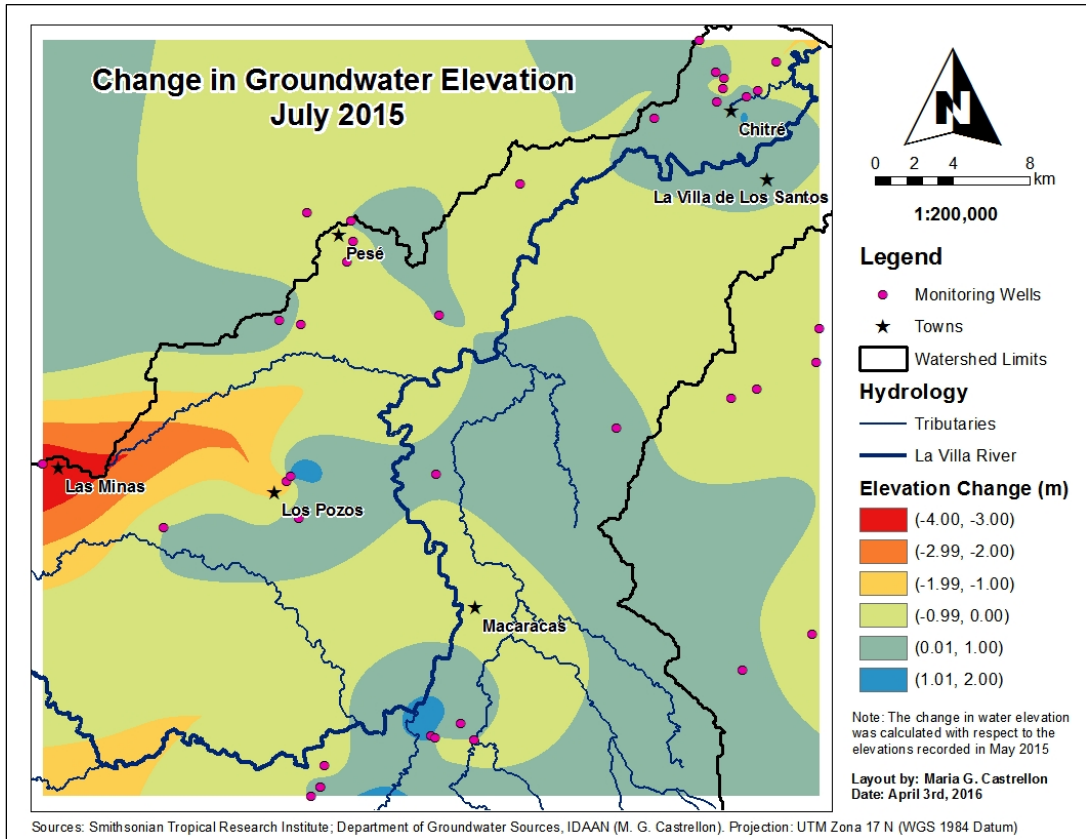
Maps of change in groundwater elevation were generated by comparing the elevations measured each month with the initial elevations measured in May 2015 (Figures 4.3a to 4.3e). The general trend observed in these maps is that the groundwater is receding from June until August, and it starts to rise in September and continuing in October 2015. Although the water is receding overall in the watershed from June to August, there are some spots that show consistent positive change throughout the observation period, with a peak occurring in September.

In September there is a significant increase in groundwater elevation in almost the entire watershed, with a peak (up to 9 meters) in the area southwest of Macaracas. In October the trend continues, with a small reduction of the maximum, but these maximum values cover larger areas. There is also consistent positive change in groundwater elevation in the area around the town of Los Pozos. In October, the groundwater elevation in this area peaks and reaches a value of up to 7 meters. This increase may be because of the recharge coming from the Pesé area in the north (Figure 4.3e).

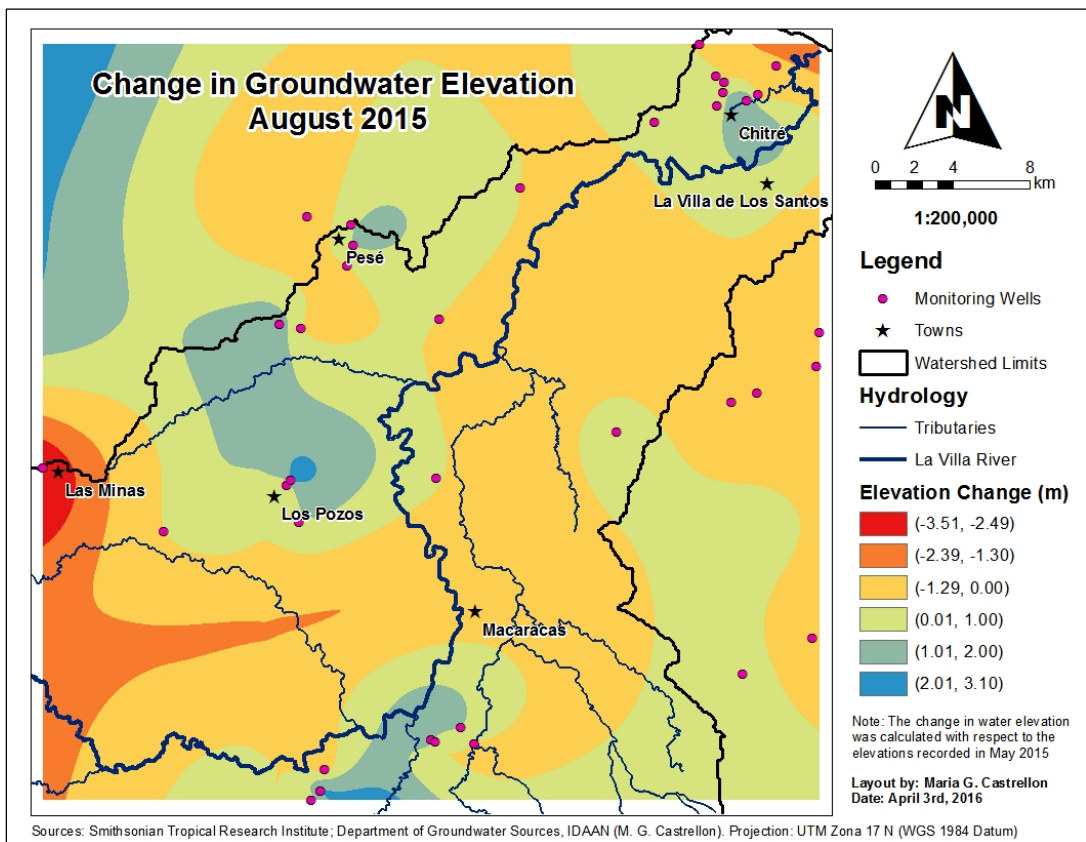


(a)

Figure 4.3: Groundwater elevation change from (a) May to June 2015.

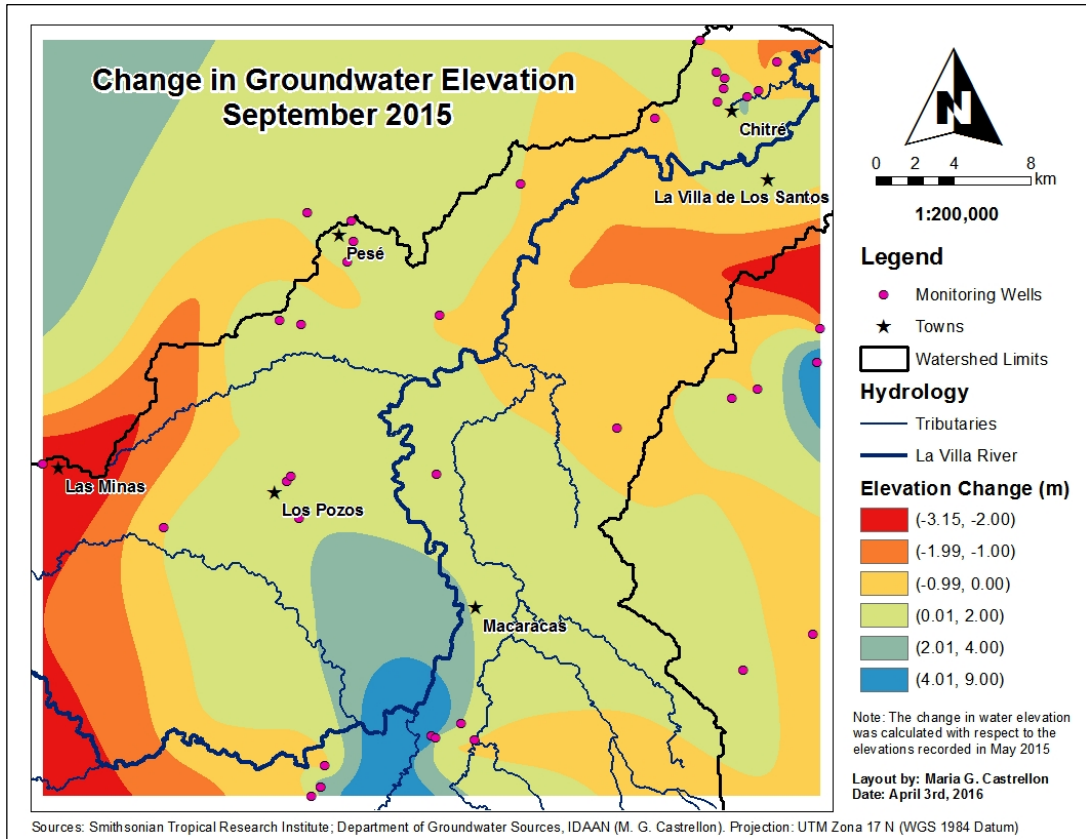


(b)

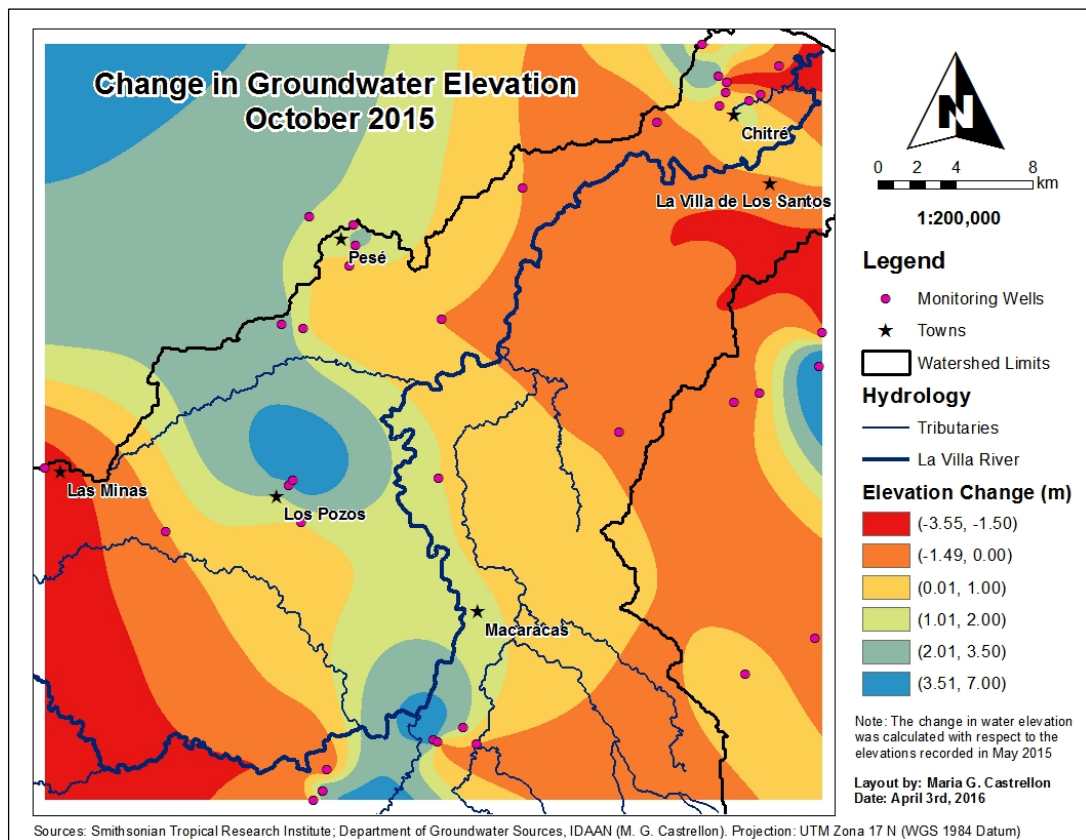


(c)

Figure 4.3: (b) May to July; (c) May to August.



(d)



(e)

Figure 4.3: (d) May to September; (e) May to October.

4.3 Hydraulic Conductivity and Transmissivity

The hydraulic conductivity values calculated from the slug tests (Appendix B, Table B5) were interpolated using the Inverse Distance Weighted method in ArcGIS. The resulting map shows the distribution of the hydraulic conductivity in the watershed (Figure 4.4). Since the slug test only has the ability to survey the upper 5 to 8 meters of the aquifer at most, the map only depicts the shallow subsurface conductivity and/or infiltration capacity of the ground. This map indicates that there are three areas with high infiltration capacity (east of La Villa de Los Santos, southwest of Macaracas and north of Pesé) and moderate hydraulic conductivity near Los Pozos. The fraction of rainfall infiltrating in these areas should be higher than the average for the entire watershed, however, this will depend on the type of soil and the land use of these areas.

The transmissivity values obtained from the analysis of the pumping test data are included in Table 4.1. A map was also created but the values were not interpolated, because of the low number of data points. Instead, the values were classified by color to represent the areas of the watershed with high and low transmissivity, respectively (Figure 4.5). This map represents the deep behavior of the aquifer since the pumping test is able to capture deeper and wider characteristics of the aquifer around the well being tested.

Table 4.1: Average transmissivities (T) and hydraulic conductivities (K) inferred from pumping tests. Depth refers to the total depth of the well and the saturated thickness (L) is the portion of the well without PVC piping.

ID	Label	Depth (m)	L (m)	T (m ² /day)	K (m/day)
LV-20	Calle El Comercio	44.21	25.91	12.88	0.497
LV-21	El Llano	91.46	76.22	0.97	0.013
LV-27	Hacia El Cedro	62.50	44.21	8.70	0.197
LV-29	Cantera	79.27	67.10	14.09	0.210
LV-30	Los Pozos Entrada	91.46	54.88	6.34	0.116
LV-39	Barriada Villa Oriente	79.27	70.12	4.39	0.063
LV-51	Hospital Anita Moreno	42.68	20.73	223.36	10.77
LV-56	La Espigadilla Arriba	24.21	18.29	5.94	0.325
LV-93	Las Lomas #1	76.22	64.02	18.77	0.293
LV-95	Las Lomas #2	44.21	24.39	15.51	0.636
LV-98	Vía El Faldar	129.57	83.84	19.92	0.238

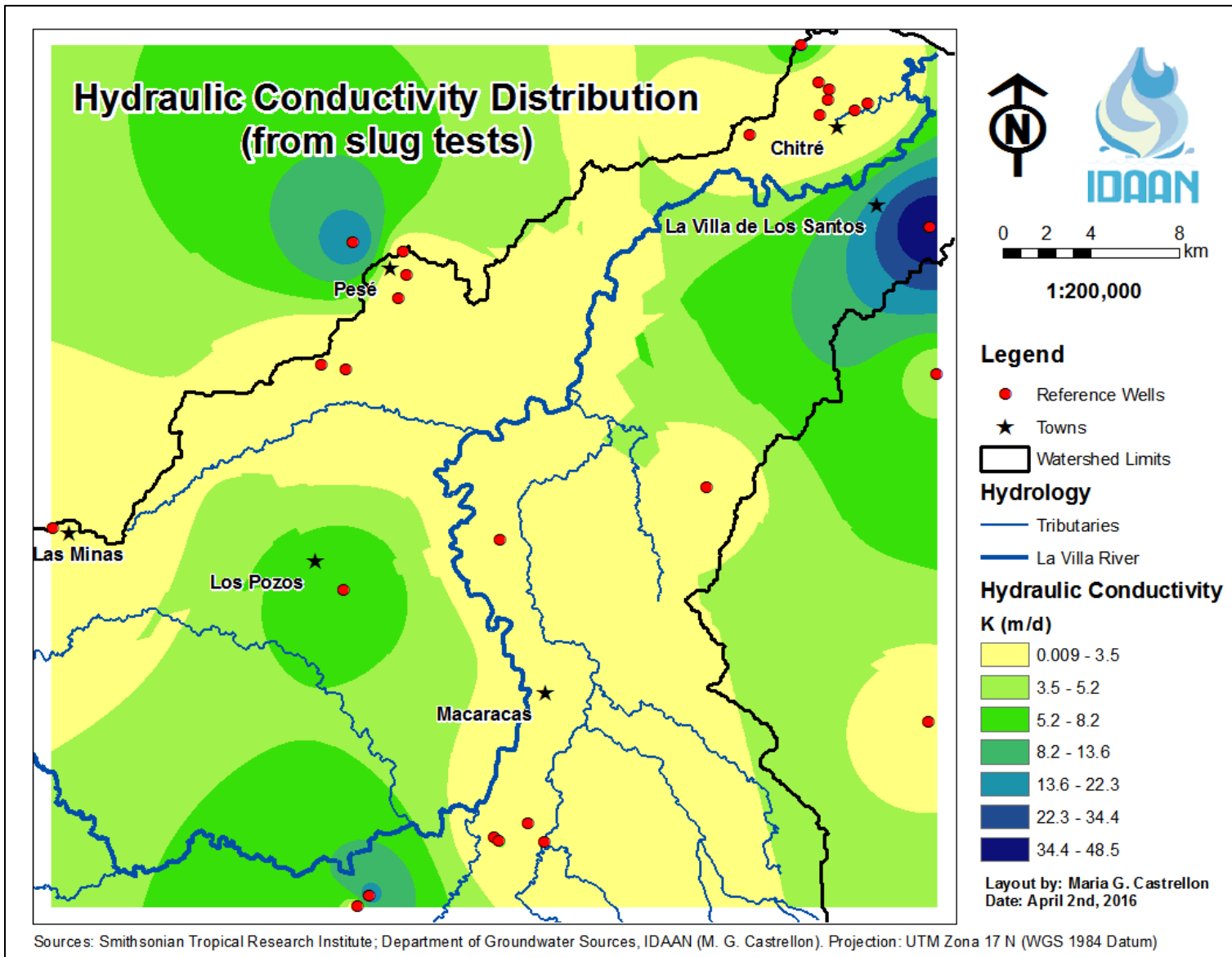


Figure 4.4: Distribution of shallow groundwater conductivity in La Villa Watershed.

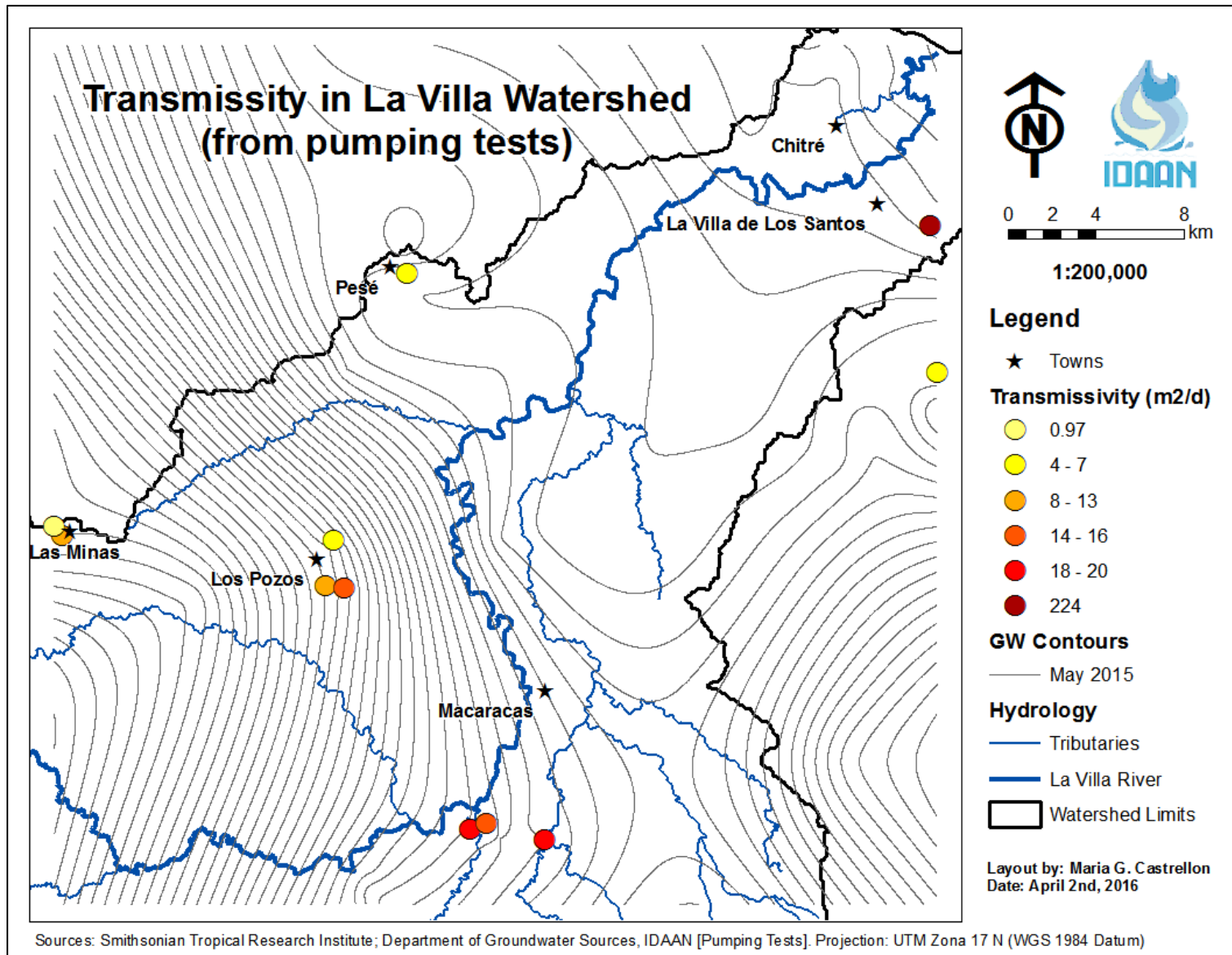


Figure 4.5: Calculated transmissivities at different points of La Villa Watershed. The GW elevation contours are 10 m.

4.4 Precipitation

In La Villa Watershed there are currently five meteorological stations collecting precipitation data. Two of them are located in the town of Macaracas, one is located in the lower part of the Watershed (Los Santos), one is located in the town of Pesé, in the mid portion of the watershed, and one is located in the highlands of the province of Herrera, southwest from the town of Los Pozos (Pan de Azúcar). The data (shown in Table 4.2) indicate that almost no precipitation occurred in the watershed during the dry season, while the higher values were registered in October.

Table 4.2: Total monthly precipitation (in mm) measured during 2015 in different met stations across La Villa Watershed (Department of Hydrometeorology, ETESA).

Label	Jan	Feb	Mar	Apr	May	Jun	Jul	Aug	Sep	Oct	Nov	Dec
Los Santos	2.5	0	0	3.5	37.3	63.8	87	57.2	37.2	171.2	90.8	0
Macaracas	0	0	0	61	29	68.5	157.5	149	204	242.5	51.5	N/D
Pesé	0	0	0	89	83.9	62.2	94.4	37.7	N/D	292.9	160.7	0
Pan de Azúcar	0	0	0	71.7	41.2	89.1	4.7	79.2	N/D	N/D	N/D	N/D
Macaracas (2)	0	0	0	61	29	68.5	125	149	162.5	229	0	0

These monthly values were interpolated using Inverse Distance Weighted in ArcGIS to generate a map of continuous precipitation across the watershed. However, with only five met stations, the resulting surface does not cover the entire watershed. The year 2015 was particularly dry and almost no precipitation was recorded during the dry season (January to March). Precipitation starts in April and continues in May, but it only starts being significant after June 2015 (Figure 4.6a). During July and August 2015, precipitation increases significantly throughout the watershed, especially in the area of Macaracas (Figures 4.6b and 4.6c). The met station located southwest of Los Pozos had no data for September 2015; therefore, the map of cumulative rainfall from April to September (Figure 4.6d) was developed by following the trend of monthly increase in precipitation.

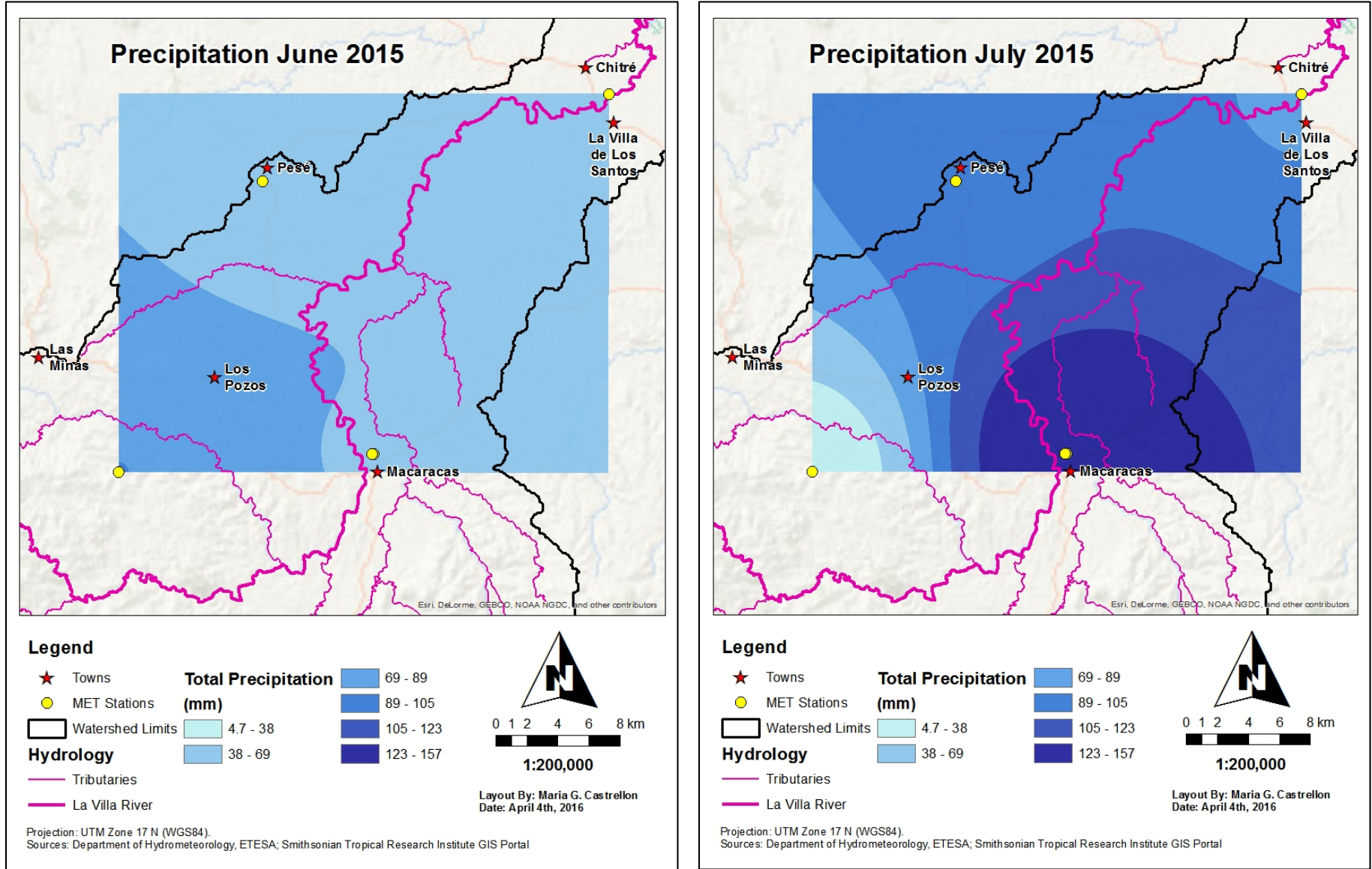


Figure 4.5: Precipitation in La Villa Watershed in June (a) and July (b) 2015 (Department of Hydrometeorology, ETESA).

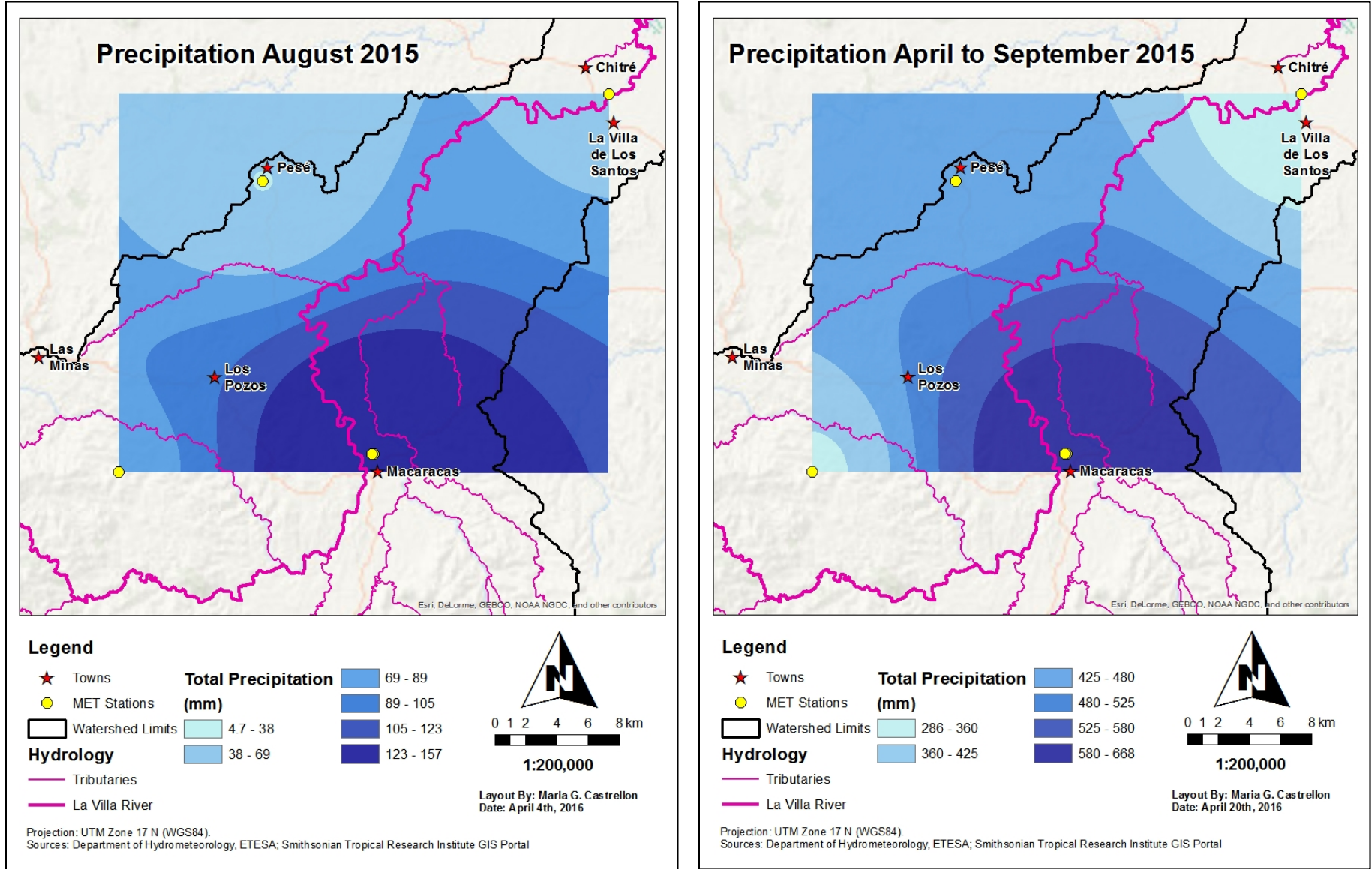


Figure 4.5: Precipitation in La Villa Watershed in August 2015 (c) and from April to September 2015 (d) (Department of Hydrometeorology, ETESA).

4.5 Recharge Areas

A possible research area for La Villa Watershed is the area between the towns of La Mesa de Macaracas and Llano de Piedras, located 7.5 and 11 km southwest of Macaracas, respectively. This area shows a significant increase in groundwater elevation (9 m in September and 7 m in August) that corresponds to an increase in precipitation as suggested by the precipitation maps. Given that the precipitation starts to peak in July and the groundwater elevation peaks in September, the groundwater response time to precipitation was estimated to be two to three months. According to geological characteristics, shallow hydraulic conductivity and slope, this area has adequate characteristics for water to infiltrate and possibly reach the deep aquifers. Boring logs in La Mesa and Llano de Piedras show the existence of layers of sandstone and fractured tuff, sometimes intercalated with layers of sand and gravel, which is a good indicator of recharge in the area. The shallow hydraulic conductivity map (Figure 4.4) indicates that the area around La Mesa has moderate to high infiltration rates (5.3 to 22.3 m/day). This area is located at the foothills of the mountains and presents mild to gentle slopes (Appendix A, Figure A10), which increases the potential for infiltration and recharge.

Another possible recharge area occurs around the town of Los Pozos, where sustained recharge is believed to be occurring. In contrast to the Macaracas Valley, this area shows a recession of groundwater levels in June, with a moderate increase from July to September (2 to 3 m) before peaking in October with an increase in 7 m. Precipitation maps reveal that this area receives less rainfall than the Macaracas Valley from April to September (Figure 4.5d); also the shallow conductivity map indicates that this area has a moderate to low infiltration rate (3.5 to 8.2 m/day), which may be the reason for the delay in response to precipitation events. This area is also characterized by mild to gentle slopes (Appendix A), which increase the potential for infiltration and thus recharge.

A third potential recharge area in the watershed is located around the town of Pesé. According to the shallow hydraulic conductivity map (Figure 4.4) the area towards the northwest of Pesé has high conductivity values (13.6 to 22.3 m/day). The groundwater elevation near Pesé is receding during June and stays almost constant or with minimum positive change (1 to 2 m) during the rest of the observation period. The maps from August and October reveal that part of the recharge of Los Pozos is coming from the Pesé area in the north, but the fact that this effect is not seen until October indicates that the areas near Pesé respond more slowly to precipitation and recharge occurring in the area. This delayed

effect is partly because directly to the south of Pesé the hydraulic conductivity is really low, thus it takes longer for the water to move in this region. In the area of Macaracas, the change in groundwater elevation responds faster to rainfall, partly because the precipitation was higher and partly because the shallow hydraulic conductivity in this area is much higher. A closer look at the transmissivity values obtained from analyzing pumping test data indicates that the Macaracas valley has higher transmissivities (14 to 20 m²/day) while Pesé and Los Pozos have lower transmissivities (4 to 13 m²/day). This supports the hypothesis that faster recharge is occurring in the southeastern part of the watershed and slower recharge is occurring in the Pesé-Los Pozos corridor.

In the province of Los Santos groundwater is entering the system from the southeastern boundary, which indicates that there may exist a source of groundwater recharge outside the delineated hydrological watershed. However, not enough data have been collected in that location, thus the existence of a recharge area cannot be ascertained.

4.6 Hydrological Analysis

In order to investigate the origin of the groundwater elevation increase, a water balance calculation was attempted. Given the size of the watershed, the water balance was performed only in the areas where recharge is believed to be occurring. For the town of Macaracas precipitation (P) data and evapotranspiration (ET) data (Table 4.3) were compiled and analyzed for the time period from April to September 2015.

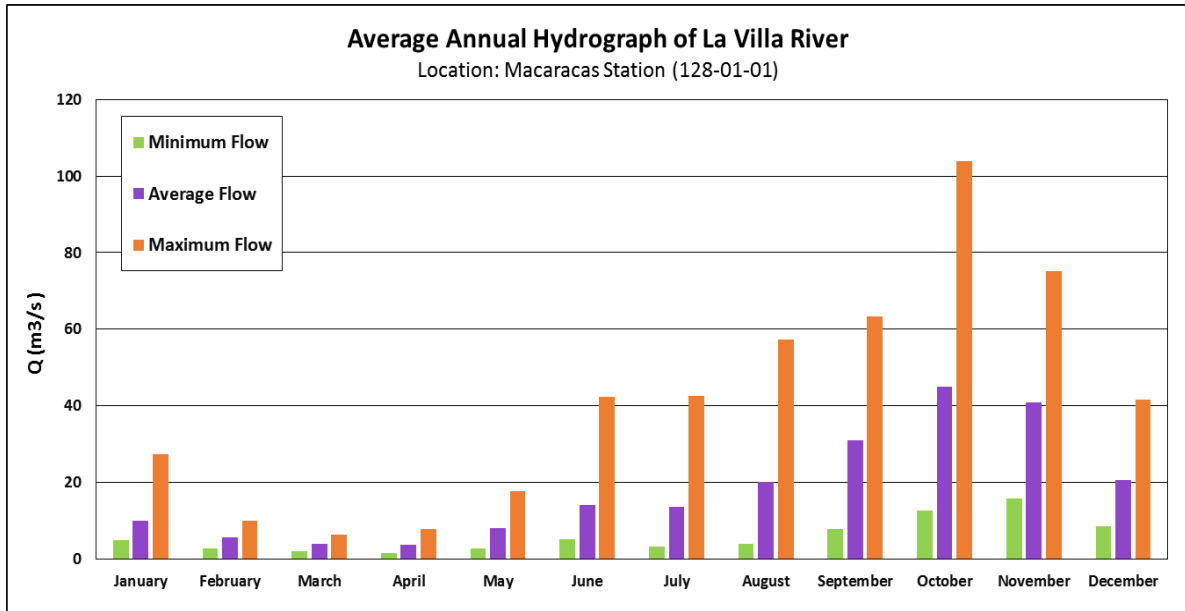
Table 4.3: Total monthly potential evapotranspiration (PET) and precipitation (P) measured during 2015 at the Macaracas#2 met station (Department of Hydrometeorology, ETESA).

	April	May	June	July	August	September	Total
PET (mm)	809.10	408.60	224.20	252.50	236.20	131.80	2062.40
P (mm)	61	29	68.5	125	149	162.5	595

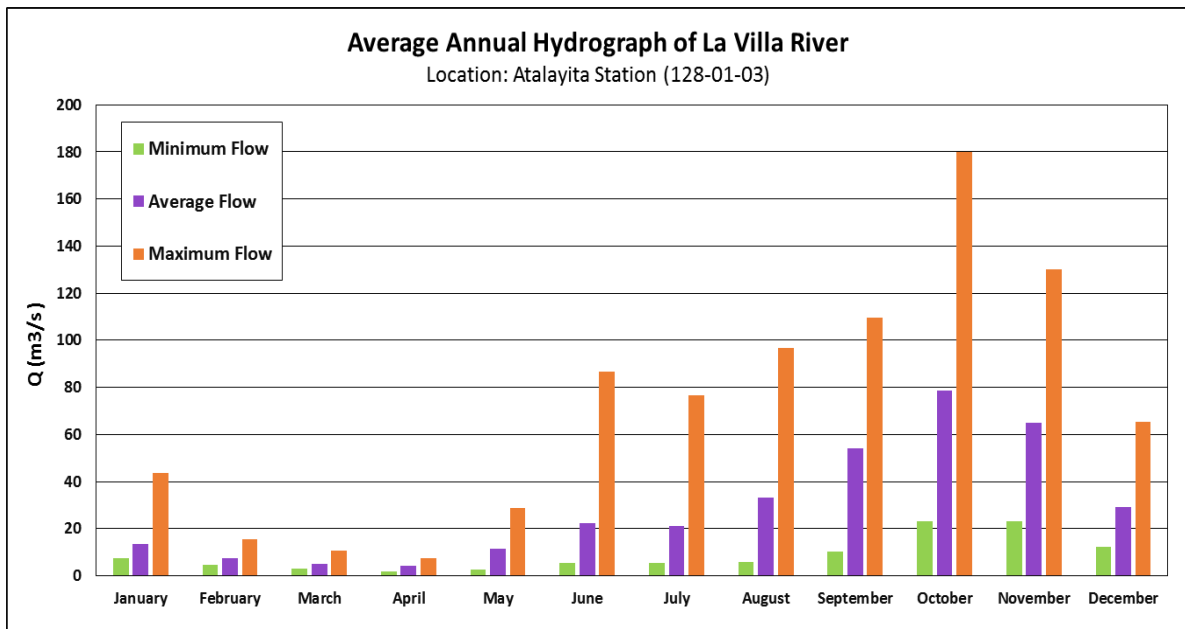
The total PET registered (2062.40 mm) is much higher than the total precipitation (595 mm). The change in groundwater elevation maps (Figure 4.3) show that water levels around Macaracas have increased up to 2 m during the observation period. The average groundwater level increase in a 0.94 km² square around the town of Macaracas, from May to October 2015, was 1.24 m or 1240 mm (see Appendix C for calculation details). Assuming a porosity value of 40%, the actual increase of groundwater elevation corresponds to 0.496 m or 496 mm. Given this value, it is believed that precipitation is the driving force behind the change in storage of groundwater locally. However, other factors

such as runoff, local groundwater flow and actual ET are required to complete a water balance for this area.

The groundwater and runoff contributions to the La Villa River were estimated by comparing the average annual hydrograph measured at the Macaracas station (Figure 4.6a) with the hydrograph measured at the Atalayita station, 30 km downstream along the La Villa River (Figure 4.6b).



(a)



(b)

Figure 4.6: Average annual hydrograph measured at the Macaracas station (a) and at the Atalayita station (b) based upon 50 years of data (Department of Hydrometeorology, ETESA).

Subtracting these two hydrographs resulted in the amount of water gained by the river in between the two stations, which corresponds to an annual average volume of $3.33\text{E}+08 \text{ m}^3$ (Appendix C). A net runoff hydrograph (Figure 4.7) was created by performing a baseflow separation consisting of subtracting the lowest flow value, which occurs in April and corresponds to $0.54 \text{ m}^3/\text{s}$, from the difference hydrograph. The area under this net runoff hydrograph is calculated by integration and is $3.16\text{E}+08 \text{ m}^3$ (Appendix C) and corresponds to the volume of water that reached the river as runoff. Therefore, the amount of groundwater flowing towards the river in the 30 km reach between Macaracas and Atalayita is the difference of $1.70\text{E}+07 \text{ m}^3$ (Appendix C).

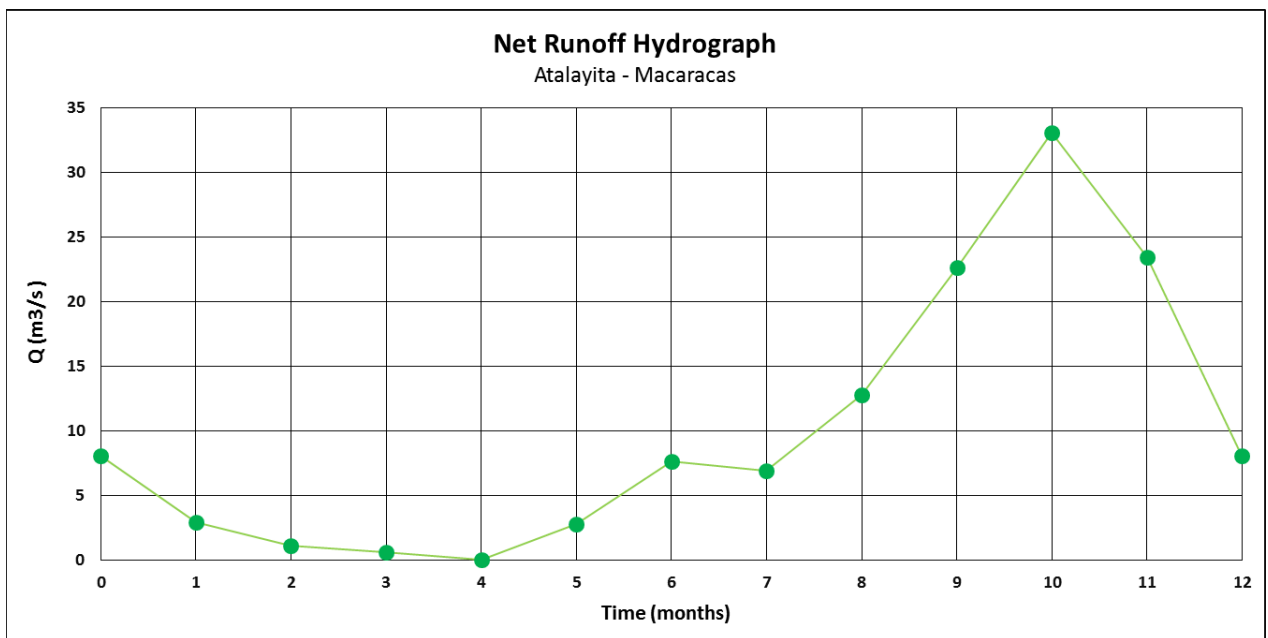


Figure 4.7: Average amount of runoff intercepted by La Villa River from Macaracas to Atalayita.

The groundwater flow lines (Figure 4.2) indicate that the groundwater intercepted by the La Villa River in the 30 km reach from Macaracas to Atalayita is mainly coming from the highlands of the province of Herrera. Using the transmissivities from the slug test and the pumping tests this groundwater flux was estimated to be in the range of $244,949 \text{ m}^3/\text{day}$ and $5,651 \text{ m}^3/\text{day}$, respectively (Appendix C). The actual amount received by the river should be between these two values since the groundwater contribution is through both shallow and deeper parts of the aquifer. The groundwater entering the river along the 30 km reach of the river was calculated as $45,479 \text{ m}^3/\text{day}$ according to the hydrograph analysis (Appendix C), which is well within the range of flow from the highlands.

A water balance was attempted for the town of Los Pozos using the runoff values previously calculated. Since this town does not have an active meteorological station, no evapotranspiration data was available and the precipitation had to be calculated using the interpolated maps. A square of 1.57 km² was drawn around the town of Los Pozos and the average cumulative precipitation within that polygon from April to September 2015 was 489 mm. The average change in groundwater elevation from May to October 2015 within the Los Pozos polygon was 1842 mm (Appendix C). Again the groundwater increase is greater than the rainfall in this area, which leads to the conclusion that this excess in groundwater is coming from the highlands of the province of Herrera. Using shallow hydraulic conductivity, this groundwater flow was estimated as 9,631 m³/day. Thus, the groundwater that entered the square surrounding the town of Los Pozos during the study period was 1100 mm (Appendix C). The area that contributes runoff to 30 km reach of the La Villa River from Macaracas to Atalayita was estimated to be 225.74 km², thus the average amount of runoff reaching the river each year is 1399.83 mm. During the observation period it is estimated that 700 mm of runoff were generated and reached the river. Based on these values, a water balance for the town of Los Pozos was performed to estimate the losses due to evapotranspiration using a budget equation for shallow layers (Eq. 4.1) and a budget equation for the deeper parts of the aquifer (Eq. 4.2):

$$P - DP - ET - R = 0 \quad (\text{Eq. 4.1})$$

$$DP + Q_{gw,local} = \Delta H_{gw} \times \eta \quad (\text{Eq. 4.2})$$

$$DP = \Delta H_{gw} \times \eta - Q_{gw,local} = (1842 \text{ mm})(0.4) - 1100 \text{ mm} = -363 \text{ mm}$$

$$ET = P - DP - R = (489 + 363 - 700) \text{ mm} = 152 \text{ mm}$$

The deep percolation (DP) was calculated from equation 4.2 as -363 mm, assuming a porosity of 40%. Using equation 4.1 the evapotranspiration (ET) was calculated as 152 mm over the observation period. Varying the porosity from 20% to 45% causes the DP to vary from -732 mm to -271 mm, respectively. The negative sign for deep percolation signifies that the deeper strata are actually replenishing the shallow aquifer in an upward fashion. This is primarily due to the significant sub-regional groundwater flow entering the Los Pozos area from the west ($Q_{gw,local}$). Consequently, the ET value calculated varies from 521 mm to 60 mm, respectively.

The difference between the highest and lowest groundwater levels occurring in October and June, respectively, for most of the watershed, provides an indication for the total volumes of groundwater that may be available for extraction. These values were calculated as $4.66\text{E}+05 \text{ m}^3$ for Macaracas and $1.16\text{E}+06 \text{ m}^3$ for Los Pozos (Appendix C). However, since the source of groundwater for these areas is uncertain, it cannot be concluded that extraction of this amount of groundwater can be sustained.

5. Conclusions

5.1 Summary

The work presented in this Thesis is the first of its kind in Panama. It provides the information necessary to better understand the behavior of groundwater in the La Villa Watershed. The groundwater in the watershed is traveling from the highlands of Herrera to the La Villa River, and from the valley of Pesé the water starts traveling parallel to the river in the direction of the Pacific Ocean. In the province of Los Santos, groundwater is entering the watershed from the southeastern border and then travels parallel to the river in the direction of the Pacific Ocean. In the valley of Macaracas, groundwater is traveling from south to north, from west to east, and from east to west and is intercepted by the tributaries of La Villa River.

The watershed has at least three main recharge areas located in Pesé, Los Pozos and in between Llano de Piedras and La Mesa, southwest of Macaracas, respectively. Each of these areas responds differently to changes in precipitation depending on the shallow hydraulic conductivity in these areas. North of Pesé there is an area of high hydraulic conductivity, but immediately south of Pesé the conductivity is really low. This slows down the effect that precipitation has on the increase in groundwater levels in the area. In the valley of Macaracas, the recharge is much faster due to the existence of areas with much higher hydraulic conductivity. It is believed that most of this recharge is coming from precipitation inputs. However, local groundwater flow and runoff need to be evaluated in order to verify that the increase in groundwater levels is not the product of recharge coming from the highlands as the flowline maps are suggesting.

The groundwater level near the town of Los Pozos remained almost constant during the observation period, and with a moderate shallow hydraulic conductivity, these results are not surprising. At the beginning of this project it was believed that the shallow aquifers in the Los Pozos area were slowly being replenished solely by precipitation. However, after

performing water balance calculations it became clear that the local groundwater flow coming from the highlands is significant, and in fact, this deeper flow is replenishing the shallow aquifers in the region.

There seems to be recharge areas for the watershed outside of the limits of the study area, namely the highland of the district of Las Minas in Herrera and the highlands of the Guararé district in the province of Los Santos, southwest of the border of the watershed. The fact that groundwater is entering the watershed from outside the delineated hydrographic watershed indicates that the La Villa groundwater basin extends beyond the La Villa watershed.

5.2 Recommendations

Although there seems to be plenty of groundwater in the watershed, especially for a very dry year, it is still unclear whether continuous pumping at maximum discharge rates is suitable. Less water should be extracted during the dry months where the groundwater levels are receding. The extraction rates could be gradually increased starting from July or August, when the groundwater levels start rising again in response to precipitation. The lack of water in the dry months could be supplied by excess water being pumped during the rainy season. In order to generate a more accurate pumping strategy for the watershed, monitoring of groundwater levels should continue and a clear pattern in the change of groundwater levels needs to be identified.

One of the main environmental problems in La Villa Watershed is the high percentage of pasture land dedicated to cattle farming. According to Hassler et al. (2011) the topsoil infiltration rates for pasture are much lower than for mature forest. It has also been proven by Ogden et al. (2013) that tropical forested watersheds present higher baseflow during the dry season than adjacent watersheds with mainly pasture. Therefore, reforestation of the recharge areas of the watershed will not only increase infiltration rates to the shallow aquifers, but also increase groundwater flow towards the river.

5.3 Further Research

Following the methodology developed by this project, a similar study should be conducted in watersheds adjacent to the La Villa Watershed, namely the Río Parita Watershed and the Guararé sub-basin. Such a study could reveal the interconnection between the groundwater flow lines of the individual watershed and will be the beginning for the delineation of a greater groundwater basin. However, in order to complete this task,

more information has to be collected to figure out what is happening with groundwater in the highlands in the provinces of Herrera and Los Santos.

Also, a complete geological model of the basin needs to be developed in order to understand the geometry of the aquifers of the region. An important aspect in the delineation of a groundwater basin is the identification of hydrological boundaries. This can only be achieved by understanding the complex geology and the relation between the different stratigraphic layers in the regions and establishing the different hydrogeological units of the region.

Once the groundwater flow in the greater La Villa Watershed is better understood, and the hydrogeological units have been identified, a hydrogeological mathematical model of the watershed could be developed. This model will provide quantitative information that will serve to describe, analyze and better understand the groundwater flow in the watershed, as well as more accurately estimate the amount of groundwater that is available for extraction, thus providing operational management strategies. This mathematical model should be accompanied by a more accurate and complete water balance of the watershed in order to understand the inputs and outputs of the system.

6. References

- ANAM, MIDA, IDIAP, ETESA and Instituto Geográfico Nacional Tommy Guardia. *Atlas De Las Tierras Secas Y Degradadas De Panamá*. N.d.
- ANAM. *Plan Nacional De Gestión Integrada De Recursos Hídricos De La República De Panamá 2010-2030*. Rep. Panamá: Autoridad Nacional Del Ambiente, 2011. Web.
- ANAM. *Las Aguas Subterráneas De La Región Del Arco Seco Y La Importancia De Su Conservación*. Rep. Panamá: Autoridad Nacional Del Ambiente, 2013. Web.
- Aizprúa, Julio César. "La Sequía Causa Estragos En Azuero." *La Prensa*. La Prensa, 3 Feb. 2016. Web. Mar. 2016.
- Caballero, Alberto. *Exploración De Aguas Subterráneas En El Arco Seco De Panamá (sector De Las Tablas) Mediante Métodos Geofísicos*. Thesis. Universidad De Barcelona, 2009. Web.
- Castillo, Jorge, and Ana E. Patiño. *Diagnóstico Y Propuesta De Desarrollo Sostenible Del Arco Seco De Panamá, 2012*. Rep. No. VIP 01-09-00-01-2012-16. Universidad De Panamá, 12 Dec. 2014. Web.
- Chow, Ven Te, David R. Maidment, and Larry W. Mays. *Applied Hydrology*. New York: McGraw-Hill, 1988. Print.
- Coates, Anthony G. "The Forging of Central America." *Central America: A Natural and Cultural History*. New Haven: Yale UP, 1997. 1-37. Print.
- Cortez, Alcibiades. "Los Santos: El Río Estivaná Se Queda Sin Agua." *La Prensa*. La Prensa, 5 Aug. 2015. Web. Mar. 2016.
- "Decreto Ejecutivo 70 De 27 De Julio De 1973." *Justia Panama*. Web. <<http://panama.justia.com/federales/decretos-ejecutivos/70-de-1973-sep-11-1973/gdoc/>>.
- ETESA. "Mapa De Clasificación Climática (según Köppen)." *Department of Hydrometeorology, ETESA*. Web. <<http://www.hidromet.com.pa/mapas.php>>.
- ETESA. "Mapa De Evapotranspiración Potencial (1971-2002)." *Department of Hydrometeorology, ETESA*. N.p., n.d. Web. <<http://www.hidromet.com.pa/mapas.php>>.
- ETESA. "Mapa De Isoyetas Anuales (1971-2002)." *Department of Hydrometeorology, ETESA*. N.p., n.d. Web. <<http://www.hidromet.com.pa/mapas.php>>.

- Driscoll, Fletcher G. "Well Hydraulics." *Groundwater and Wells*. St. Paul, MN: Johnson Division, 1986. 205-67. Print.
- Donovan, Kelly. "UF Study: Isthmus of Panama Formed as Result of Plate Tectonics." University of Florida News. University of Florida, 29 July 2008. Web.
- Fetter, C. W. "Slug Tests". *Applied Hydrogeology*. Upper Saddle River, NJ: Prentice Hall, 2001. 190-205. Print.
- Harmon, Russell S. "Geological Development of Panama." *The Río Chagres, Panama: A Multidisciplinary Profile of a Tropical Watershed*. Vol. 52. Dordrecht, Netherlands: Springer, 2005. 45-62. Water Science and Technology Library.
- Hassler, S. K., B. Zimmermann, M. van Bruegel, J. S. Hall, and H. Elsenbeer, (2011), Recovery of saturated hydraulic conductivity under secondary succession on former pasture in the humid tropics, *For. Ecol. Manage.*, 261, 1634–1642.
- Herring, David. "What Is El Nino? Fact Sheet: Feature Articles." *Earth Observatory*. NASA, 27 Apr. 1999. Web. 4 Feb. 2016.
- Hesh, Wayne et al. Conceptual Model Development for MODFLOW or FEFLOW models. FEFLOW Conference. *Schlumberger Water Services*. 2009. Web.
- Kumar, Arun. "Geology of the Isthmus of Panama, History of the Panama Canal and a Visit to the Barro Colorado Island." *Earth Science India VI (IV)*. Popular Issue (2013): 1-13. Oct. 2013. Web.
- Kruseman, G. P., and N. A. De Ridder. *Analysis and Evaluation of Pumping Test Data*. Wageningen, Netherlands: International Institute for Land Reclamation and Improvement, 1994. SamSam Water. Web. Mar. 2016.
- L'Heureux, Michelle. "What Is the El Niño–Southern Oscillation (ENSO) in a Nutshell?" *Climate.gov*. NOAA, 5 May 2014. Web. 4 Feb. 2016.
- MacDonald, Donald F. "Contributions to Panama Geology". *The Journal of Geology* 45.6 (1937): 655–662. Web.
- Ogden, F. L., T. D. Crouch, R. F. Stallard, and J. S. Hall (2013). Effect of land cover and use on dry season river runoff, runoff efficiency, and peak storm runoff in the seasonal tropics of Central Panama, *Water Resour. Res.*, 49, 8443–8462, doi:10.1002/2013WR013956.
- Olmedo, Berta. *Estado Actual De Las Condiciones Del Océano Pacífico Y Su Posible Evolución Durante El Año 2015-2016*. Rep. Department of Hydrometeorology, ETESA, Aug. 2015. Web.

- Rubio, Angel. *Notas Sobre Geología De Panamá*. Panamá: Universidad De Panamá, 1949.
- Sterrett, Robert J. *Groundwater and Wells*. Bloomington, MN: Johnson Screens, 2007. Print.
- Sjunnesson, Lena, and Malin Svendenius. *Investigation of the Groundwater Situation in Pesé Stream Area, Panama*. Rep. Department of Land and Water Resources Engineering, Royal Institute of Technology, Stockholm, 2004. Web.
- Souifer, Anatoli. *Delimitación De Acuíferos Y Establecimiento De Zonas De Recarga, Para Identificar Su Vulnerabilidad Y El Desarrollo De Una Estrategia Para Su Protección Y Conservación En El Arco Seco Del País*. Rep. Panamá: Nómadas De Centroamérica, 2010.
- Tejeira, Eric, Raúl Corro, Roddy Marquez, and Abdiel F. Mendoza. *Situación Actual De La Gestión Del Agua Subterránea En Panamá*. Sept. 2010. Programa De Formación Iberoamericano En Materia De Aguas.

7. Appendices

7.1 Appendix A: Figures and Maps

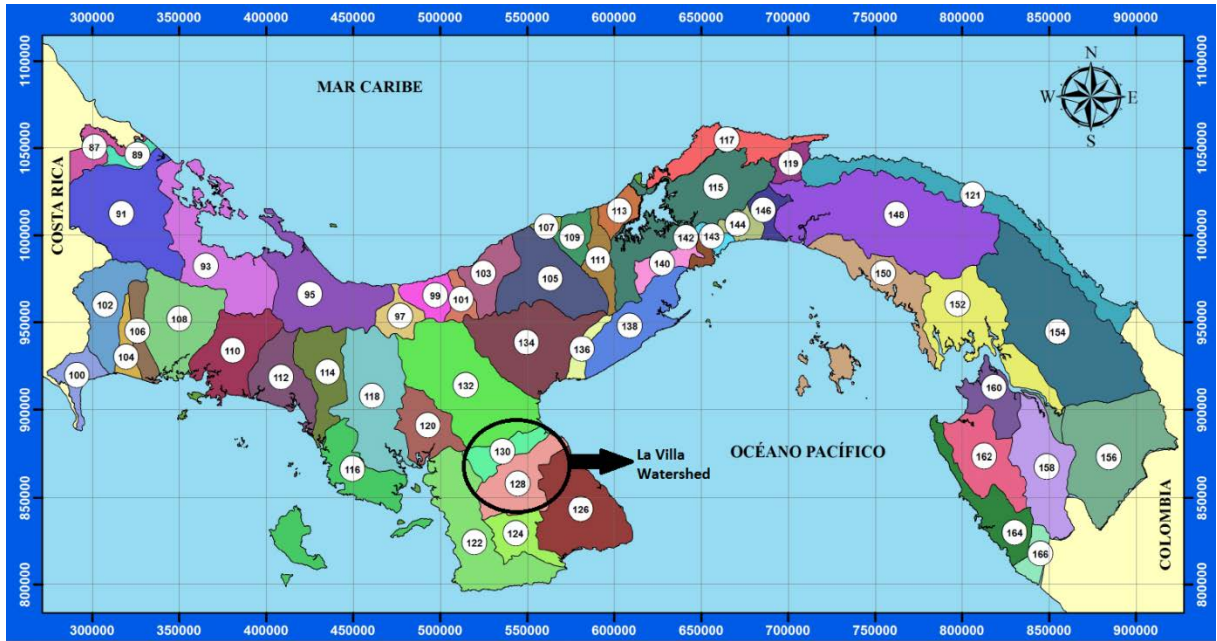


Figure A1: The watersheds of Panama. The territory of Panama is divided into 52 watersheds. La Villa Watershed is No. 128 in this map (<http://www.hidromet.com.pa/cuencas.php>).

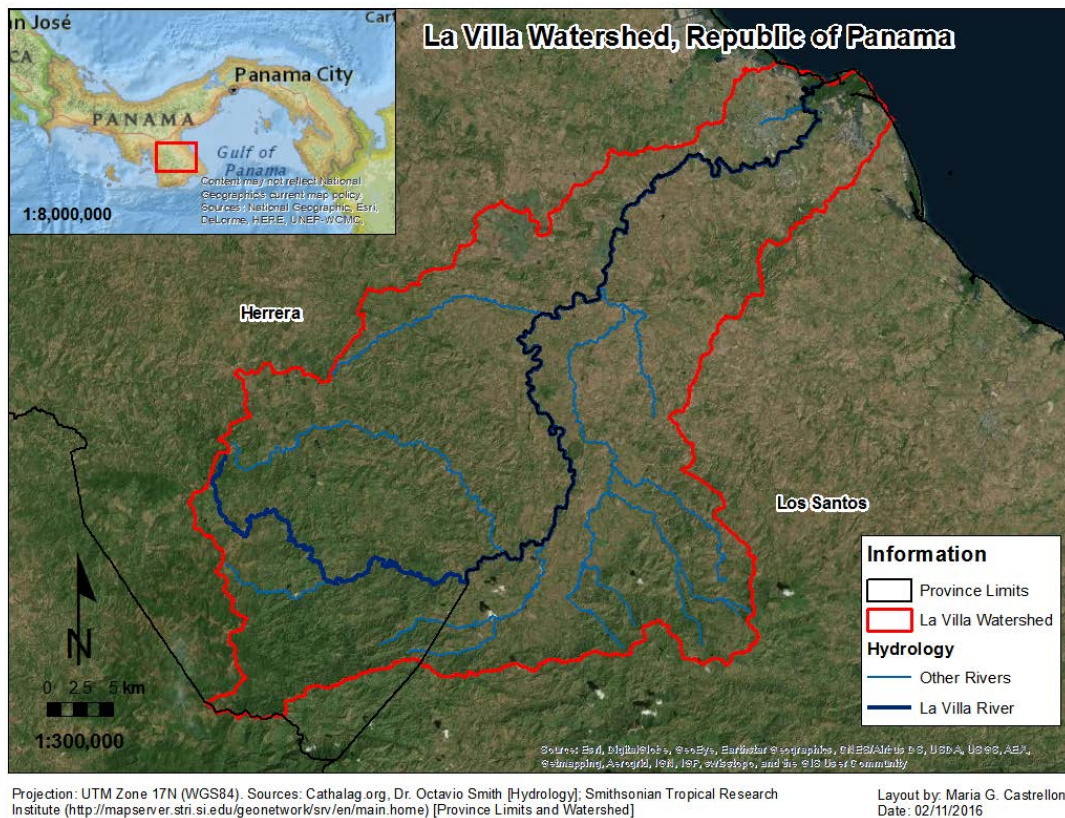
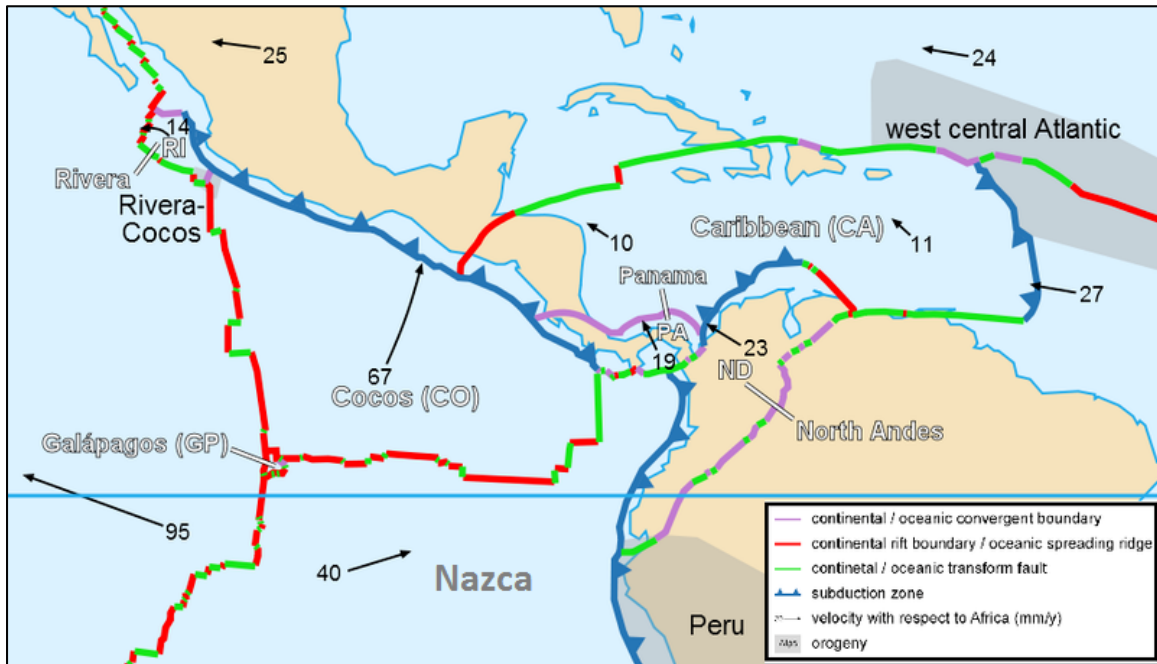
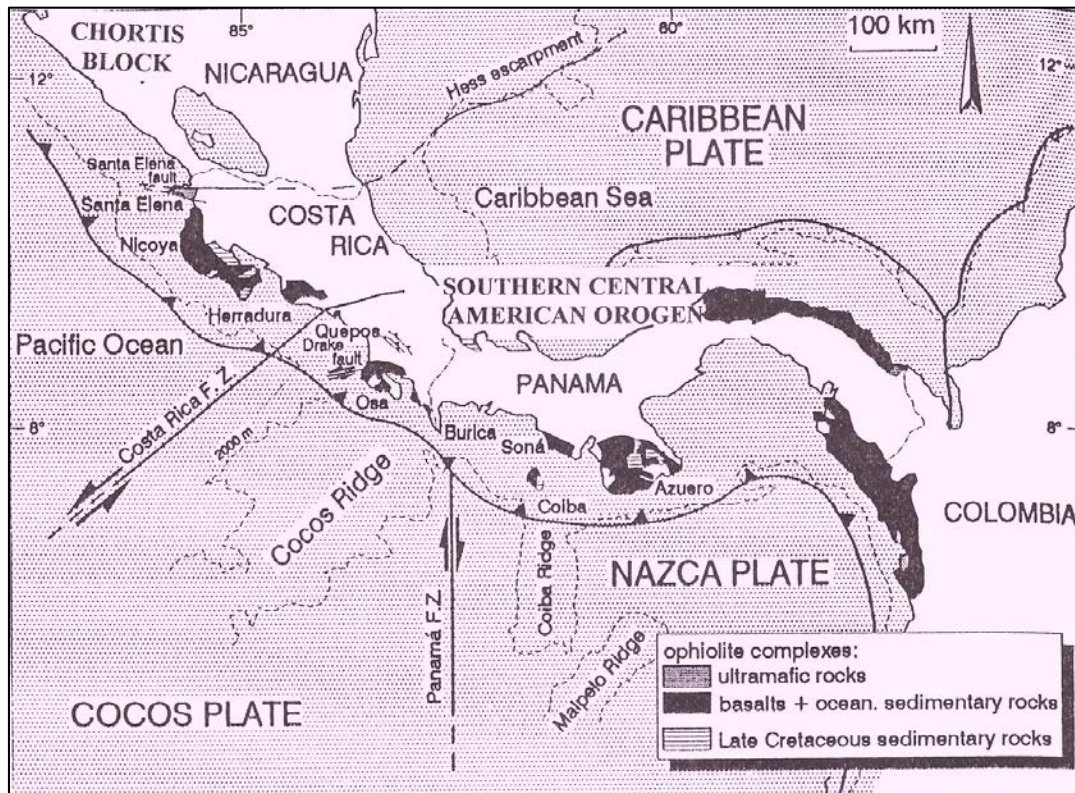


Figure A2: La Villa Watershed (red line) is located between the provinces of Herrera and Los Santos in the Azuero Peninsula of Panama. The La Villa River (dark blue line) is the limit between the two provinces.



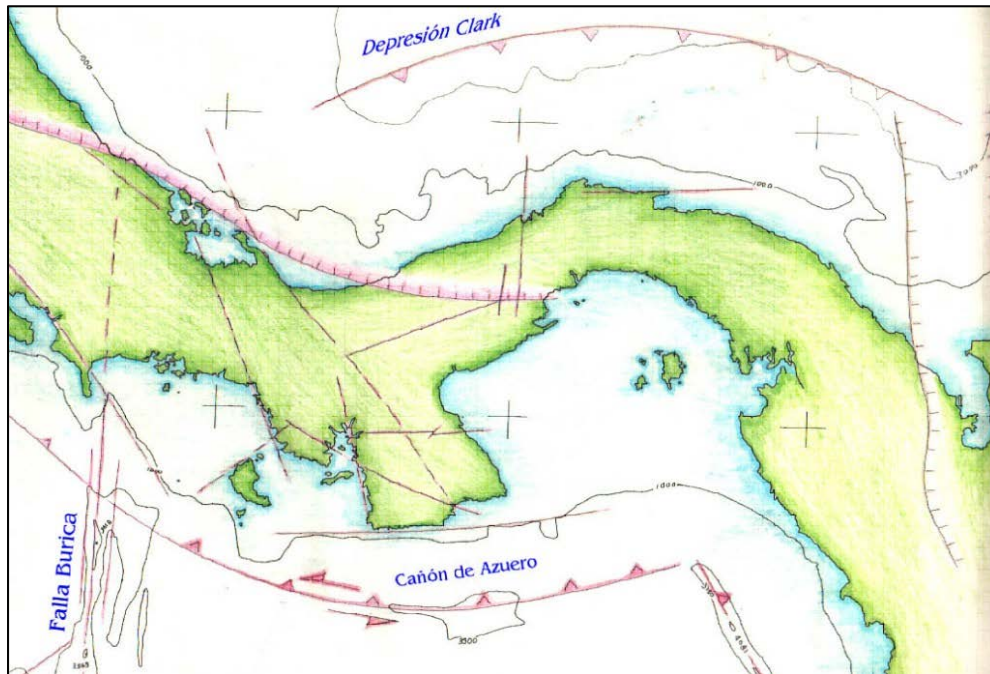
Source: http://i.livescience.com/images/i/000/053/736/i02/Caribbean_plate_tectonics.jpg?1371062515

Figure A3: Panama is located in the frontier of three oceanic plates, the Cocos, the Nazca and the Caribbean. Over the past 150 million years, the relative motion of these plates, as well as the North and South American continental plates, shaped Panama as the isthmus that it is today (Harmon, 2005).



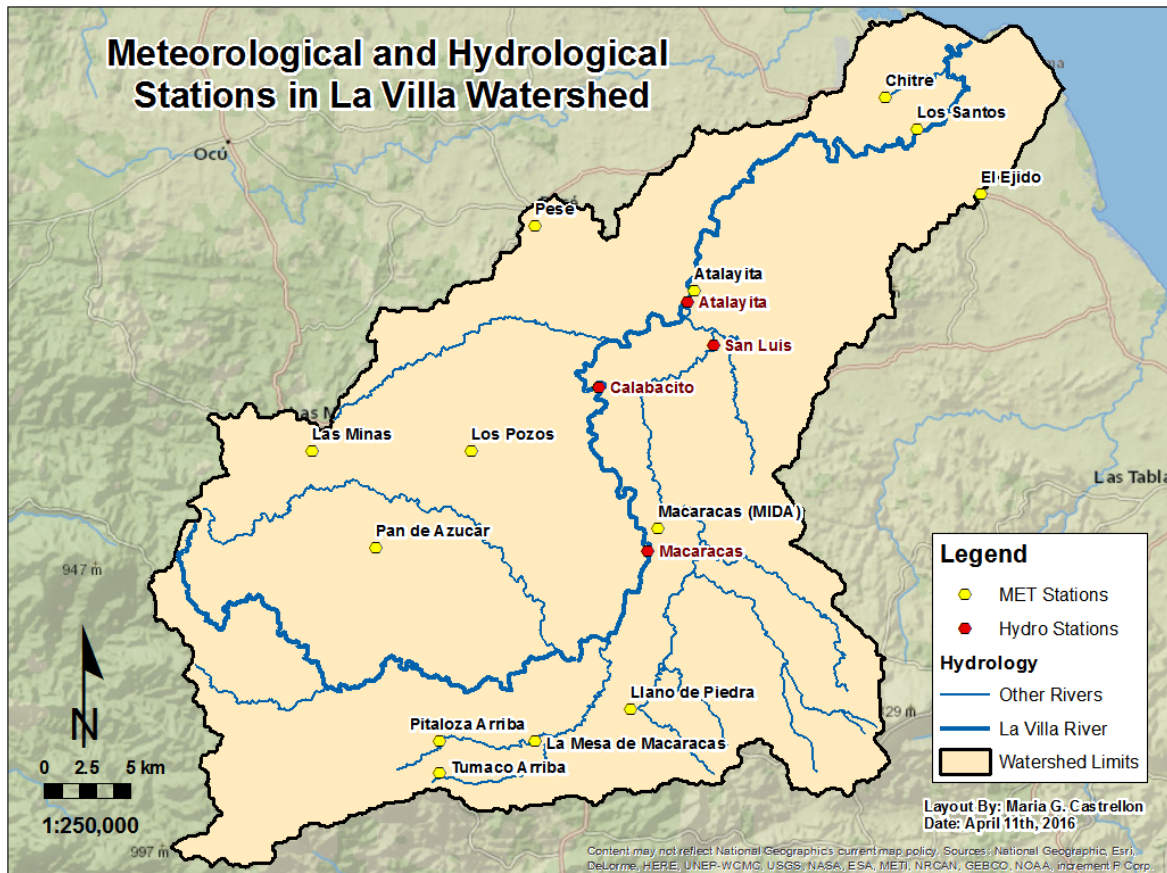
Source: <http://www.soldeosa.com/editorial/images/figure%203.jpg>

Figure A4: Location of the exotic terranes of Panama and Costa Rica. The basalts that conform the peninsulas of Azuero, Burica, Soná, Osa and Nicoya formed in the southern and western Pacific Ocean and traveled to their current location by the movement of the tectonic plates (Coates, 1997; Harmon 2005).



Source: http://geologia.azueropanamia.org/wp-content/uploads/2009/08/FALLAS_REG-1024x734.jpg

Figure A5: Faults of Panama. Redlines indicate location of faults and arrows indicate the relative movement of the major faults. Faults in the Pacific are more active than in the Caribbean (Harmon, 2005).



Projection: UTM Zone 17 N (WGS 84). Source: Smithsonian Tropical Research Institute GIS Portal; Department of Hydrometeorology, ETESA.

Figure A6: Location of the meteorological and hydrological stations in La Villa River Watershed. These stations are managed by the Department of Hydrometeorology of ETESA.

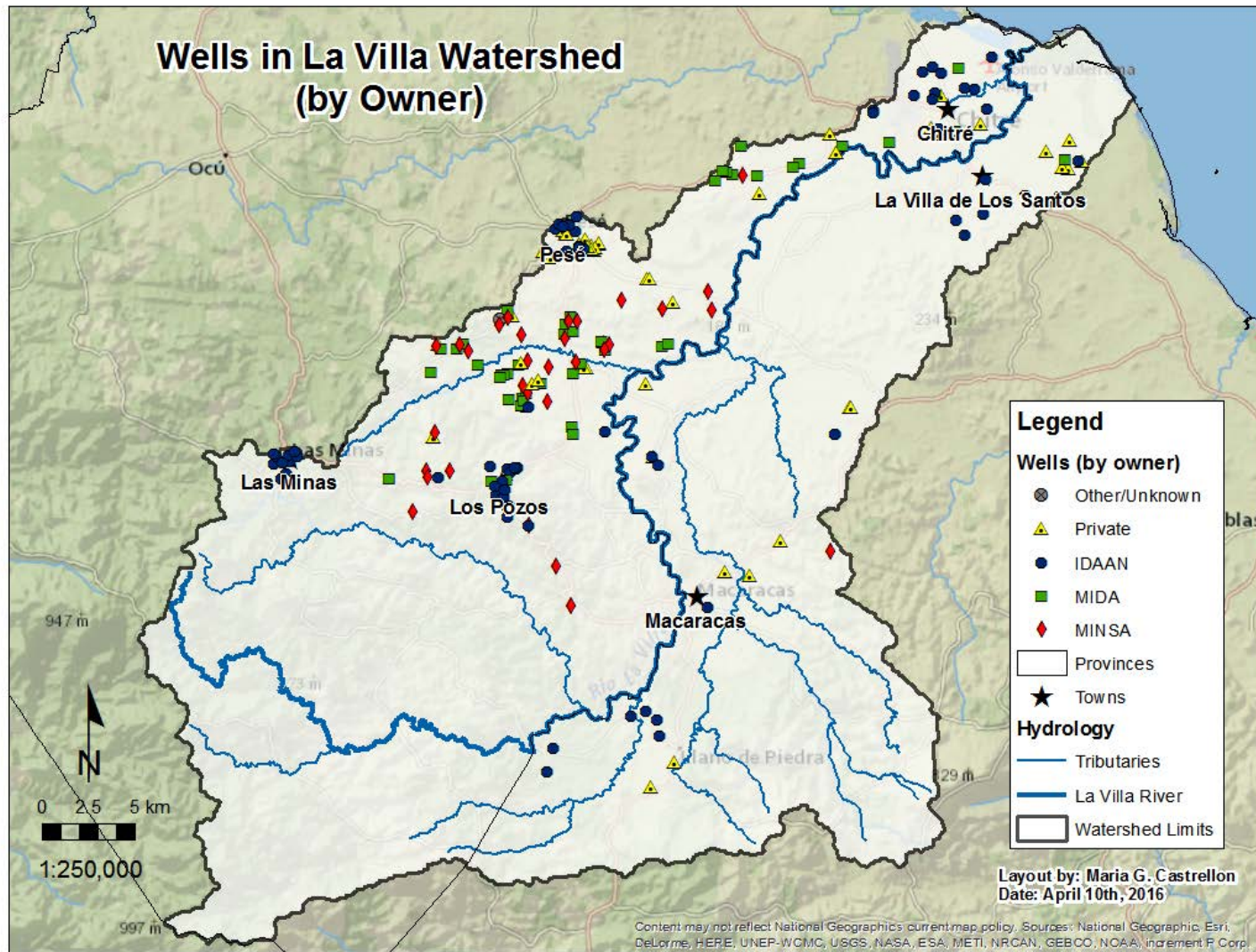


Figure A7: Location of 205 wells around La Villa River Watershed classified according to the government institution which drilled and operates the well. This map also contains the location of some private wells.

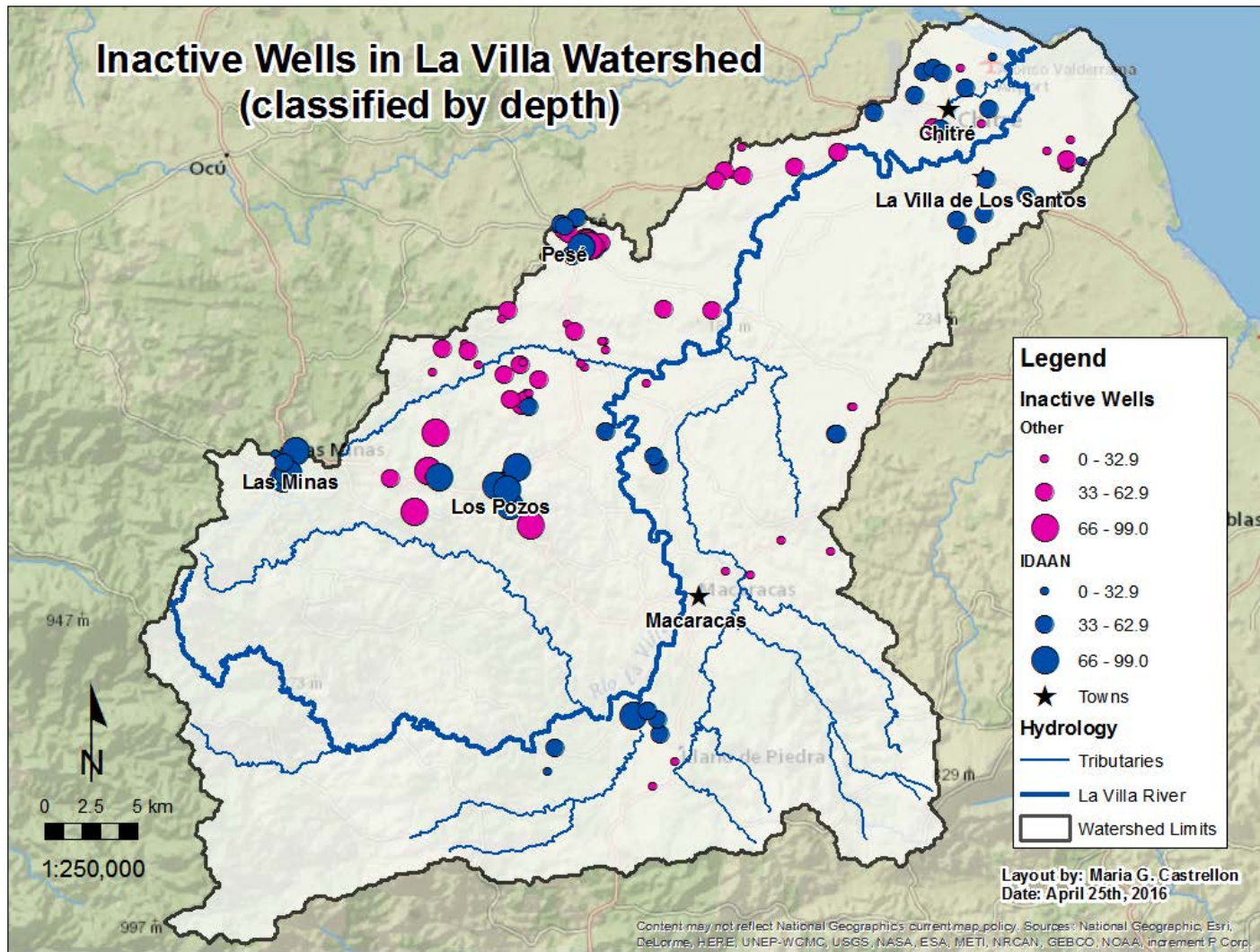


Figure A8: Inactive Wells in La Villa Watershed, classified according to their depth in meters below ground surface.

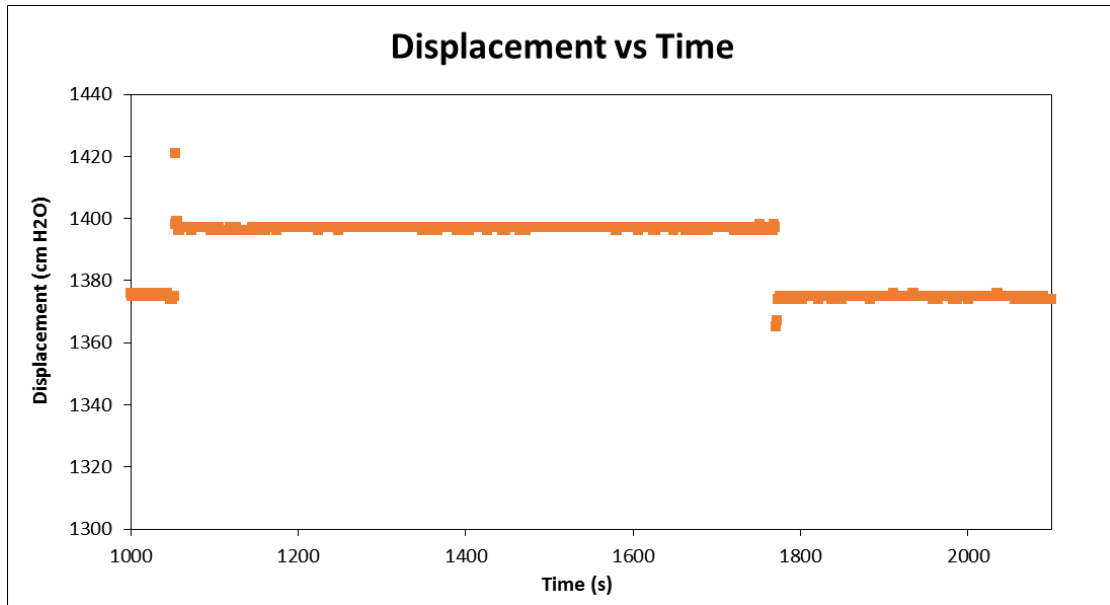


Figure A9: Example of slug test data that could not be analyzed because there is no logarithmic decay and also the water level did not recover to its original level.

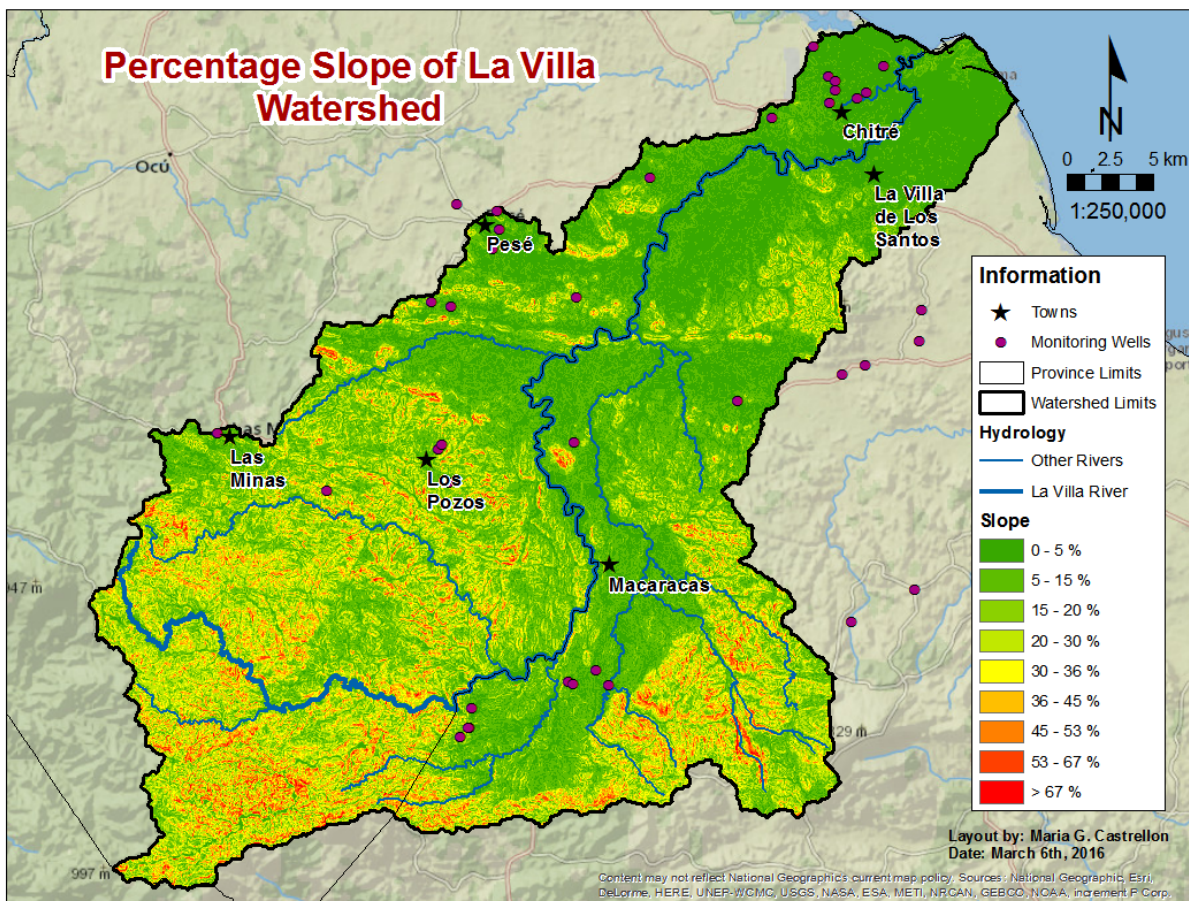


Figure A10: Slope, measured as percentage, in la Villa Watershed. Generated from the DEM of the watershed.

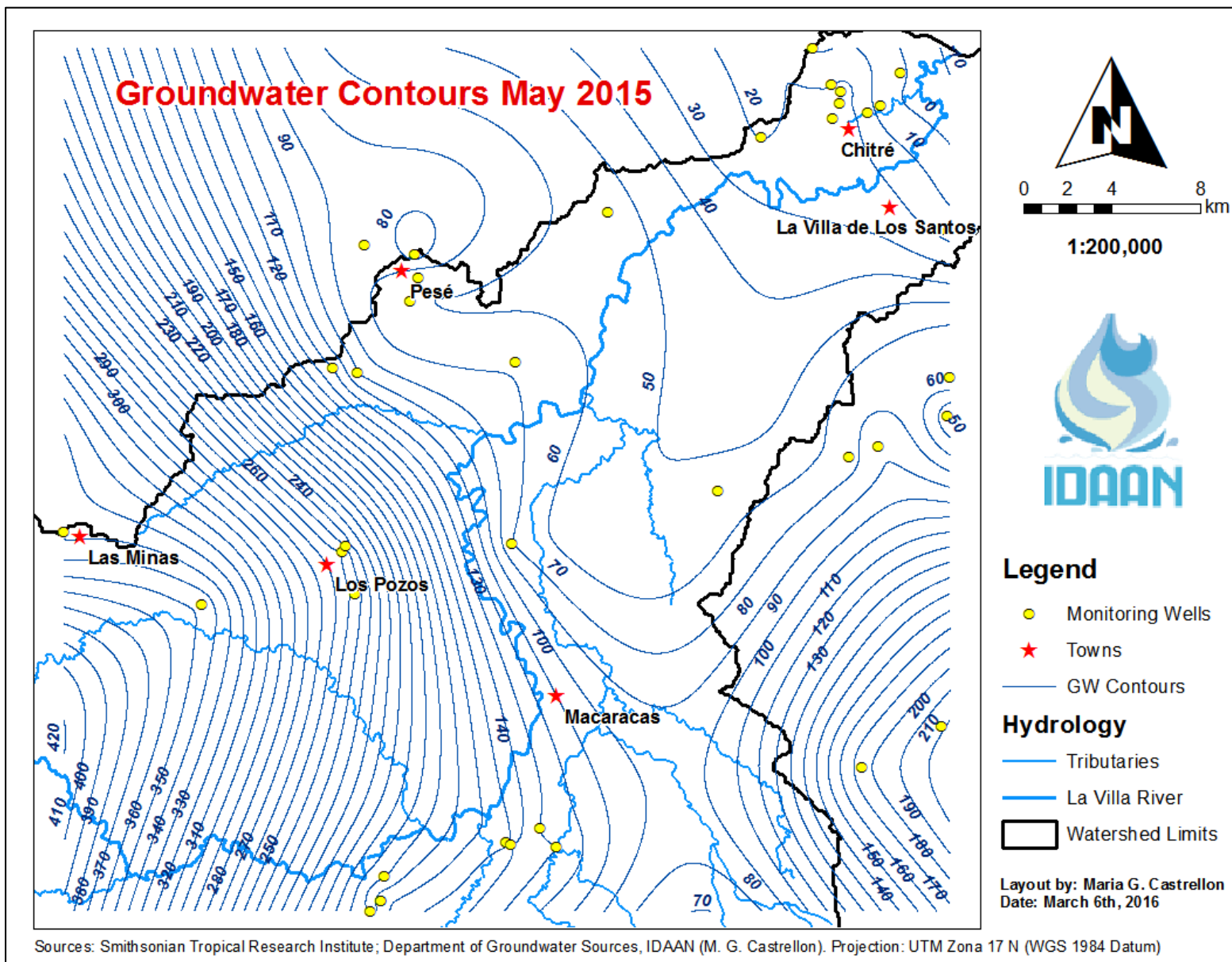


Figure A11: Groundwater elevation contours drawn each 10 meters for May 2015.

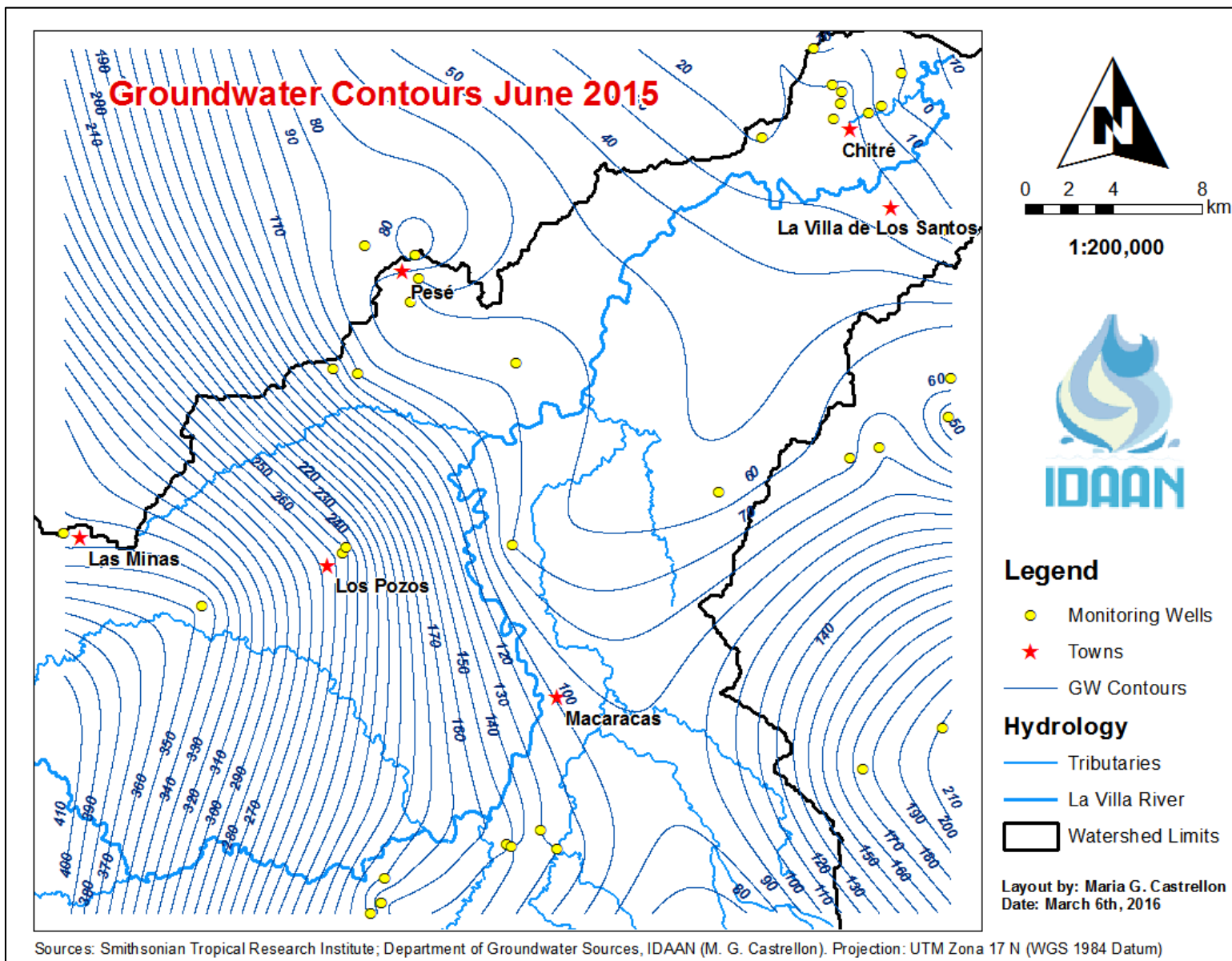


Figure A12: Groundwater elevation contours drawn each 10 meters for June 2015.

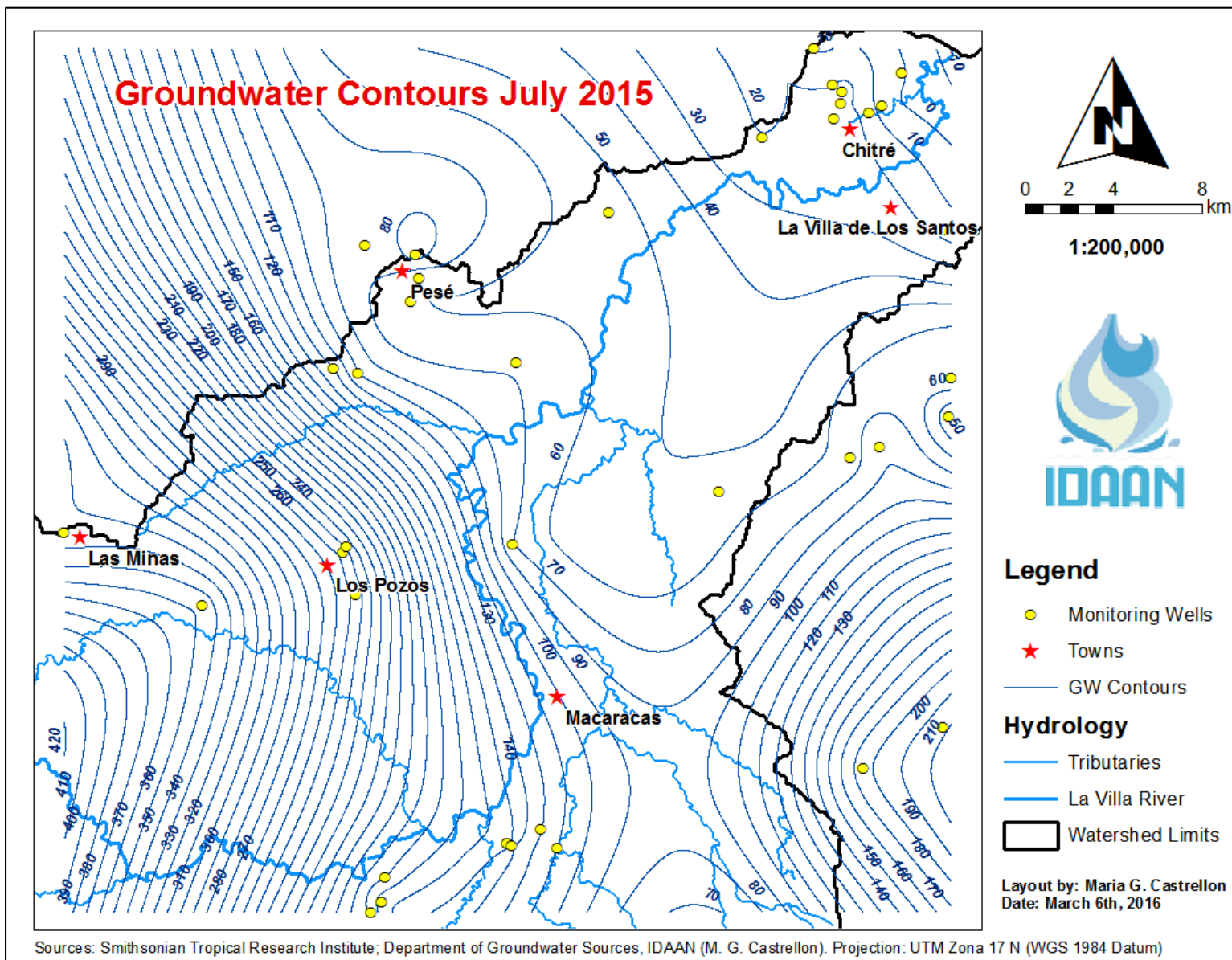


Figure A13: Groundwater elevation contours drawn each 10 meters for July 2015.

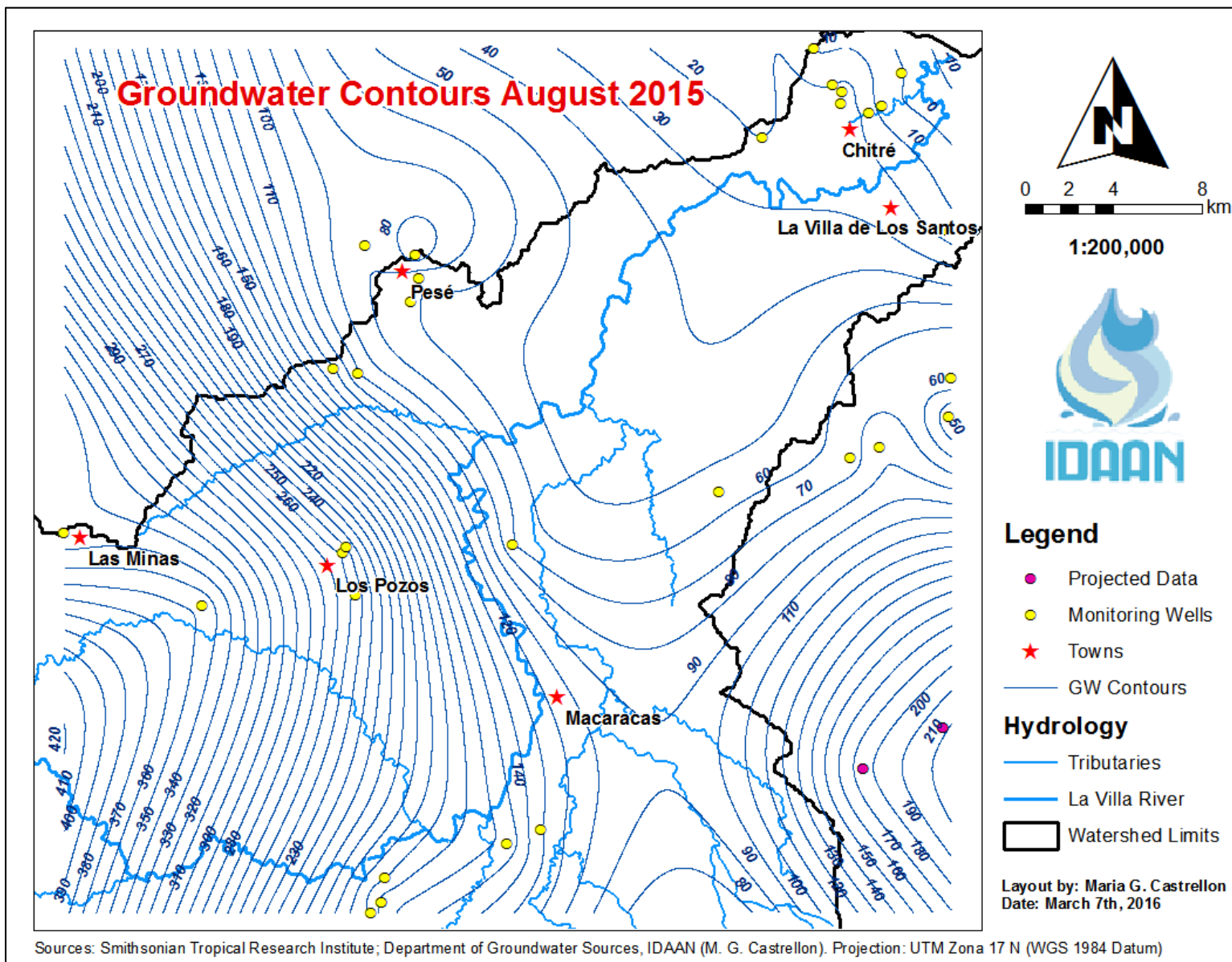


Figure A14: Groundwater elevation contours drawn each 10 meters for August 2015.

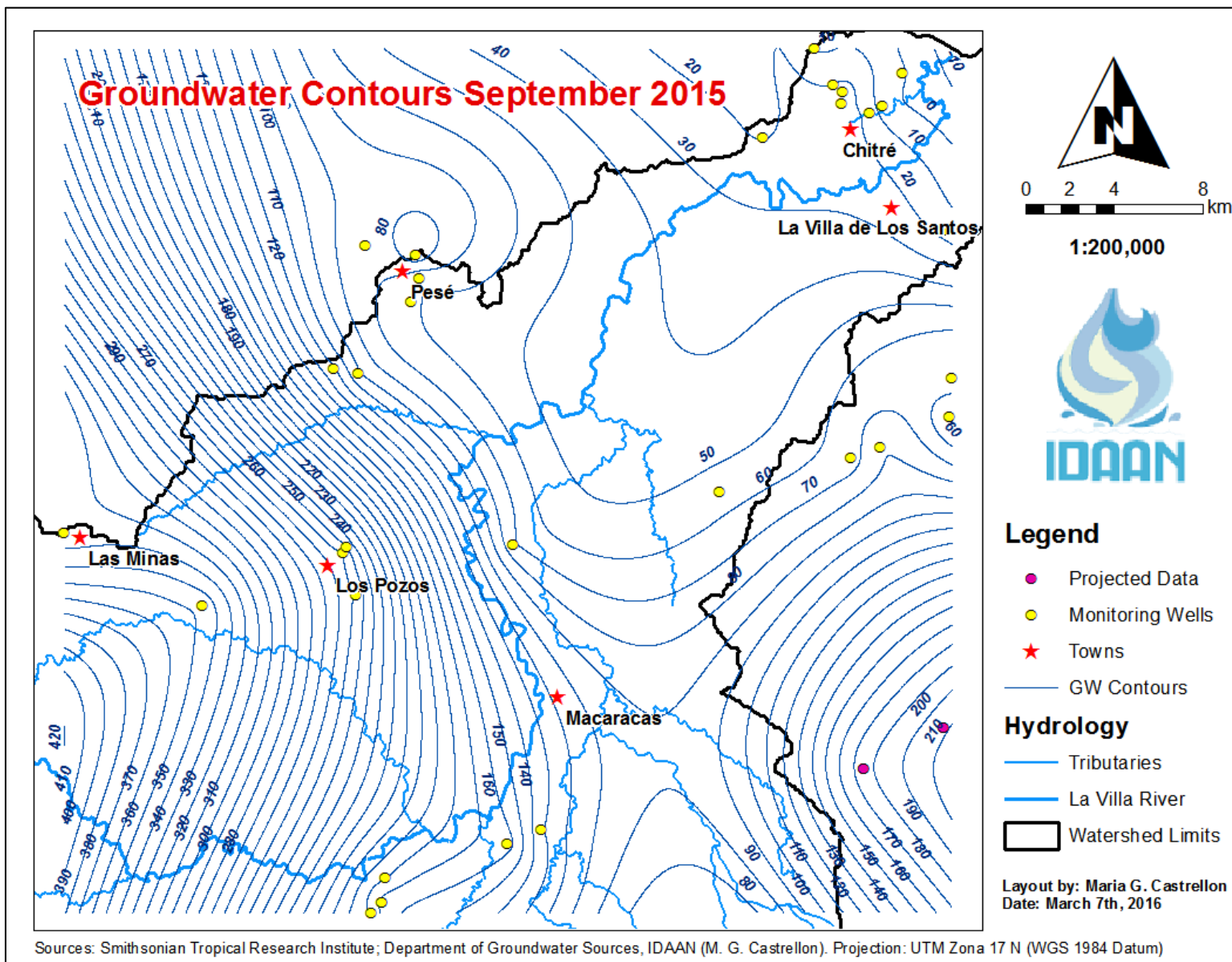


Figure A15: Groundwater elevation contours drawn each 10 meters for September 2015.

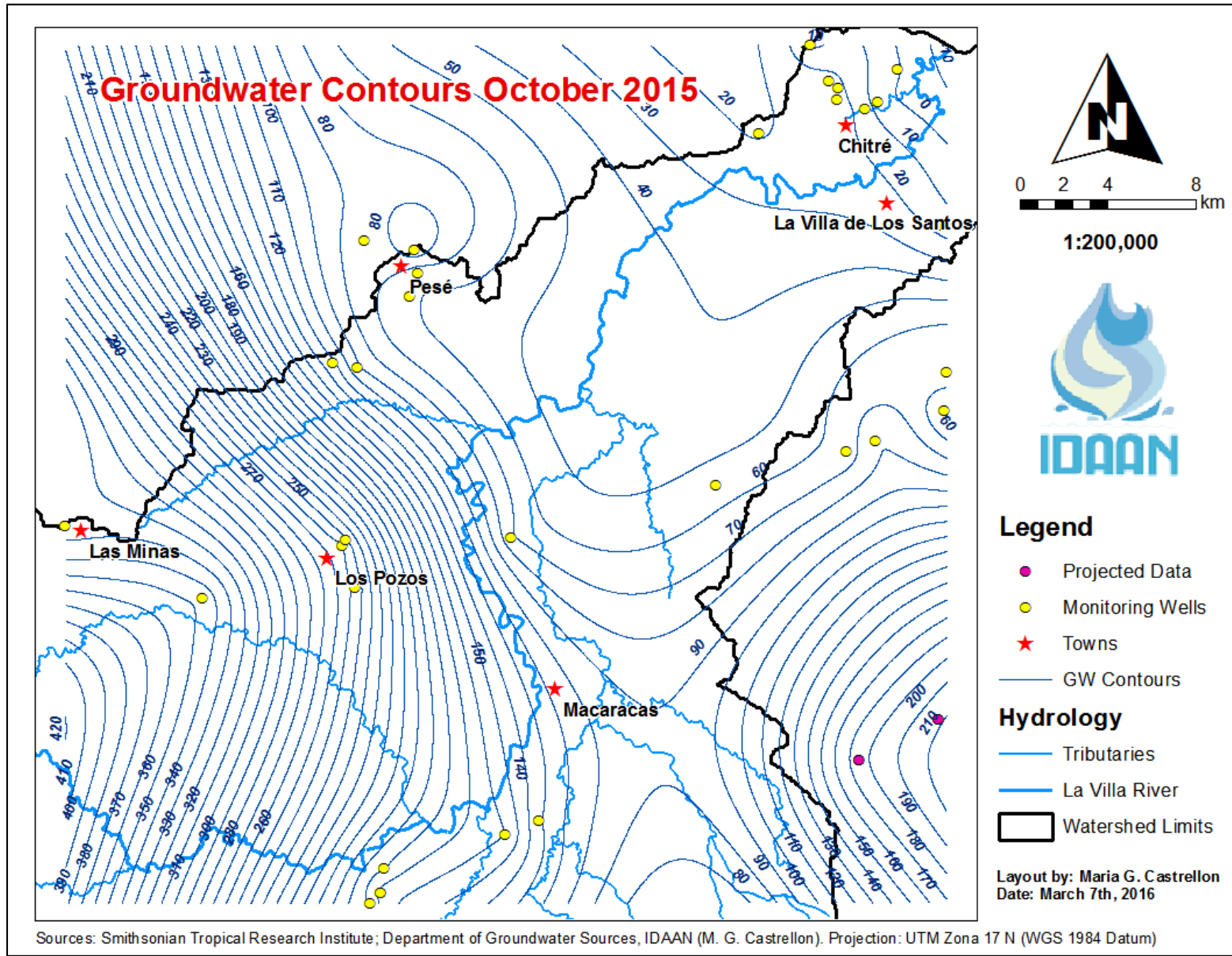


Figure A16: Groundwater elevation contours drawn each 10 meters for October 2015.

7.2 Appendix B: Tables

Table B1: Historic average monthly precipitation (mm) measured in the ETESA MET stations of La Villa Watershed (Souifer, 2010).

Station	Jan.	Feb.	Mar.	Apr.	May	Jun.	Jul.	Aug.	Sept.	Oct.	Nov.	Dec.	Total
Los Santos	5.27	0.75	0.59	20.97	118.07	133.86	98.36	128.42	161.73	214.17	111.3	51.89	1045.36
Macaracas	5.32	4.38	4.46	48.43	200.18	215.7	162.67	203.31	242.53	267.93	205.27	70.26	1630.44
Pesé	8.01	2.69	6.08	36.12	209.68	168.34	163.25	173.54	232.56	256.75	170.1	60.03	1487.13
Pan de Azúcar	14.38	10.32	16.5	66.14	200.11	212.68	173.66	241.86	289.45	318.78	173	51.1	1767.99

Table B2: Historic Average monthly streamflow (m^3/s) measured at the Atalayita Hydrological Station station (128-01-03), summarized by Souifer (2010).

	Jan.	Feb.	Mar.	Apr.	May	Jun.	Jul.	Aug.	Sept.	Oct.	Nov.	Dec.
Min.	7.38	4.44	2.97	1.76	2.52	5.25	5.32	5.7	10.34	23.01	23.3	12.08
Avg.	13.49	7.41	5.08	4.22	11.42	22.31	21.15	33.38	54.15	78.7	64.99	29.29
Max.	43.51	15.66	10.73	7.26	28.84	86.62	76.45	96.62	109.61	179.96	130.17	65.26

Table B3: Historic Average monthly streamflow (m^3/s) measured at the Macaracas Hydrological station (128-01-01), summarized by Souifer (2010).

	Jan.	Feb.	Mar.	Apr.	May	Jun.	Jul.	Aug.	Sept.	Oct.	Nov.	Dec.
Min.	4.83	2.86	2.02	1.56	2.71	5.08	3.33	3.87	7.79	12.61	15.83	8.53
Avg.	10.02	5.72	3.92	3.68	8.09	14.14	13.69	20.04	30.95	45.07	41.02	20.7
Max.	27.33	10.01	6.41	7.82	17.76	42.47	42.48	57.38	63.23	103.84	75.09	41.72

Table B4: Difference in average monthly historic hydrograph from Macaracas to Atalayita (m^3/s), adapted from Souifer (2010).

	Jan.	Feb.	Mar.	Apr.	May	Jun.	Jul.	Aug.	Sept.	Oct.	Nov.	Dec.
Min.	2.55	1.58	0.95	0.2	-0.19*	0.17	1.99	1.83	2.55	10.4	7.47	3.55
Avg.	3.47	1.69	1.16	0.54	3.33	8.17	7.46	13.34	23.2	33.63	23.97	8.59
Max.	16.18	5.65	4.32	-0.56*	11.08	44.15	33.97	39.24	46.38	76.12	55.08	23.54

*The negative values mean the flow in Macaracas was higher than the flow in Atalayita.

Table B4: Average historic monthly net runoff that reached the La Villa River in 30 km reach from Macaracas to Atalayita (m^3/s), calculated from Souifer (2010).

	Jan.	Feb.	Mar.	Apr.	May	Jun.	Jul.	Aug.	Sept.	Oct.	Nov.	Dec.
Avg.	2.93	1.15	0.62	0	2.79	7.63	6.92	12.8	22.66	33.09	23.43	8.05

Table B5: Average transmissivities (T) and hydraulic conductivities (K) inferred from slug tests. Depth refers to the total depth of the well and the saturated thickness (L) is the portion of the well without PVC piping.

ID	Location	Depth (m)	L (m)	K (m/day)	T (m ² /day)
PM-01	La Arena	48.78	30.49	1.63	49.84
PM-02	Llano Bonito	67.07	48.78	0.13	6.43
PM-03	Llano Bonito	24.37	80.79	0.01	0.73
PM-05	San Juan Bautista	23.19	24.00	0.39	9.37
PM-06	Monagrillo	32.85	36.59	0.86	31.32
PM-07	Monagrillo	35.50	14.63	8.94	130.79
PM-08	Monagrillo	46.48	27.44	1.72	47.11
PM-09	Monagrillo	54.88	21.34	1.05	22.35
PM-10	Las Minas	91.46	76.22	0.04	2.82
PM-12	Los Pozos	79.27	54.88	7.67	420.87
PM-16	El Pedregoso	31.04	30.50	20.53	626.27
PM-18	Pesé	34.00	70.12	1.15	80.76
PM-19	Pesé	47.26	44.20	2.28	100.91
PM-20	Sábana Grande	80.20	73.17	1.54	112.99
PM-21	Rincón Hondo	43.60	43.60	1.12	48.70
PM-22	Sábana Grande	42.68	30.50	0.04	1.16
PM-24	Las Trancas	17.00	19.11	2.41	46.05
PM-25	La Espigadilla	22.46	18.29	3.58	65.46
PM-28	Las Guabas	91.46	57.93	2.30	133.35
PM-29	Los Santos	50.30	26.83	48.46	1300.20
PM-31	Chupá	42.68	32.00	1.89	60.35
PM-33	La Mesa	42.68	18.29	1.16	21.23
PM-35	La Mesa	30.49	24.39	17.14	418.00
PM-36	Llano de Piedra	54.88	54.88	0.51	27.93
PM-37	Llano de Piedra	76.22	62.50	2.35	146.97
PM-38	Llano de Piedra	42.68	42.68	4.08	173.94
PM-39	Llano de Piedra	129.57	83.84	1.94	162.65

Table B6: Example of lithological description found in IDAAN drilling registries. This description corresponds to LV-10 located in Chitré.

HGUID	Top Elevation (m)	Bottom Elevation (m)	Description
4	8.00	-1.15	Clay
1	-1.15	-4.20	Altered Agglomerate
1	-4.20	-7.24	Fractured Agglomerate
1	-7.24	-10.29	Agglomerate
2	-10.29	-19.44	Andesite
4	-19.44	-22.49	Gray Clay

7.3 Appendix C: Calculations

- Groundwater elevation change in Macaracas:

$$\text{Area of polygon around Macaracas } (A_{poly.}) = 0.94 \text{ km}^2 = 9.40 \times 10^5 \text{ m}^2$$

$$\text{Number of Pixels in the polygon} = 1044$$

$$\text{Total GW elevation change in polygon} = \sum_1^{1044} (\Delta H_{gw})_i = 1294.448 \text{ m}$$

$$\text{Average GW elevation change in polygon } (\Delta H_{gw}) = 1294.448 \text{ m} / 1044 = 1.240 \text{ m}$$

- Total volume of groundwater available for extraction in Macaracas (assuming a soil porosity of 40%):

$$\text{Actual GW elevation change} = (\Delta H_{gw}) \times (\eta) = (1.240 \text{ m}) \times (0.40) = 0.496 \text{ m}$$

$$\text{Total volume} = (\text{Actual GW elevation change}) \times (\text{Polygon Area})$$

$$\text{Total volume } (0.496 \text{ m}) \times (9.40 \times 10^5 \text{ m}^2) = 4.66 \times 10^5 \text{ m}^3$$

- Area beneath average difference hydrograph (Polygon Method):

$$\text{Average monthly flow } (Q_{avg}) = (Q_i + Q_{i+1})/2 = (8.59 + 3.47)/2 = 6.03 \text{ m}^3/\text{s}$$

$$\text{Time step } (\Delta t) = 30 \text{ days}$$

$$\text{Volume } (V) = (Q_{avg}) \times (\Delta t) = (6.03 \text{ m}^3/\text{s}) \times (86400 \text{ s/d}) \times (30 \text{ d}) = 1.56 \times 10^7 \text{ m}^3$$

Time (days)	Q (m ³ /s)	AVG Q (m ³ /s)	Volume (m ³)
0	8.59	6.03	1.56E+07
30	3.47	2.58	6.69E+06
60	1.69	1.425	3.69E+06
90	1.16	0.85	2.20E+06
120	0.54	1.935	5.02E+06
150	3.33	5.75	1.49E+07
180	8.17	7.815	2.03E+07
210	7.46	10.4	2.70E+07
240	13.34	18.27	4.74E+07
270	23.2	28.415	7.37E+07
300	33.63	28.8	7.46E+07
330	23.97	16.28	4.22E+07
360	8.59	--	--

$$\text{Total Volume} = \sum_1^{12} V_i = 3.33 \times 10^8 \text{ m}^3$$

- Area beneath average net runoff hydrograph (Polygon Method):

$$\text{Average monthly flow } (Q_{avg}) = (Q_i + Q_{i+1})/2 = (8.05 + 2.93)/2 = 5.49 \text{ m}^3/\text{s}$$

$$\text{Time step } (\Delta t) = 30 \text{ days}$$

$$\text{Volume } (V) = (Q_{avg}) \times (\Delta t) = (5.49 \text{ m}^3/\text{s}) \times (86400 \text{ s/d}) \times (30 \text{ d}) = 1.42 \times 10^7 \text{ m}^3$$

Time (days)	Q (m ³ /s)	AVG Q (m ³ /s)	Volume (m ³)
0	8.05	5.49	1.42E+07
30	2.93	2.04	5.29E+06
60	1.15	0.885	2.29E+06
90	0.62	0.31	8.04E+05
120	0	1.395	3.62E+06
150	2.79	5.21	1.35E+07
180	7.63	7.275	1.89E+07
210	6.92	9.86	2.56E+07
240	12.8	17.73	4.60E+07
270	22.66	27.875	7.23E+07
300	33.09	28.26	7.32E+07
330	23.43	15.74	4.08E+07
360	8.05	--	--

$$\text{Total Runoff Volume} = \sum_1^{12} V_i = 3.16 \times 10^8 \text{ m}^3$$

- Total amount of groundwater reaching La Villa River in the 30 km reach:

$$V_{gw} = \text{Total Volume} - \text{Runoff Volume}$$

$$V_{gw} = 3.33 \times 10^8 \text{ m}^3 - 3.16 \times 10^8 \text{ m}^3 = 1.70 \times 10^7 \text{ m}^3$$

- Flow of water towards La Villa River from the highlands of Herrera:

a. Using transmissivities (T) from pumping tests in the town of Los Pozos

ID	Label	Well Depth (m)	Saturated Thickness (m)	T (m ² /day)
LV-27	Hacia El Cedro	62.50	44.21	8.70
LV-29	Cantera	79.27	67.10	14.09
LV-30	Los Pozos Entrada	91.46	54.88	6.34

$$\text{Average Transmissivity } (T_{avg}) = (8.70 + 14.09 + 6.34)/3 = 9.71 \text{ m}^2/\text{day}$$

$$\text{Hydraulic gradient, measured from contour map } (I) = 0.0194$$

$$\text{Width of flow through section } (w) = 30,000 \text{ m}$$

$$Q_{pt} = T_{avg} * I * w = (9.71 \text{ m}^2/\text{day})(0.0194)(30,000 \text{ m}) = 5651 \text{ m}^3/\text{day}$$

b. Using transmissivity (T) from slug test in Los Pozos - Cantera

Transmissivity from slug test in Los Pozos (T_{st}) = 420.875 m²/day

$$Q_{st} = T_{st} * I * w = (420.875 \text{ m}^2/\text{day})(0.0194)(30,000 \text{ m}) = 244,949 \text{ m}^3/\text{day}$$

- Rainfall in Los Pozos:

Area of polygon around Los Pozos ($A_{poly.}$) = 0.94 km² = 1.57 × 10⁶ m²

Number of Pixels in the polygon = 1748

$$\text{Total rainfall accumulated in polygon} = \sum_1^{1748} P_i = 855.294 \text{ m}$$

$$\text{Average rainfall accumulated in polygon (P)} = 855.294 \text{ m}/1748 = 0.489 \text{ m}$$

- Groundwater elevation change in Los Pozos:

$$\text{Total GW elevation change in polygon} = \sum_1^{1748} (\Delta H_{gw})_i = 3219.631 \text{ m}$$

$$\text{Average GW elevation change in polygon } (\Delta H_{gw}) = 3219.631 \text{ m}/1748 = 1.842 \text{ m}$$

- Total volume of groundwater available for extraction in Los Pozos (assuming a soil porosity of 40%):

$$\text{Total volume} = (\Delta H_{gw}) \times (\eta) \times A_{poly.}$$

$$\text{Total volume} = (1.842 \text{ m}) \times (0.40) \times (1.57 \times 10^6 \text{ m}^2) = 1.16 \times 10^6 \text{ m}^3$$

- Groundwater flow reaching Los Pozos from the highlands:

Transmissivity from slug test in Los Pozos (T_{st}) = 420.875 m²/day

Hydraulic gradient, measured from contour map (I) = 0.0194

Width of flow through section, corresponding to size of polygon (w) = 1,180 m

$$Q^* = T_{st} * I * w = (420.875 \text{ m}^2/\text{day})(0.0194)(1,180 \text{ m}) = 9631 \text{ m}^3/\text{day}$$

Area of polygon around Los Pozos ($A_{poly.}$) = 0.94 km² = 1.57 × 10⁶ m²

Observation period (t) = 6 months = 180 days

$$Q_{gw,local} = \frac{(Q^*) \times (t)}{A_{poly.}} = \frac{(9631 \text{ m}^3/\text{day})(180 \text{ days})}{1.57 \times 10^6 \text{ m}^2} = 1.10 \text{ m}$$